NOAA Project
Report

Tsunami Inundation Maps Development for the Gulf of Mexico

Final Report to the
National Tsunami Hazard Mitigation Program (NTHMP)
in Completion of Project Awards
NA22NWS4670022

Authors

Juan J Horrillo	Texas A&M University at Galveston
Wei Cheng	
Collaborators:	

Under the guidance of
NTHMP Mapping and Modeling Subcommittee

National Tsunami Hazard Mitigation Program

National Oceanic and Atmospheric Administration

Ocean Engineering
Texas A&M University at Galveston
Galveston, Texas, 77553

December 2024

Contents

List of Figures

List of Tables

1 Executive Summary

Potential tsunami sources for the GOM are local submarine landslides, which have been examined in the past by the Atlantic and Gulf of Mexico Tsunami Hazard Assessment Group [ten Brink et al., 2009b]. In their findings, they stated that submarine landslides in the GOM are considered a potential tsunami hazard. However, the probability of such an event (tsunamis generated by large landslides) is low. The probability of occurrence is related to ancient (geological) massive landslides which were probably active prior to 7,000 years ago when large quantities of sediments were emptied into the Gulf of Mexico. Nowadays, sediment continues to empty into the Gulf of Mexico mainly from the Mississippi River. This sediment supply contributes to the slope steepening and the increase of fluid pore pressure in sediments, which may lead to further landslide activities and hence, the reason for this study in determining the potential tsunami hazard and its effects in the Gulf of Mexico.

For the triggering mechanism (tsunami generation) we use five geological sources, i.e., the Eastbreaks, Mississippi Canyon, West Florida landslides, and two Yucatán landslides introduced in [Horrillo et al., 2018]. A probabilistic approach was implemented in our previous study, see [Horrillo et al., 2015], to fill gaps along the continental shelf between the geological landslide sources by adding synthetic landslide sources (four in total) to cover the entire northern part of the GOM. Our probabilistic approach confirmed a recurrence period of major landslide events of around 8000 years, consistent with findings by [Geist et al., 2013].

These geological and probabilistic tsunami sources (nine in total) are used as the maximum credible events that could happen in the region according to the local bathymetry, seafloor slope, and sediment information. These credible events are then used to determine the inundation impact on selected communities along the GOM. The extent and magnitude of the tsunami inundation in those selected locations are achieved by using a combination of 3D and 2D coupled-numerical models. For instance, the 3D model, TSUNAMI3D, is used for tsunami generation to determine the initial dynamic wave or initial source and results are passed as an input to the 2D non-hydrostatic model, NEOWAVE, to determine the tsunami wave propagation and the detailed runup and inundation extent in each of the communities. Tsunami flooding inland-extent, maximum inundation water depth, momentum flux and direction, current velocity and vorticity can then be determined within the inundation-prone areas of the selected communities. Also, tsunami inundation and hurricane category flooding can be compared to access tsunami hazard in unmapped locations.

This project focused on the implementation of recent developments in the tsunami science recommended by the National Tsunami Hazard Mitigation Program - Modeling Mapping Subcommittee - Strategic Plan (NTHMP-MMS-SP) into our current Gulf of Mexico (GOM) tsunami mitigation products. Four main developments for tsunami mitigation have been created under this project for communities in the GOM that will provide guidance to state emergency managers for tsunami hazard mitigation and warning purposes.

The first is the development of tsunami inundation maps in Rosemary Beach, FL and North Tampa Bay, FL. Maximum tsunami inundation extent, water height, and momentum flux magnitude and direction are determined from each landslide sources, as well as the maximum of maximum inundation maps from all nine landslide sources. The two new

tsunami inundation map products add to the existing 20 mapped locations, which provide so far good coverage of the most populous coastal areas along the GOM.

The second is a continuing study of the comparison between existing SLOSH hurricane flooding data and our tsunami inundation result, in order to provide temporal-low-order estimate for tsunami hazard areas (community) where inundation studies have not yet been assigned/executed or where little bathymetric and elevation data exists. The adopted approach to define a quick estimate of tsunami vulnerability areas in the GOM has been taken from the existing hurricane storm surge flooding results along coastal areas, in which storm flooding map products are based on hurricane category. The existing storm surge flooding maps cover almost the entire GOM coastal regions and thus they are very well known among GOM regional emergency managers and other parties.

The third is to produce the velocity and vorticity magnitude maps for all the landslide scenarios, for Rosemary Beach, FL and North Tampa Bay, FL. Based on these maritime maps, location of strong currents and their damaging levels are identified. The tsunami hazard maritime products such as tsunami current magnitude, vorticity, safe/hazard zones would be central for future developments of maritime hazard maps, maritime emergency response and as well as infrastructure planning. We hope that the results herein may assist the maritime communities, port managers and other NTHMP's interested parties.

?????The fourth task is a continuation of the study to obtain an understanding of meteotsunami through the characterization of physical parameters in GOM [Cheng et al., 2021, Horrillo et al., 2020, 2021]. In this project, we expanded the previous parameter study from 1260 runs (on 1 arcminute resolution grid) to 17280 runs (15 arcsecond grid) for each subregion (northeastern & northwestern GOM), thanks to the huge performance increase using CUDA on our newly built multi-GPU workstation. The GPU workstation is able to run our meteotsunami CUDA Fortran code 50 – 100 times faster than it CPU versoin, depending on the grid. The result is a significantly improved resolution of different incident wave direction, forward speed and trajectory position, and their effect on maximum gauge water elevation across the whole GOM. In addition, characterization of meteotsunamis in northern GOM using meteotsunami rose charts and an application of ANN in meteotsunami water elevation prediction are performed on the new data generated from the parameter study

Although the recurrence of destructive tsunami events have been verified to be quite low in the GOM, our work has confirmed that submarine landslide events with similar characteristics to those used here, have indeed the potential to cause severe damage to GOM coastal communities. Therefore, this work is intended to provide guidance to local emergency managers to help managing urban growth, evacuation planning, and public education with final objective to mitigate potential tsunami hazards in the GOM.

2 Introduction

2.1 Background

The U.S. Tsunami Warning System has included Gulf of Mexico (GOM) coasts since 2005 in order to enable local emergency management to act in response to tsunami warnings. To

plan for the warning response, emergency managers must understand what specific areas within their jurisdictions are threatened by tsunamis. Coastal hazard areas susceptible to tsunami inundation can be determined by historical events, by modeling potential tsunami events (worst-case scenarios), or by using a probabilistic approach to determine the rate of recurrence or likelihood of exceeding a certain threshold. As the GOM coastal regions have no significant recent historical tsunami records, numerical modeling and probabilistic methodologies for source identification must be used to determine coastal hazard zones.

Potential tsunami sources for the GOM are local submarine landslides [ten Brink et al., 2009b]; sources outside the GOM are considered a very low threat and may not significantly impact GOM coastal communities or infrastructure [Knight, 2006]. Although a massive tsunamigenic underwater landslide in the GOM is considered a potential hazard, the frequency of such events (though not well-constrained) is probably quite low based on historical evidence [Dunbar and Weaver, 2008] and available data on ages of failures which suggest they were probably active prior to 7,000 years ago when large quantities of sediments were emptied into the GOM [ten Brink et al., 2009b]. However, sediments continue to empty into the GOM, mainly from the Mississippi River, contributing to slope steepening and the increase of fluid pore pressure in sediments which may lead to unstable slopes that can be subsequently triggered to failure by seismic loading [Masson et al., 2006, ten Brink et al., 2009a, Dugan and Stigall, 2010, Harbitz et al., 2014]. In addition, the unique geometry of the GOM basin makes even unlikely tsunami events potentially hazardous to the entire Gulf Coast. Waves tend to refract along continental slopes; thus, given the curved geomorphology of the GOM shelf and the concave shape of the coastline, any outgoing tsunami wave could potentially affect the opposite coast in addition to the coast close to the landslide source.

Five large-scale geological submarine landslides with tsunamigenic potential have been identified within the GOM [ten Brink et al., 2009b, Chaytor et al., 2016], representing possible worst-case tsunami scenarios affecting GOM coasts in the past. In order to generate a more complete picture of landslide tsunami potential in the GOM, a probabilistic approach has been implemented to develop four additional synthetic landslide sources which fill gaps along the continental shelf between the geological landslide sources [Pampell-Manis et al., 2016]. These probabilistic tsunami sources are considered to be the maximum credible events that could happen in a particular region of the GOM according to the local bathymetry, seafloor slope, sediment information, and seismic loading. The probabilistic maximum credible events together with the geological sources form a suite of tsunami sources that have been used within coupled 3D and 2D numerical models to model tsunami generation and propagation throughout the GOM and to develop high-resolution inundation maps for the inundation-prone areas of two new communities along the Gulf Coast: Rosemary Beach, FL and North Tampa Bay, FL. These inundation studies showed that tsunamis triggered by massive submarine landslides have the potential to cause widespread and significant inundation of coastal cities. All of the 22 communities from both previous and current work and nine landslide sources are shown in Fig. 1.

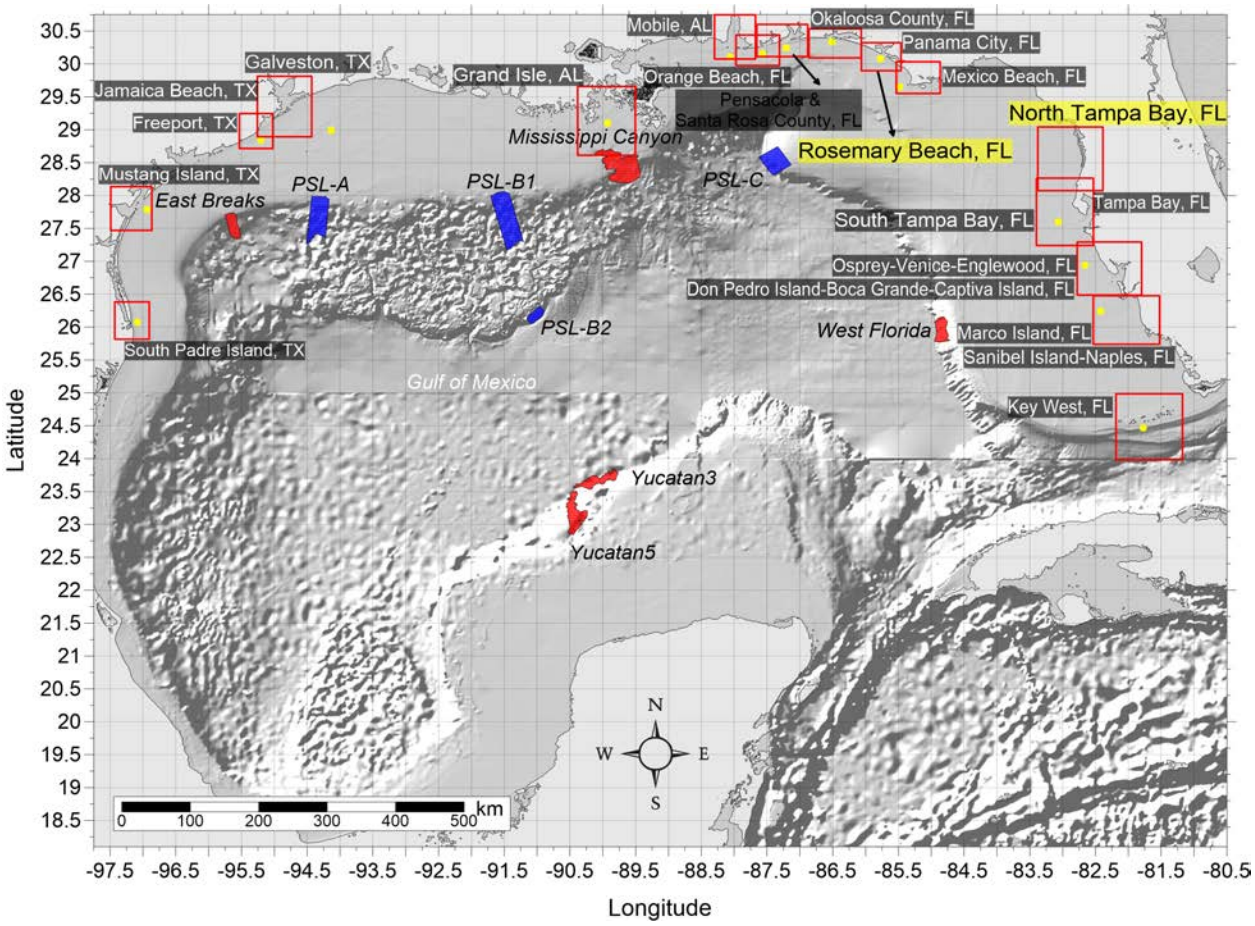

Figure 1: Selected communities or geography regions along the US GOM coastline where tsunami maps have been developed. Red rectangles denote 3 arcsecond (∼90m) domains of coastal communities where tsunami inundation has been modeled (highlighted Rosemary Beach, FL and North Tampa Bay, FL are developed in the current project); red hatched areas are geological landslide sources; blue hatched areas are Probabilistic Submarine Landslide (PSL) sources; yellow dots are locations of numerical wave gauges. The zero-meter elevation contour is drawn to show the GOM coastline.

While high-resolution tsunami inundation studies have been completed for these 22 communities and are planned for additional locations, vulnerability assessments are still essential for coastal locations where inundation studies have not yet been performed or planned, or where there is a lack of high-resolution bathymetric and/or elevation data. Therefore, we aim to extend the results of the completed mapping studies in order to provide estimates of tsunami inundation zones for hazard mitigation efforts in unmapped locations. Inundation maps with even low resolution are useful to emergency managers to create first-order evacuation maps, and some methods currently exist to provide low-resolution estimates of hazard zones for regions which do not currently have or warrant high-resolution maps. For example, guidance given by the National Tsunami Hazard Mitigation Program (NTHMP) Mapping and Modeling Subcommittee in "Guidelines and Best Practices to Establish Areas of Tsunami Inundation for Non-modeled or Low-hazard Regions" (available from `https://nws.weather.gov/nthmp/documents/3nonmodeledregionguidelines.pdf`) recommends that coastal areas and areas along ocean-connected waterways that are below 10 m (33 ft) elevation are at risk for most tsunamis, and rare and large tsunamis may inundate above this elevation. However, in low-lying coastal regions such as along the Gulf Coast, the 10 m (33 ft) elevation contour is too far inland to be reasonably applicable for estimating potential tsunami inundation zones. The guidance additionally suggests that low-lying areas are prone to inundation within 3 km (1.9 mi) inland for locally-generated tsunamis and within 2 km (1.3 mi) inland for distant sources. While these distances may be reasonable for some regions of the Gulf Coast, prevalent bathymetric and topographic features such as barrier islands/peninsulas complicate the method of delineating inundation-prone areas based on distance from the shoreline. As a result, the purpose of the current work is to improve the methodology which compares modeled tsunami inundation to modeled/predicted hurricane storm surge. Specifically, we aim to identify the hurricane category which produces modeled maximum storm surge that best approximates the maximum tsunami inundation in the two new locations modeled in this project. Even though many physical aspects of storm surge inundation are completely different from those of tsunamis (time scale, triggering mechanism, inundation process, etc.), good agreement or clear trends between tsunami and storm surge flooding on a regional scale can be used to provide first-order estimates of potential tsunami inundation in communities where detailed inundation maps have not yet been developed or are not possible due to unavailability of high-resolution bathymetry/elevation data. Additionally, since tsunamis are not well-understood as a threat along the Gulf Coast, while hurricane hazards are well-known, this method of predicting tsunami inundation from storm surge provides a way for GOM emergency managers to better prepare for potential tsunami events based on more understandable and accessible information. This hurricane-tsunami comparison was first carried out in Horrillo et al. [2016] (award number NA14NWS4670049) where five previously mapped locations were studied, namely South Padre Island, TX, Galveston, TX, Mobile, AL, Panama City, FL, and Tampa, FL; then as a regular procedure for all the newly mapped locations during the following mapping projects.

Past tsunamis have shown that the maritime community requires additional information and guidance about tsunami hazards and post-tsunami recovery [Wilson et al., 2012, 2013]. To accomplish mapping and modeling activities to meet NTHMP's planning/response purposes for the maritime community and port emergency management and other customer

requirements, it is necessary to continue the process to include maritime products in our current inundation map development. These activities will include tsunami hazard maritime products generated by GOM's tsunami sources (submarine landslides) that may impact specifically ship channels, bay inlets, harbors, marinas, and oil infrastructures (e.g., designated lightering and oil tanker waiting zones), which has already been applied in other tsunami risk regions, e.g., California, Oregon and Washington. It is worth noting that Galveston was the first city where we implemented the maritime products [Horrillo et al., 2016]. South Padre Island, TX, Mobile, AL, Panama City, FL, and Tampa, FL, Pensacola, FL, Key West, FL, Okaloosa County, FL, Santa Rosa County, FL and Mustang Island, TX, were implemented in project NA15NWS4670031 and NA16NWS4670039 [Horrillo et al., 2017], and then as a regular procedure for all the newly mapped locations during the following mapping projects.

2.2 Regional and Historical Context

All the locations and cities mentioned in the following regional context are in Florida, so the shortcut FL will be omitted from here on.

Rosemary Beach, FL

This mapping area covers the coastal communities from Miramar Beach to Panama City Beach, with Grayton Beach, Seaside, Seacrest, and Rosemary Beach in between. This study area was selected for this project to fill in the gap between Destin to the west and Panama City & Mexico Beach to the east, which were investigated in Horrillo et al. [2017, 2016], respectively.

Unlike its adjacent coastal communities like Santa Rosa Island & Destin to the west and Panama City to the East, the Rosemary Beach mapping area features widening barrier island from Miramar Beach to Graton Beach and coasts gradually merged to the mainland at Seaside, Seacrest, and Rosemary Beach. This can be seen on the project overview figure (1) between Okaloosa County, FL and Panama City, FL. The state highway 98 passes through the whole area, which is connected to the mainland via State Road 293 (Mid-Bay Bridge), State Road 331, and State Road 79, from west to east, which can be used for evacuation in case of emergencies.

Similar to most Florida coastal communities, the population of the studying area saw a growth in the last decade. Miramar Beach (Walton County) had a population of 8,002 in 2020 up from 6,146 in 2010. Rosemary Beach's population is 14,551 according to the U.S. Census Bureau. Laguna Beach (Bay County) population was 3,932 at the 2010 census. Between 2020 and 2021, the population of Panama City Beach saw a 40.3% increase from 12,747 to 17,882.

Hurricane Michael, the first Category 5 hurricane to hit the contiguous United States since 1992, made landfall near Mexico Beach, Florida, on October 10, 2018. Originating as a tropical depression in the Caribbean Sea, it rapidly intensified in the Gulf of Mexico, reaching Category 5 status with peak winds of 160 mph. The storm caused at least 74 deaths, including 59 in the U.S. and 15 in Central America, with an estimated $25.1 billion

in damages. Panama City Beach experienced significant storm surge, with surge inundation exceeding 5.3 feet along the coast. The area also faced severe roof and siding damage, due to gusts reaching 87 mph. Marinas and boats docked in port were almost entirely destroyed. The overall impact on Panama City Beach included damage to structures, vehicles, and infrastructure, highlighting the severity of the hurricane in this coastal area of Bay County.

Hurricane Dennis, a major storm during the 2005 Atlantic hurricane season, formed in July and briefly held the record for the strongest Atlantic hurricane before August. Making landfall twice in Cuba as a Category 4 hurricane and later hitting the Florida Panhandle as a Category 3, it caused 88 fatalities and $3.98 billion in damages, with $2.5 billion occurring in the United States. Dennis followed closely after Hurricane Ivan in the same region. The worst property damage from Hurricane Dennis transpired in Walton County to Wakulla County, resulting in the destruction of 1,000 homes. The coastal areas, particularly in Walton, Bay, Gulf, Franklin, and Wakulla counties, experienced significant beach erosion as a consequence of the storm.

North Tampa Bay, FL

Encompassing the Hernando Beach in southern Hernando County, the coastal stretch from all of Pasco County, and Clearwater Beach and Belleair Beach (and the immediate mainland portions) in Pinellas County, this mapping area joins the Tampa Bay mapping area done in Horrillo et al. [2016], making all of southern Florida populated GOM coastal communities mapped for tsunami inundation.

The North Tampa Bay study area features barrier island system in the Pinellas County portion and open coasts in the northern parts. State Hwy 19 is the main road running along the coastline through the study area. In case of hurricanes or tsunamis, Hernando Beach can reach the mainland through Osowaw Blvd to State Hwy 19. In Pinellas County, the Clearwater Beach is connected to the mainland via Clearwater Memorial Causeway, and similarly Belleair Beach via Belleair Bridge.

Hernando Beach has a 2024 population of 2,558. Hernando Beach is currently declining at a rate of annually and its population has increased by 2.08% since the most recent census, which recorded a population of 2,506 in 2020. The coastal communities in Pasco County, FL, including Hudson, Bayonet Point, Jasmine Estates, Port Richey, New Port Richey, New Port Richey East, Elfers, Beacon Square, Key Vista, and Holiday, had a total population of 135,304 in 2024, up from a total population of 139,694 in 2020. Among the coastal communities in Pasco County, FL, Port Richey experienced the highest positive growth rate at 17.3The coastal communities in Pinellas County, FL, including Tarpon Springs, Palm Harbor, Dunedin, Clearwater, and Belleair Beach, had a total population of 242,680 in 2024, up from a total population of 242,383 in 2020.

Hurricane Idalia, a Category 4 storm in August 2023, originated from a low-pressure area crossing Central America and gradually intensified while meandering in the western Caribbean. Upgraded to a tropical storm on August 27, it underwent rapid intensification in the Gulf of Mexico, reaching Category 4 status briefly before making landfall in Florida's Big Bend region at Category 3 strength on August 30. The hurricane maintained its intensity through Northern Florida and Southeast Georgia, transitioning into a tropical storm over

the Carolinas. The storm caused significant damage, particularly in Florida, with record-breaking storm surge and a tornado outbreak, resulting in four storm-related deaths and estimated insured losses between $2.2–5 billion. Hurricane Idalia caused substantial damage across Hernando, Pasco, and Pinellas counties in Florida. In Pasco County, approximately 2,000 homes suffered damage as up to 5 feet of water inundated structures, leading to around 150 rescues. Two fatal traffic accidents occurred in Pasco and Alachua counties due to hazardous driving conditions. Hernando Beach experienced storm surge hindering firefighters from reaching a burning unoccupied house, necessitating neighbors to attempt containment with garden hoses. In Pinellas County, Tampa Bay and Clearwater witnessed over 3 feet of storm surge, while waves damaged the northbound side of the Howard Frankland Bridge, partially flooding it. At least 75 people were rescued near St. Petersburg, and widespread power outages affected over 278,000 customers.

Hurricane Irma was a powerful Category 5 hurricane in September 2017 followed by Hurricane Maria two weeks later. It became the most powerful hurricane in the open Atlantic at the time until surpassed by Hurricane Dorian in 2019. Irma caused extensive devastation in the northeastern Caribbean and the Florida Keys, being the third-strongest Atlantic hurricane at landfall. Irma originated near the Cape Verde Islands, rapidly intensifying into a Category 5 storm with sustained winds of 180 mph. It resulted in at least 134 deaths across various regions, making it a highly impactful and widely searched event in 2017. In Pinellas County during Hurricane Irma, gusts of up to 96 mph caused widespread damage, leaving 63% of the county without power. Severe damage to homes in Clearwater amounted to over $1.3 million, with an overall countywide estimate of $594.45 million. Two fatalities were reported, including an indirect fatality during cable wire repairs. Pasco County experienced winds ranging from 69 to 81 mph, leaving 37% without power. Heavy rainfall led to major flooding, causing about $8.16 million in damage, including significant losses to citrus crops. One indirect fatality occurred as a man evacuating crashed into a tree. Hernando County faced winds of 39 to 58 mph, resulting in widespread damage to homes and significant power outages. Heavy rainfall led to flooding along the Withlacoochee River, causing about $5 million in damage. The county saw 26 homes or businesses destroyed and one indirect fatality due to storm-related accidents.

2.3 Summary

Although the probability of a large-scale tsunami event in the GOM is low, this and previous studies have indicated that tsunami events with characteristics similar to those detailed in Horrillo et al. [2015] have the potential to cause severe flooding and damage to GOM coastal communities that is similar to or even greater than that seen from major hurricanes, particularly in open beach and barrier island regions. Tsunami hazard maritime products such as tsunami current magnitude, vorticity, safe/hazard zones would be central for future developments of maritime hazard maps, maritime emergency response as well as infrastructure planning. The results of this work are intended to provide guidance to local emergency managers to help with managing urban growth, evacuation planning, and public education with the vision to mitigate potential GOM tsunami hazards.

This report is organized as follows. Section 3 briefly describes all 9 landslide sources used

for tsunami modeling (3.1) and the numerical models used for simulations (3.2). Section 4 covers the inundation and momentum flux maps for Rosemary Beach, FL and North Tampa Bay, FL. The comparison between tsunami inundation and hurricane storm surge inundation (tsunami inundation in terms of hurricane category) is given in Section 5 for the two new Gulf Coast communities. Current velocity and vorticity maps are described in Section 6 for the two new communities.

3 Tsunami Inundation Modeling

3.1 Landslide Tsunami Sources

Nine large-scale landslide configurations were created assuming an unstable (gravity-driven) sediment deposit condition. Five of these landslide configurations are geological events identified by ten Brink et al. [2009b]: the Eastbreaks, Mississippi Canyon, and West Florida submarine landslides; and Chaytor et al. [2016]: the Yucatán #3 and Yucatán #5 landslides, which are shown as red hatched regions in Fig. 1. The Yucatán Shelf/Campeche Escarpment was the last remaining area of the GOM that had not been evaluated for landslide tsunami hazards, until high-resolution mapping data collected in 2013 [Paull et al., 2014] shows that the Yucatán Shelf/Campeche Escarpment margin has been subjected to intense modifications by Cenozoic mass wasting processes. Although no known tsunami events have been linked to these Yucatán sources, numerical modeling result shows that they are capable of generating tsunamis that could propagate throughout the GOM Basin [Chaytor et al., 2016]. The other four were obtained using a probabilistic methodology based on work by Maretzki et al. [2007] and Grilli et al. [2009] and extended for the GOM by Pampell-Manis et al. [2016]. The probabilistic landslide configurations were determined based on distributions of previous GOM submarine landslide dimensions through a Monte Carlo Simulation (MCS) approach. The MCS methodology incorporates a statistical correlation method for capturing trends seen in observational data for landslide size parameters while still allowing for randomness in the generated landslide dimensions. Slope stability analyses are performed for the MCS-generated trial landslide configurations using landslide and sediment properties and regional seismic loading (Peak Horizontal ground Acceleration, PHA) to determine landslide configurations which fail and produce a tsunami. The probability of each tsunamigenic failure is calculated based on the joint probability of the earthquake PHA and the probability that the trial landslide fails and produces a tsunami wave above a certain threshold. Those failures which produce the largest tsunami amplitude and have the highest probability of occurrence are deemed the most extreme probabilistic events, and the dimensions of these events are averaged to determine maximum credible probabilistic sources. The four maximum credible Probabilistic Submarine Landslides (PSLs) used as tsunami sources for this study are termed PSL-A, PSL-B1, PSL-B2, and PSL-C and are shown as blue hatched regions in Fig. 1. For a more complete discussion of GOM submarine landslide sources, the reader can consult Horrillo et al. [2015, 2018], Pampell-Manis et al. [2016].

Table 1: Submarine Landslide general information.

Submarine Landslide	Location (Lon, Lat)	Age/Recurrence (Years)	Area (km^2)	Volume (km^3)	Excavation Depth (m)	Modeled Volume (km^3)
East Breaks	-95.68, 27.70	$\sim 10000 - 25000$	~ 519.52	~ 21.95	~ 160	26.7
Mississippi	-90.00, 28.60	$\sim 7500 - 11000$	~ 3687.26	~ 425.54	~ 300	425
West Florida	-84.75, 25.95	> 10000	~ 647.57	~ 16.2	~ 150	18.4
Yucatán #3	-90.07, 23.00	–	~ 578	~ 38	~ 278	39.3
Yucatán #5	-89.80, 23.54	–	~ 1094	~ 70.2	~ 385	69.5
PSL-A	-94.30, 27.98	$\sim 7700 - 7800$	~ 1686	~ 57	~ 67	58
PSL-B1	-91.56, 28.05	$\sim 5400 - 5500$	~ 3118	~ 69	~ 44	57.3
PSL-B2	-91.01, 26.17	$\sim 4700 - 4800$	~ 282	~ 45	~ 323	68
PSL-C	-87.20, 28.62	$\sim 550 - 650$	~ 1529	~ 315	~ 404	357

3.2 Numerical Models

For the nine landslide tsunami sources considered here, tsunami wave development and subsequent propagation and inundation of coastal communities was modeled using coupled 3D and 2D numerical models [Horrillo et al., 2015]. The tsunami generation phase was modeled using the 3D model TSUNAMI3D [Horrillo, 2006, Horrillo et al., 2013], which solves the finite difference approximation of the full Navier-Stokes equations and the incompressibility (continuity) equation. Water and landslide material are represented as Newtonian fluids with different densities, and the landslide-water and water-air interfaces are tracked using the Volume of Fluid (VOF) method of Hirt and Nichols [1981], which is simplified to account for the large horizontal/vertical aspect ratio of the tsunami wave and the selected computational cell size required to construct an efficient 3D grid. The pressure term is split into hydrostatic and non-hydrostatic components. Although TSUNAMI3D has the capability of variable grids, the nesting capability necessary for modeling detailed inundation of coastal regions is too computationally intensive within the fully 3D model; thus, detailed inundation modeling is achieved by coupling the 3D model to a 2D model. Once the tsunami wave generated by the 3D model is fully developed, the wave is passed as an initial condition to the 2D model for modeling wave propagation and coastal inundation. The generated wave is considered fully developed when the total wave energy (potential plus kinetic) reaches a maximum and before the wave leaves the computational domain, as discussed in López-Venegas et al. [2015]. The 2D model used here is NEOWAVE [Yamazaki et al., 2008], a depth-integrated and non-hydrostatic model built on the nonlinear shallow water equations which includes a momentum-conserved advection scheme to model wave breaking and two-way nested grids for modeling higher-resolution wave runup and inundation. Propagation and inundation are calculated via a series of nested grids of increasing resolution, from 15 arcsecond (450 m) resolution for a domain encompassing the entire northern GOM (Fig. 1), to finer resolutions of 3 arcseconds (90 m, from NOAA NCEI Coastal Relief Models), 1 arcsecond (30 m), and 1/3 arcsecond (10 m, from NOAA NCEI Tsunami Inundation Digital Elevation Models [DEMs]) to model detailed inundation of the most populated/ inundation-prone areas of each coastal community. The 3 arcsecond (90 m) subdomains encompassing each coastal community studied here are shown by red rectangles in Fig. 1.

4 Tsunami Maps

Tsunami inundation depth and extent has been modeled for two selected coastal communities: Rosemary Beach, FL and Tampa Bay North, FL. Inundation (flooding) is determined by subtracting land elevation from water elevation, and elevations used are in reference to the Mean High Water (MHW) tidal datum. For this study, the tsunami inundation depth/extent modeled for each community is the maximum-of-maximums (MOM) inundation, which is calculated as the maximum inundation depth from an ensemble of inundation depths produced by each of the nine tsunami sources considered. That is, once inundation in a community has been modeled for each of the nine sources, the overall maximum inundation depth in each computational grid cell is taken as the MOM tsunami inundation in that cell. This approach gives a worst-case scenario of estimated tsunami inundation for each coastal community.

In this section, the numerical results (inundation and momentum flux maps) for each landslide source are presented for Rosemary Beach, FL and Tampa Bay North, FL. The MOM inundation map from all sources and the maximum inundation map by source are also shown. A summary table of each location's numerical gauge (at an approximate water depth of 20 m) shows maximum wave amplitude and arrival time after each landslide failure.

It is worth noting, however, that for both communities, the MOM tsunami inundation is produced solely by the Mississippi Canyon submarine landslide failure. That geological failure is the largest in both area and volume of material removed, and therefore produces the highest amplitude wave of all sources simulated.

4.1 Rosemary Beach, FL

Table 2: Maximum tsunami wave amplitude and corresponding arrival time after landslide failure at Rosemary Beach, FL (same as Okaloosa County, FL gauge) numerical wave gauge: 30°14'45.00"N, 87°12'30.00"W (Fig. 1), approximate water depth 21 m.

Tsunami Source	Maximum Wave Amplitude (m)	Arrival Time After Landslide Failure (hr)
East Breaks	0.28	2.9
PSL-A	0.41	2.5
PSL-B1	0.43	1.7
PSL-B2	0.35	1.9
Mississippi Canyon	4.38	1.2
PSL-C	1.82	1.1
West Florida	0.40	1.8
Yucatán #3	0.58	2.1
Yucatán #5	0.34	2.2

RosemaryBeach, FL
East Breaks submarine landslide
Maximum Momentum Flux

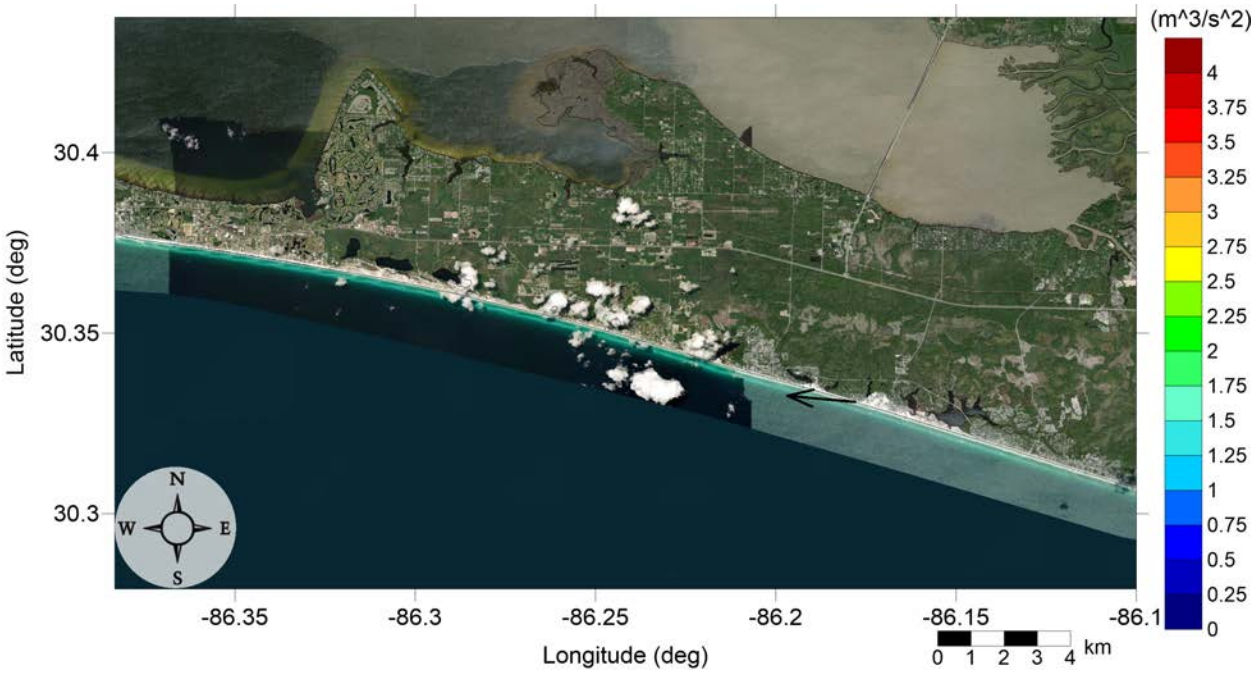

Figure 2: Maximum momentum flux (m^3/s^2) caused by the East Breaks submarine landslide in Miramar Beach, FL. Arrows represent direction of maximum momentum flux. Contour drawn is the zero-meter contour for land elevation.

RosemaryBeach, FL
East Breaks submarine landslide
Maximum Momentum Flux

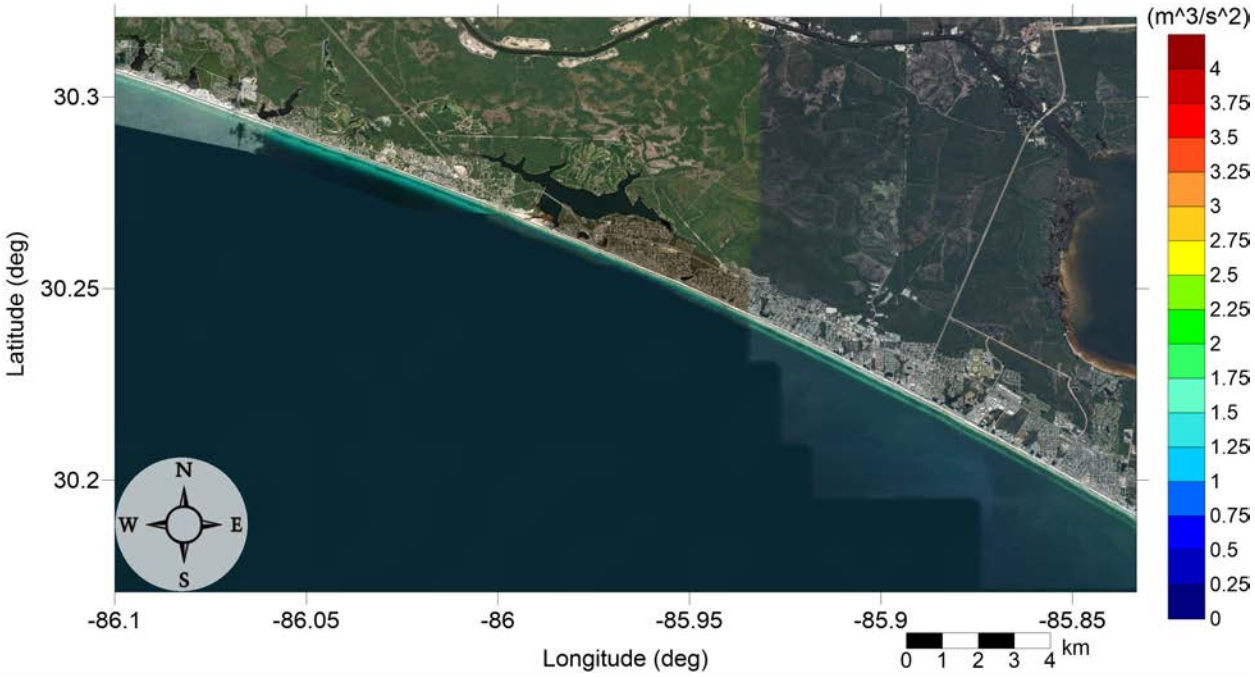

Figure 3: Maximum momentum flux (m^3/s^2) caused by the East Breaks submarine landslide in Panama City Beach, FL. Arrows represent direction of maximum momentum flux. Contour drawn is the zero-meter contour for land elevation.

RosemaryBeach, FL
East Breaks submarine landslide
Maximum Inundation Depth

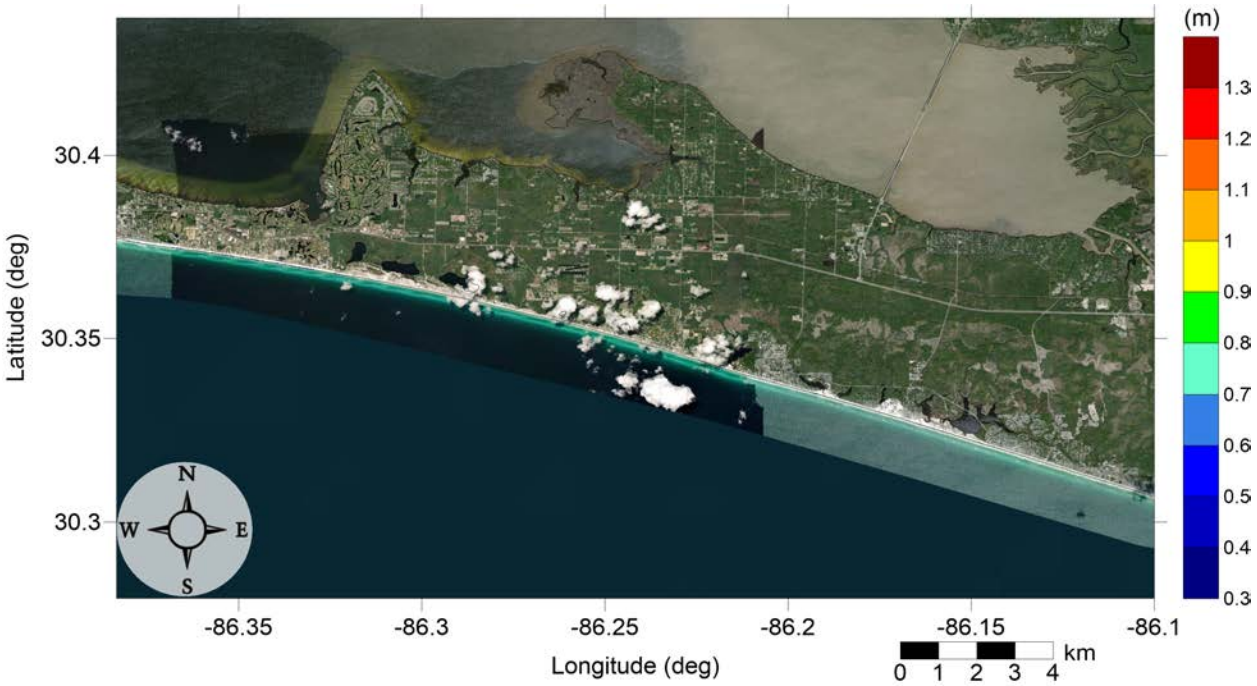

Figure 4: Maximum inundation depth (m) caused by the East Breaks submarine landslide in Miramar Beach, FL. Contour drawn is the zero-meter contour for land elevation.

RosemaryBeach, FL
East Breaks submarine landslide
Maximum Inundation Depth

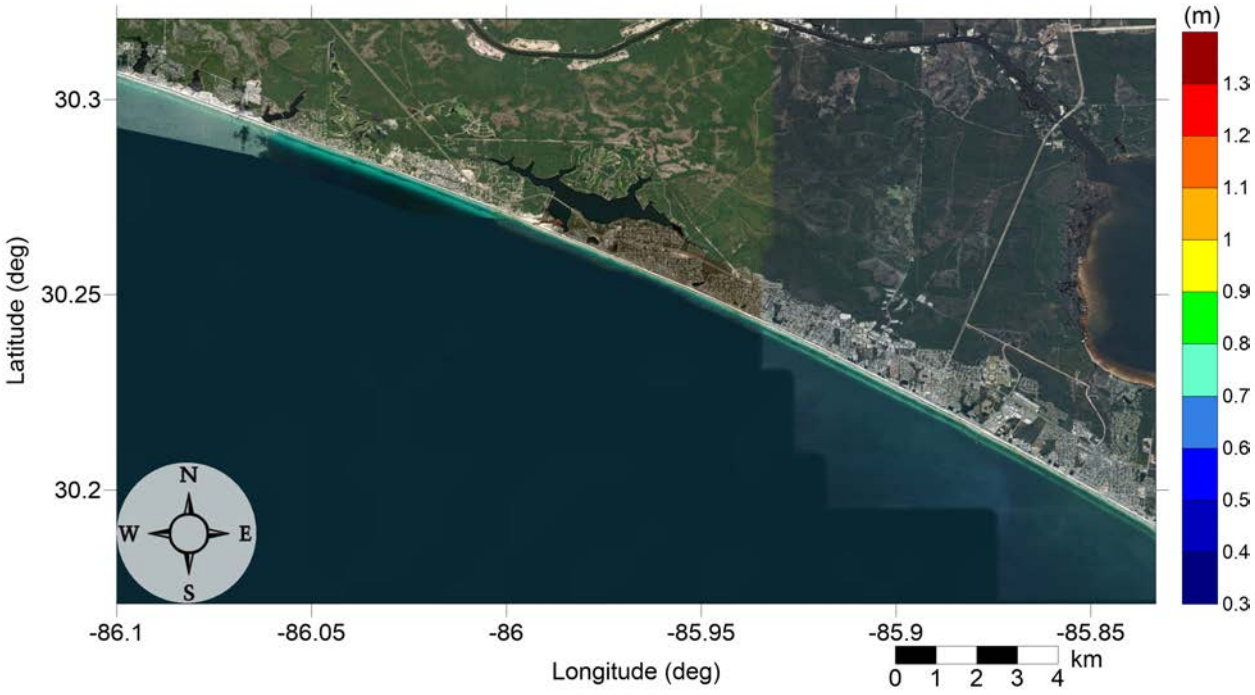

Figure 5: Maximum inundation depth (m) caused by the East Breaks submarine landslide in Panama City Beach, FL. Contour drawn is the zero-meter contour for land elevation.

RosemaryBeach, FL
Probabilistic Submarine Landslide A
Maximum Momentum Flux

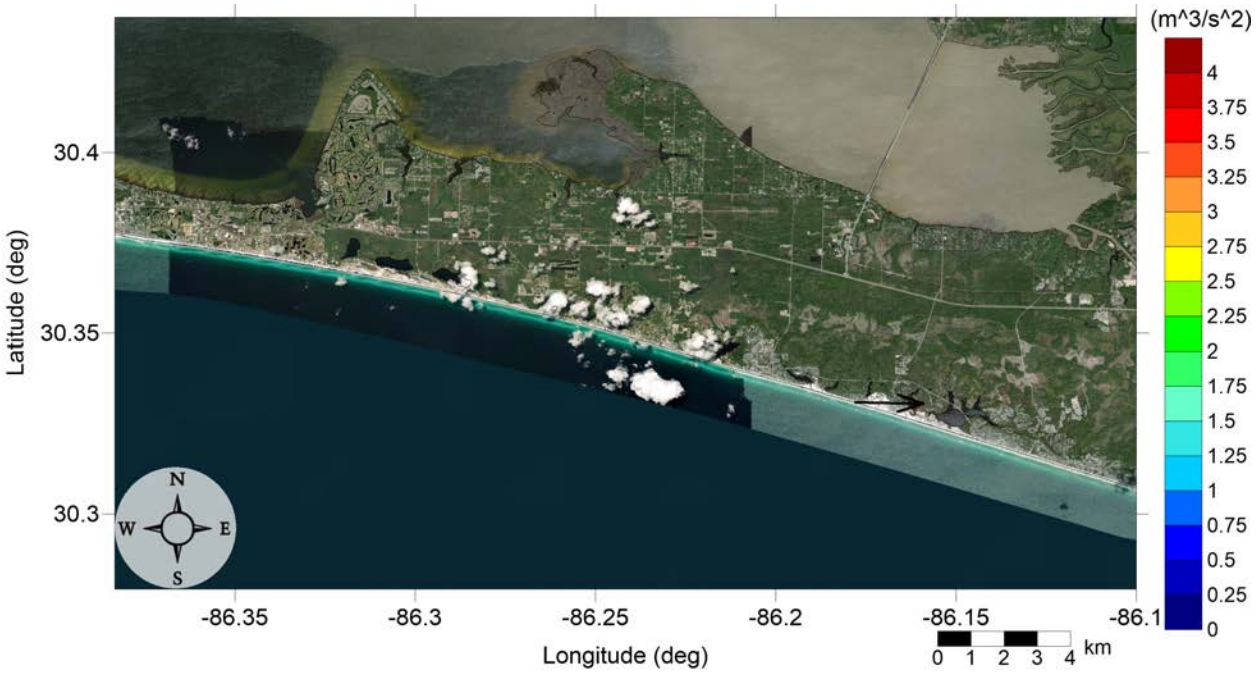

Figure 6: Maximum momentum flux (m^3/s^2) caused by the Probabilistic Submarine Landslide A in Miramar Beach, FL. Arrows represent direction of maximum momentum flux. Contour drawn is the zero-meter contour for land elevation.

RosemaryBeach, FL
Probabilistic Submarine Landslide A
Maximum Momentum Flux

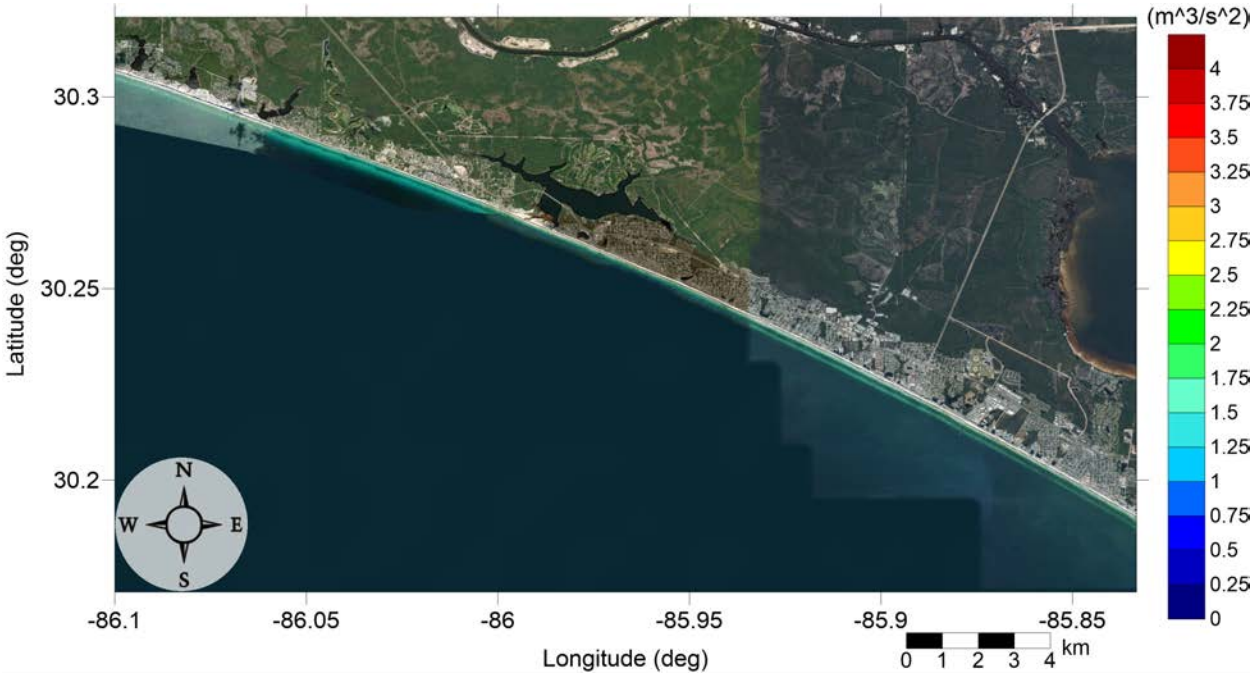

Figure 7: Maximum momentum flux (m^3/s^2) caused by the Probabilistic Submarine Landslide A in Panama City Beach, FL. Arrows represent direction of maximum momentum flux. Contour drawn is the zero-meter contour for land elevation.

RosemaryBeach, FL
Probabilistic Submarine Landslide A
Maximum Inundation Depth

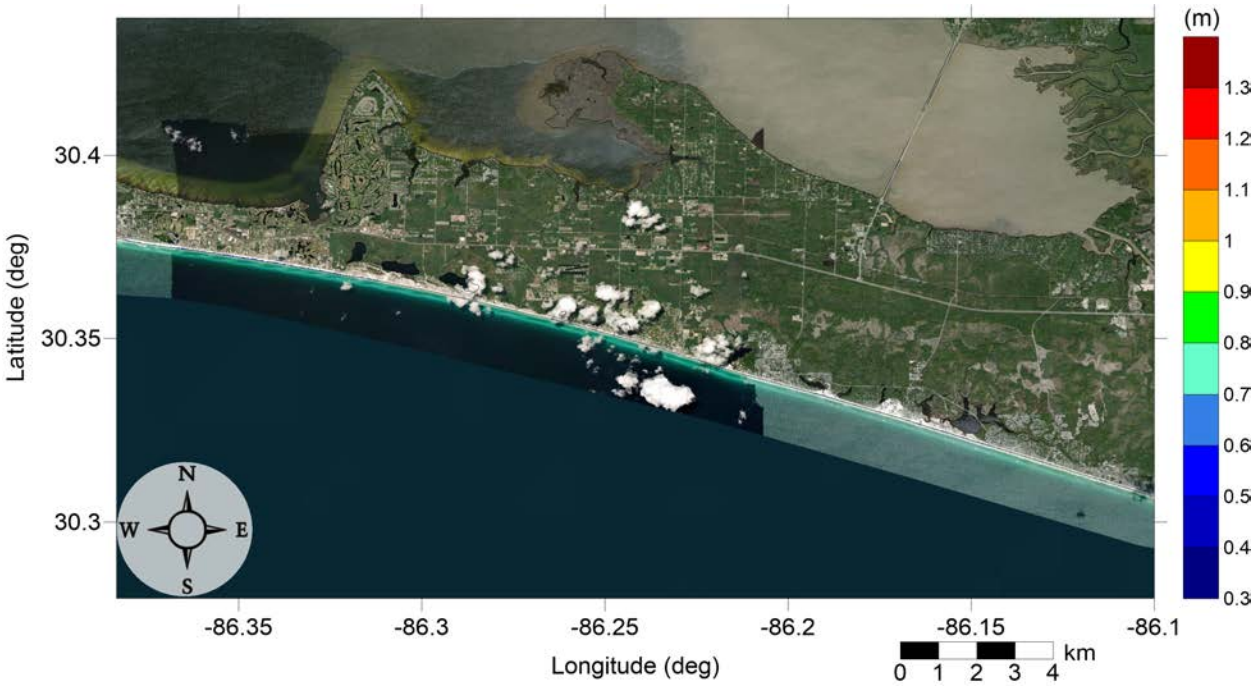

Figure 8: Maximum inundation depth (m) caused by the Probabilistic Submarine Landslide A in Miramar Beach, FL. Contour drawn is the zero-meter contour for land elevation.

RosemaryBeach, FL
Probabilistic Submarine Landslide A
Maximum Inundation Depth

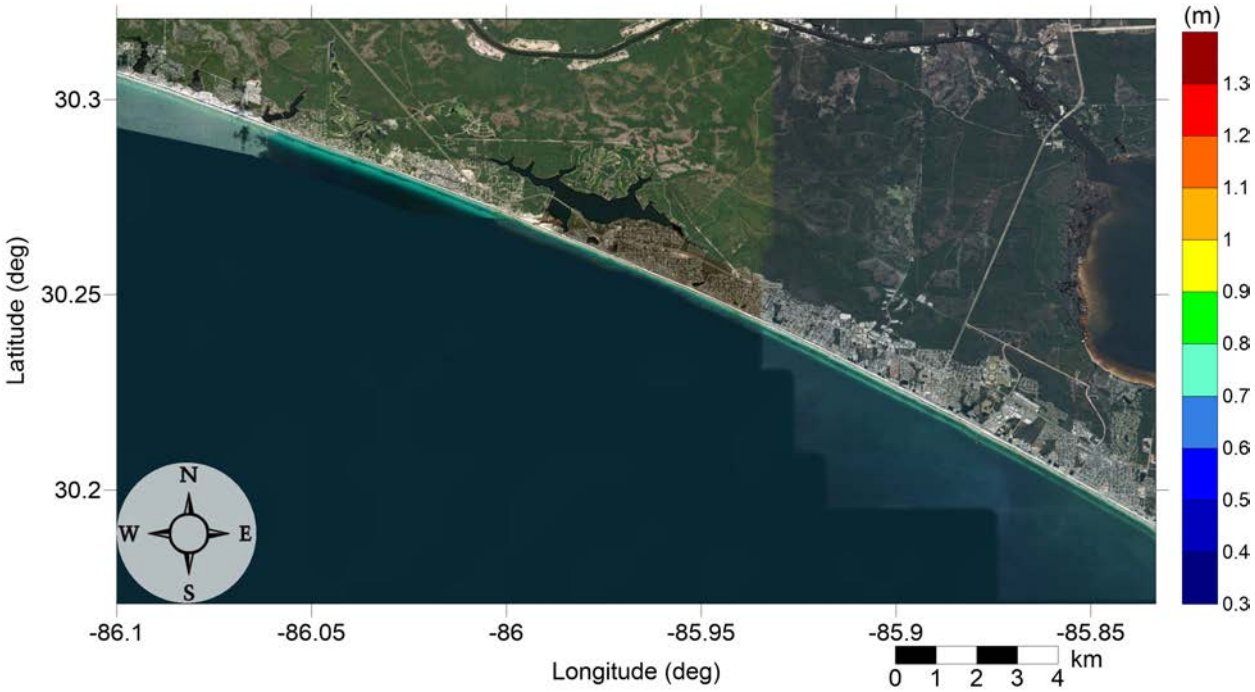

Figure 9: Maximum inundation depth (m) caused by the Probabilistic Submarine Landslide A in Panama City Beach, FL. Contour drawn is the zero-meter contour for land elevation.

RosemaryBeach, FL
Probabilistic Submarine Landslide B1
Maximum Momentum Flux

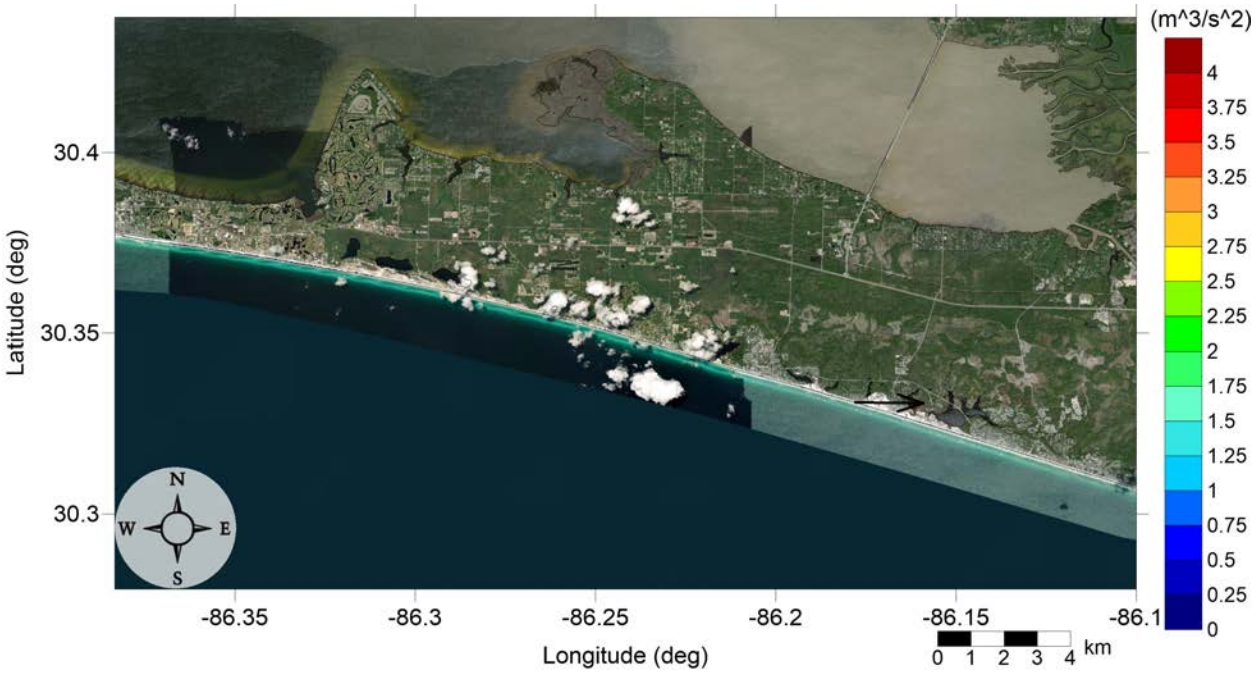

Figure 10: Maximum momentum flux (m^3/s^2) caused by the Probabilistic Submarine Landslide B1 in Miramar Beach, FL. Arrows represent direction of maximum momentum flux. Contour drawn is the zero-meter contour for land elevation.

RosemaryBeach, FL
Probabilistic Submarine Landslide B1
Maximum Momentum Flux

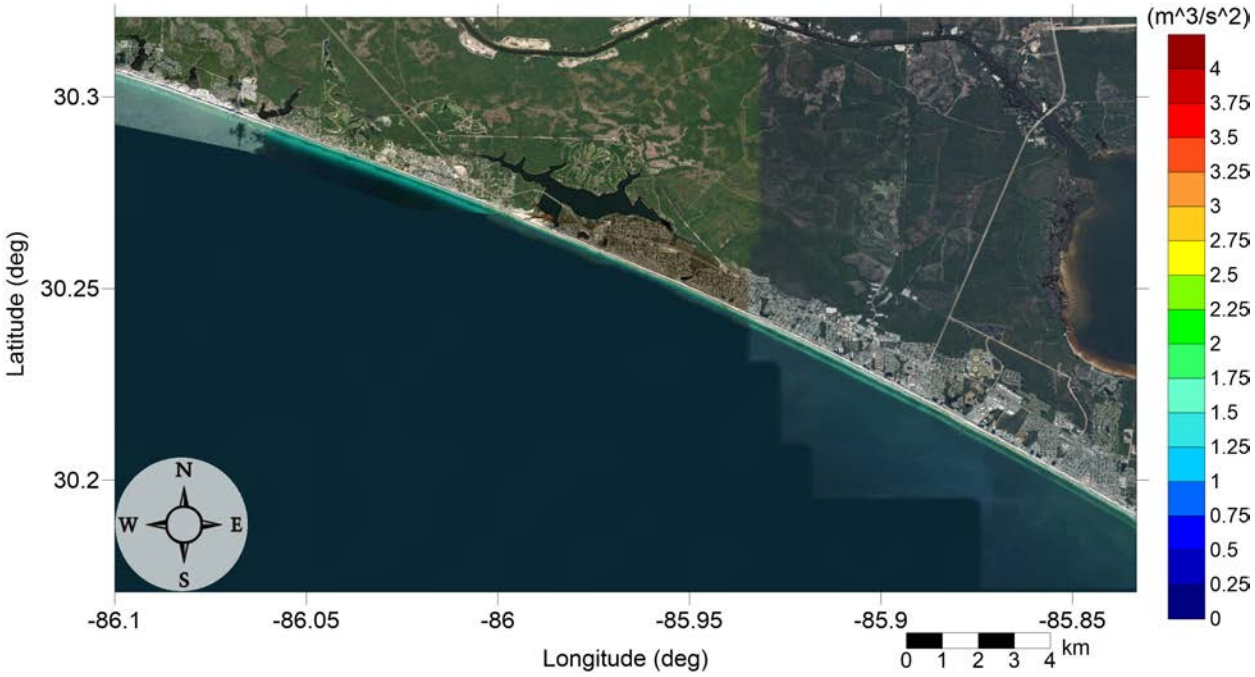

Figure 11: Maximum momentum flux (m^3/s^2) caused by the Probabilistic Submarine Landslide B1 in Panama City Beach, FL. Arrows represent direction of maximum momentum flux. Contour drawn is the zero-meter contour for land elevation.

RosemaryBeach, FL
Probabilistic Submarine Landslide B1
Maximum Inundation Depth

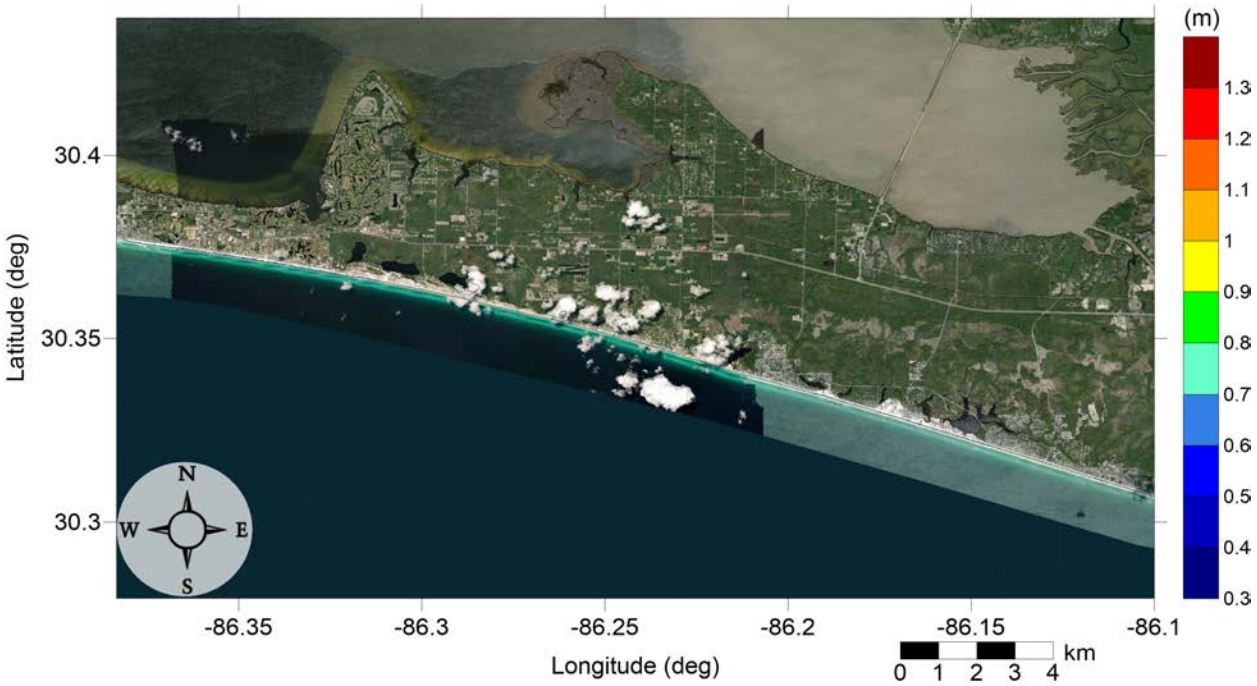

Figure 12: Maximum inundation depth (m) caused by the Probabilistic Submarine Landslide B1 in Miramar Beach, FL. Contour drawn is the zero-meter contour for land elevation.

RosemaryBeach, FL
Probabilistic Submarine Landslide B1
Maximum Inundation Depth

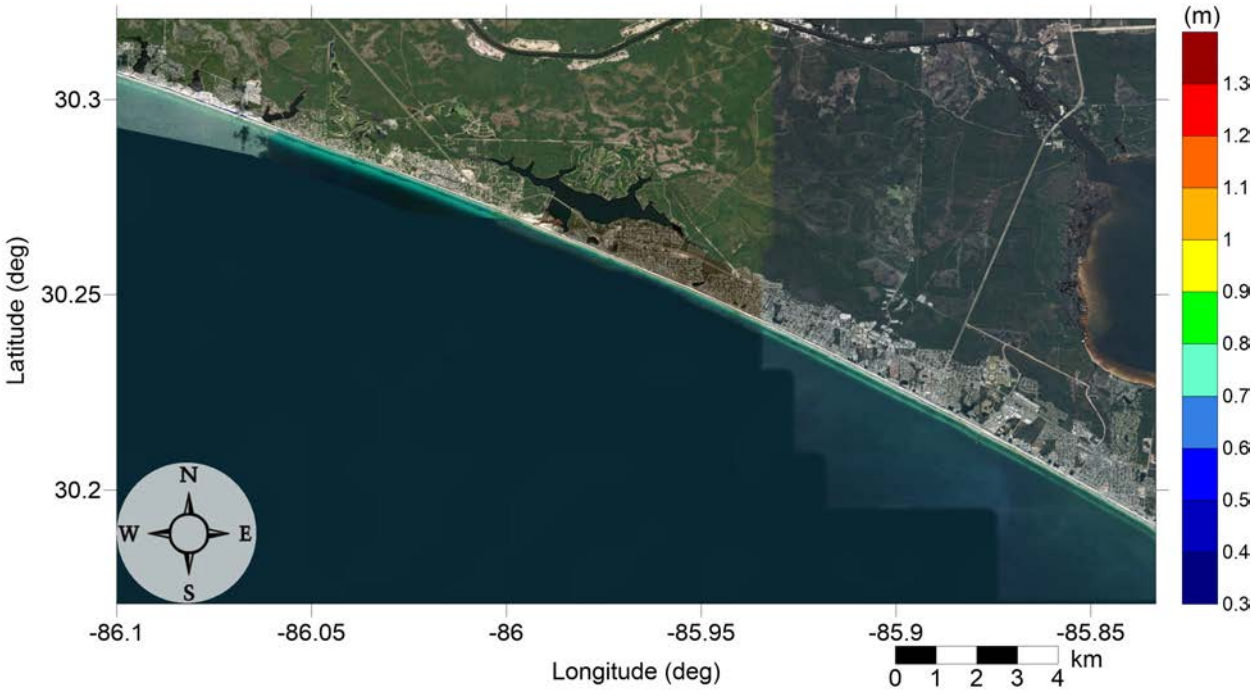

Figure 13: Maximum inundation depth (m) caused by the Probabilistic Submarine Landslide B1 in Panama City Beach, FL. Contour drawn is the zero-meter contour for land elevation.

RosemaryBeach, FL
Probabilistic Submarine Landslide B2
Maximum Momentum Flux

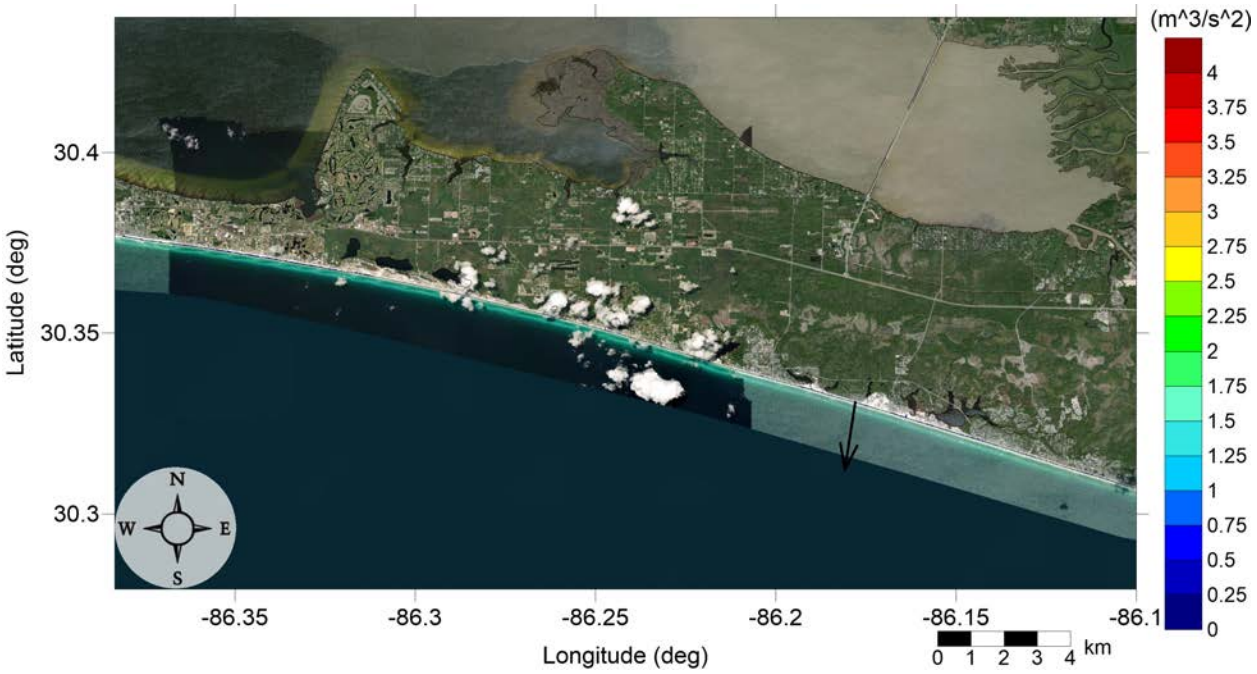

Figure 14: Maximum momentum flux (m^3/s^2) caused by the Probabilistic Submarine Landslide B2 in Miramar Beach, FL. Arrows represent direction of maximum momentum flux. Contour drawn is the zero-meter contour for land elevation.

RosemaryBeach, FL
Probabilistic Submarine Landslide B2
Maximum Momentum Flux

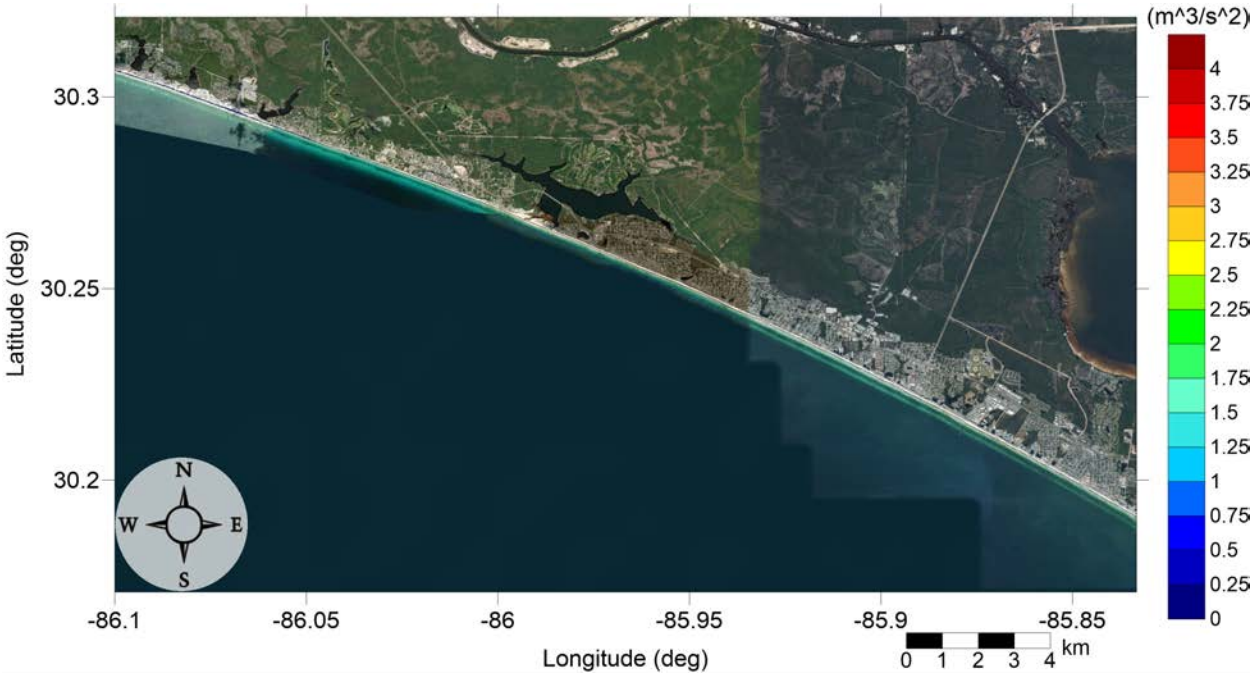

Figure 15: Maximum momentum flux (m^3/s^2) caused by the Probabilistic Submarine Landslide B2 in Panama City Beach, FL. Arrows represent direction of maximum momentum flux. Contour drawn is the zero-meter contour for land elevation.

RosemaryBeach, FL
Probabilistic Submarine Landslide B2
Maximum Inundation Depth

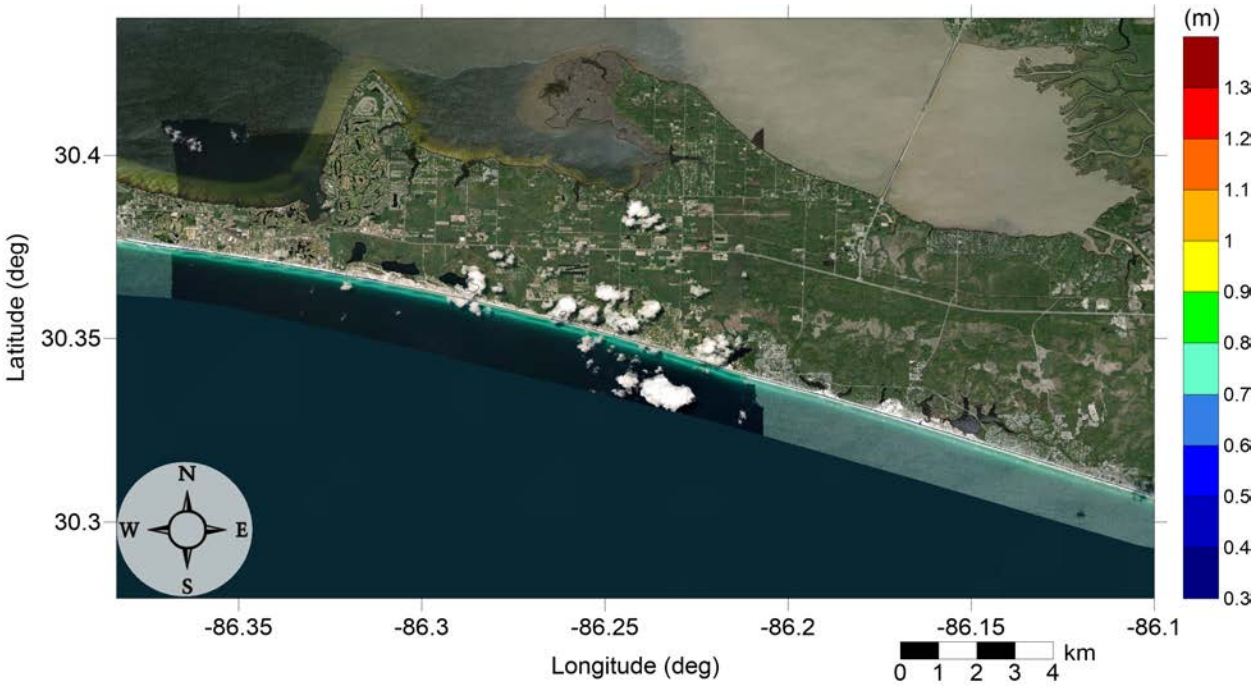

Figure 16: Maximum inundation depth (m) caused by the Probabilistic Submarine Landslide B2 in Miramar Beach, FL. Contour drawn is the zero-meter contour for land elevation.

RosemaryBeach, FL
Probabilistic Submarine Landslide B2
Maximum Inundation Depth

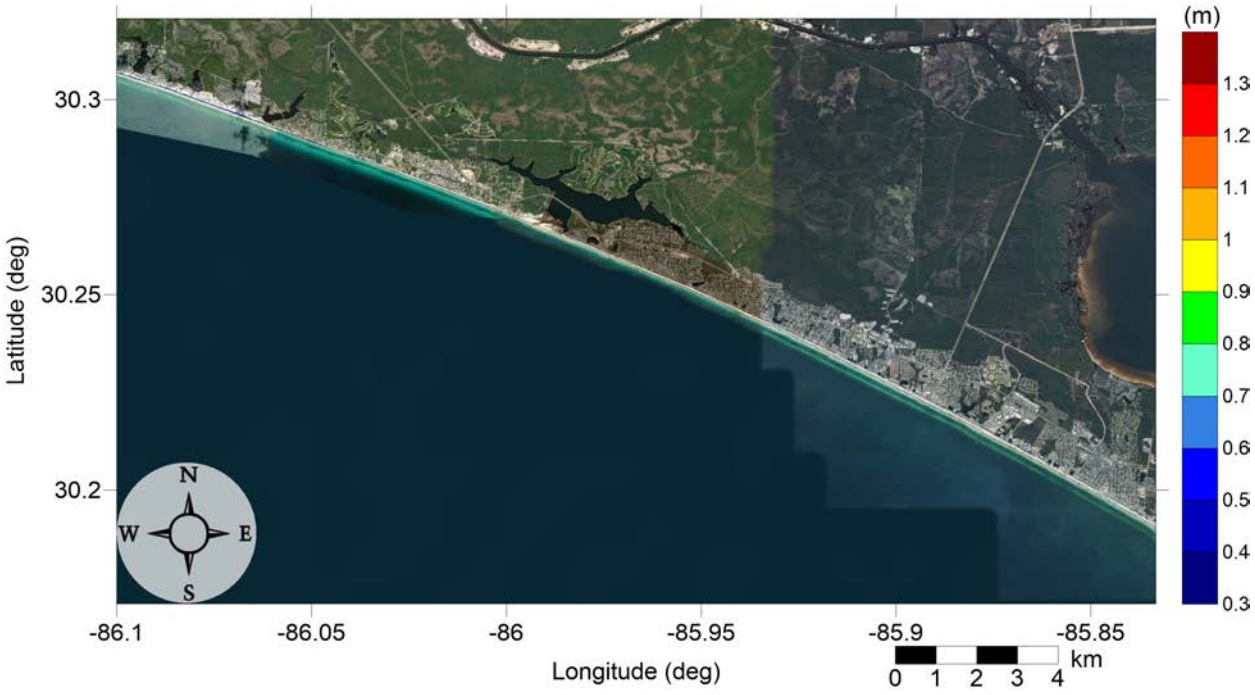

Figure 17: Maximum inundation depth (m) caused by the Probabilistic Submarine Landslide B2 in Panama City Beach, FL. Contour drawn is the zero-meter contour for land elevation.

RosemaryBeach, FL
Mississippi Canyon submarine landslide
Maximum Momentum Flux

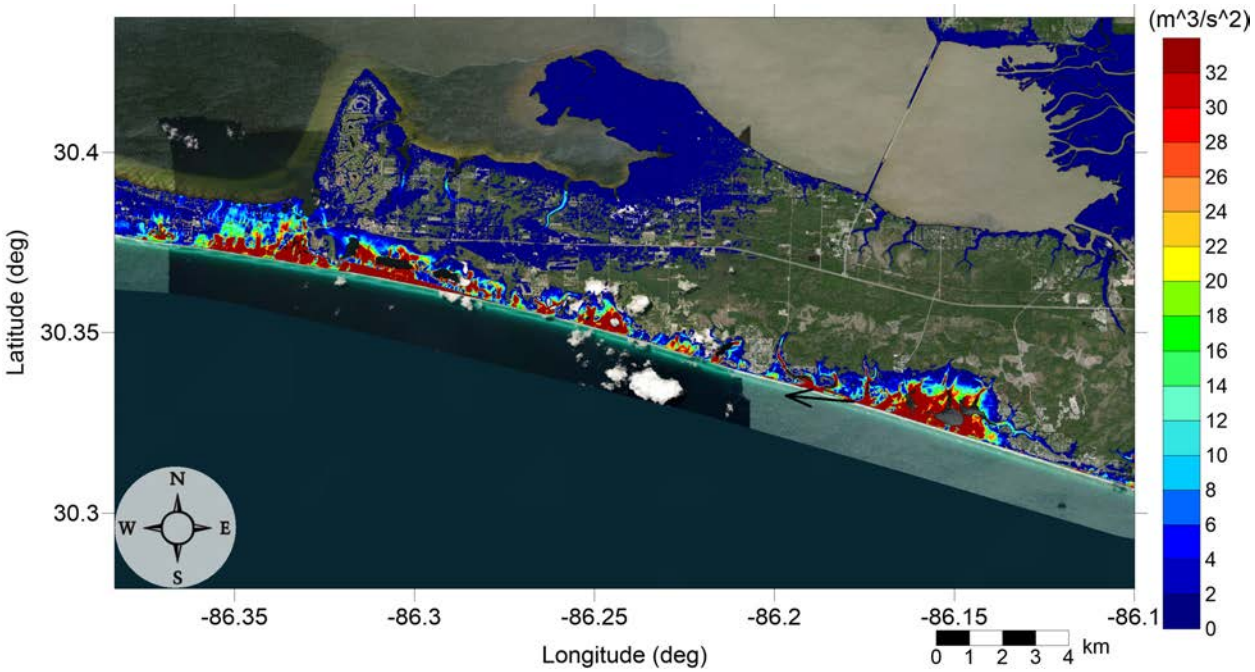

Figure 18: Maximum momentum flux (m^3/s^2) caused by the Mississippi Canyon submarine landslide in Miramar Beach, FL. Arrows represent direction of maximum momentum flux. Contour drawn is the zero-meter contour for land elevation.

RosemaryBeach, FL
Mississippi Canyon submarine landslide
Maximum Momentum Flux

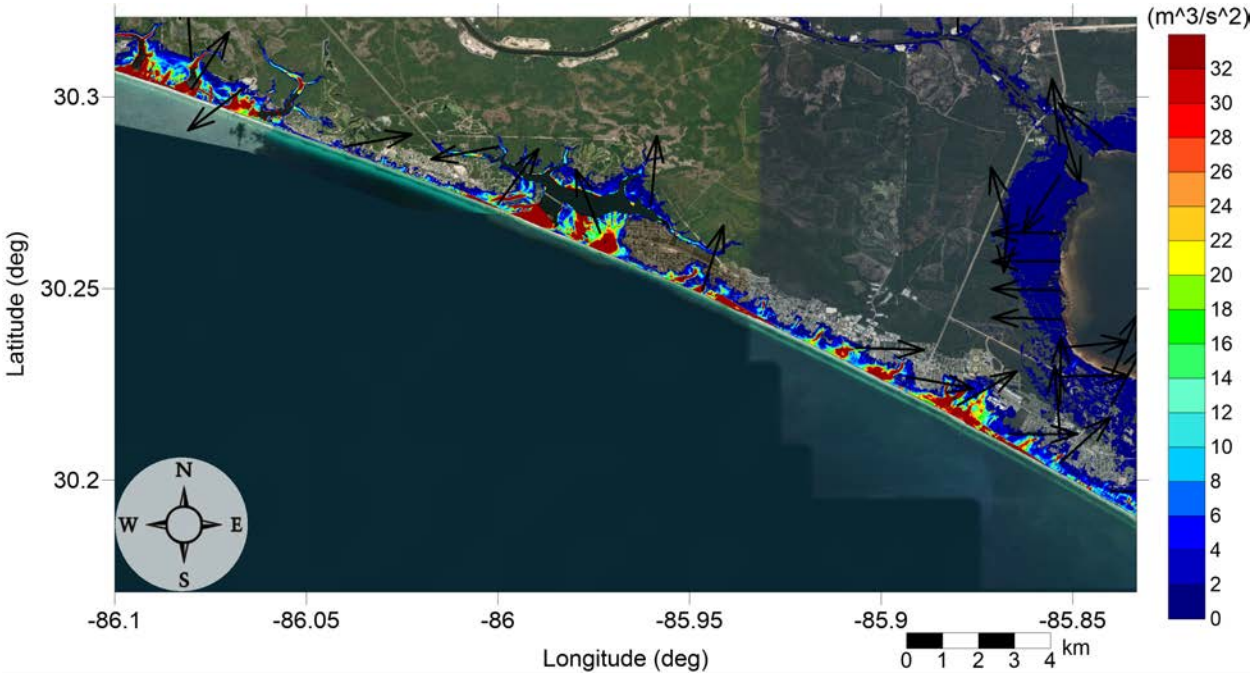

Figure 19: Maximum momentum flux (m^3/s^2) caused by the Mississippi Canyon submarine landslide in Panama City Beach, FL. Arrows represent direction of maximum momentum flux. Contour drawn is the zero-meter contour for land elevation.

RosemaryBeach, FL
Mississippi Canyon submarine landslide
Maximum Inundation Depth

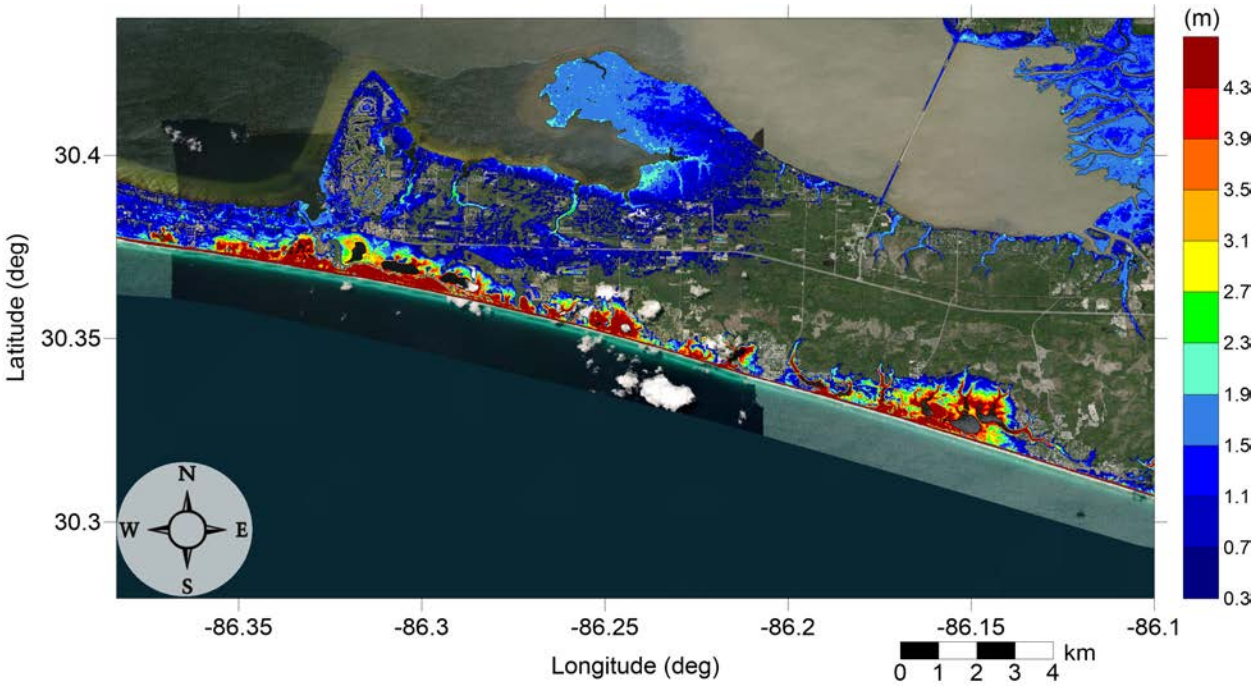

Figure 20: Maximum inundation depth (m) caused by the Mississippi Canyon submarine landslide in Miramar Beach, FL. Contour drawn is the zero-meter contour for land elevation.

RosemaryBeach, FL
Mississippi Canyon submarine landslide
Maximum Inundation Depth

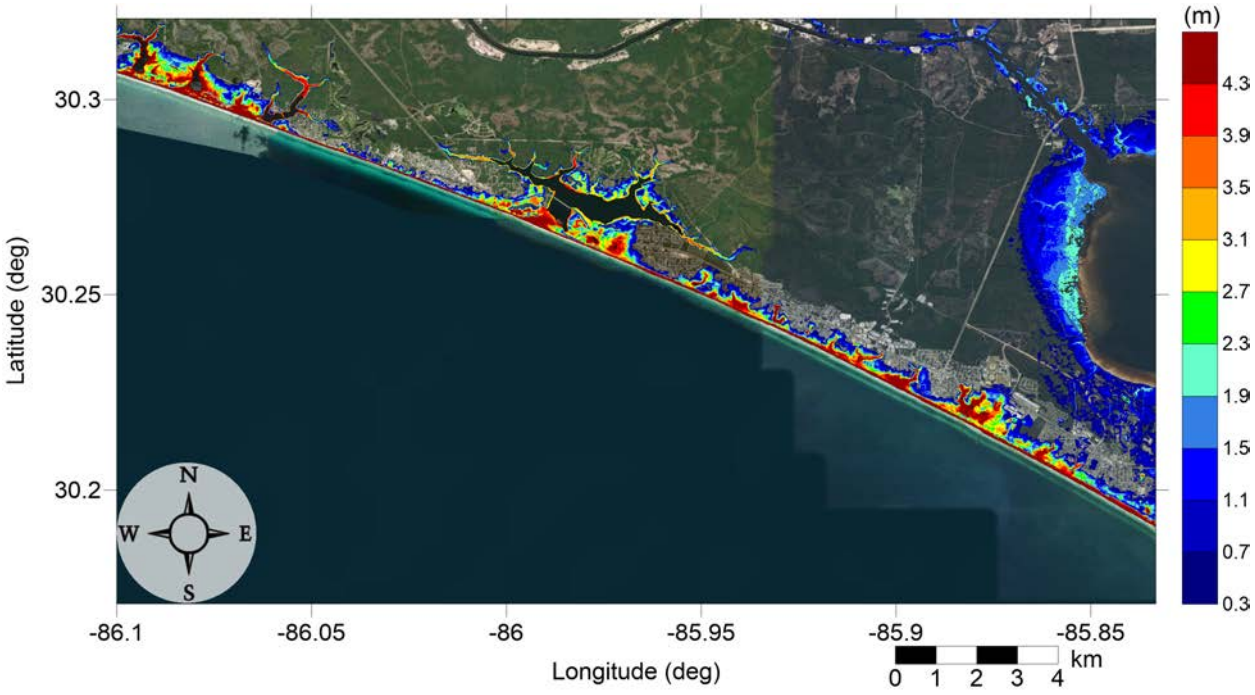

Figure 21: Maximum inundation depth (m) caused by the Mississippi Canyon submarine landslide in Panama City Beach, FL. Contour drawn is the zero-meter contour for land elevation.

RosemaryBeach, FL
Probabilistic Submarine Landslide C
Maximum Momentum Flux

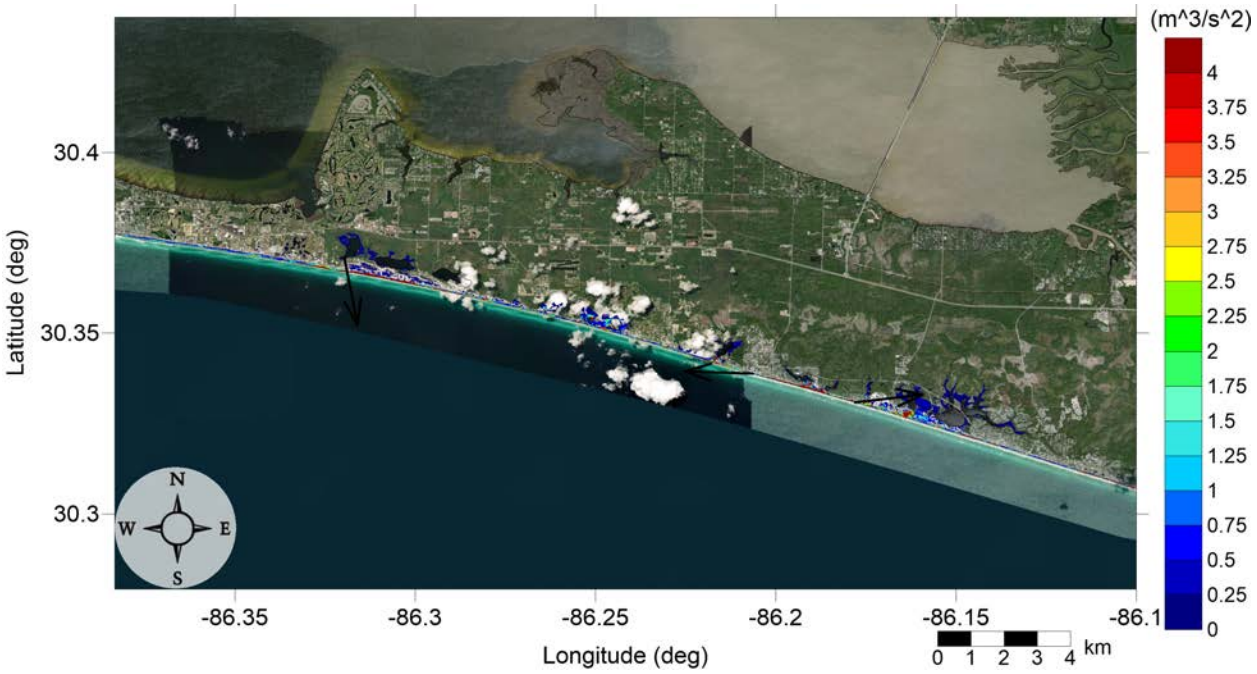

Figure 22: Maximum momentum flux (m^3/s^2) caused by the Probabilistic Submarine Landslide C in Miramar Beach, FL. Arrows represent direction of maximum momentum flux. Contour drawn is the zero-meter contour for land elevation.

RosemaryBeach, FL
Probabilistic Submarine Landslide C
Maximum Momentum Flux

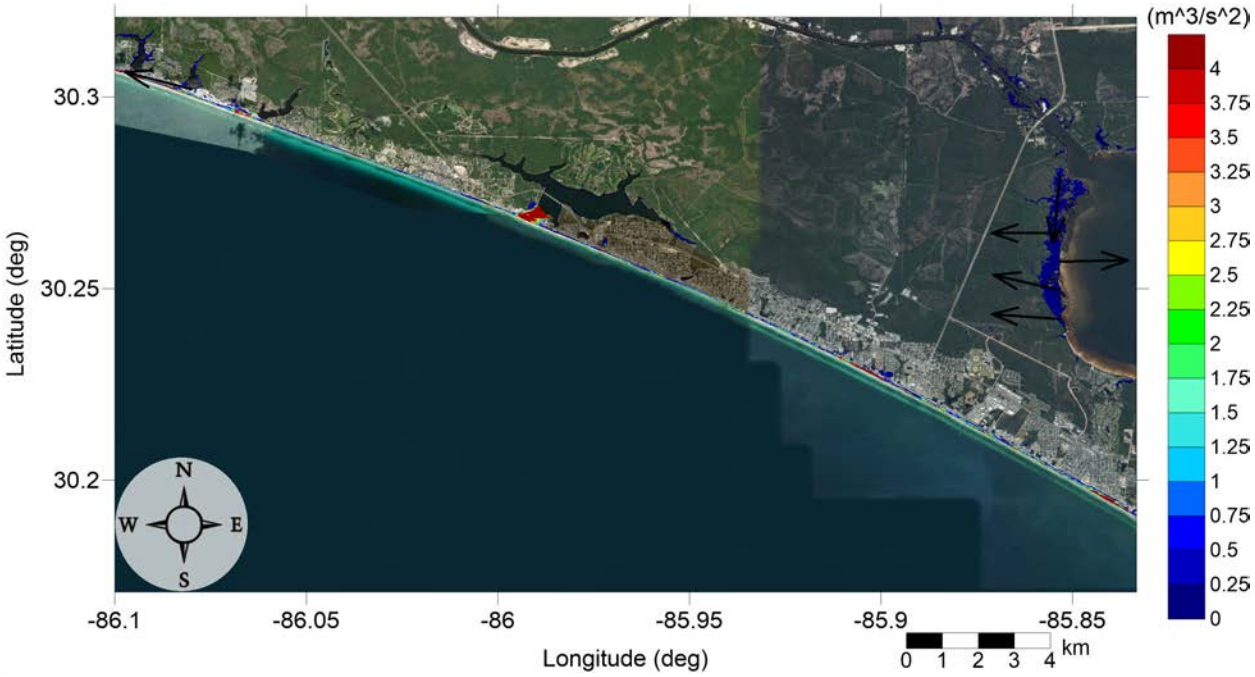

Figure 23: Maximum momentum flux (m^3/s^2) caused by the Probabilistic Submarine Landslide C in Panama City Beach, FL. Arrows represent direction of maximum momentum flux. Contour drawn is the zero-meter contour for land elevation.

RosemaryBeach, FL
Probabilistic Submarine Landslide C
Maximum Inundation Depth

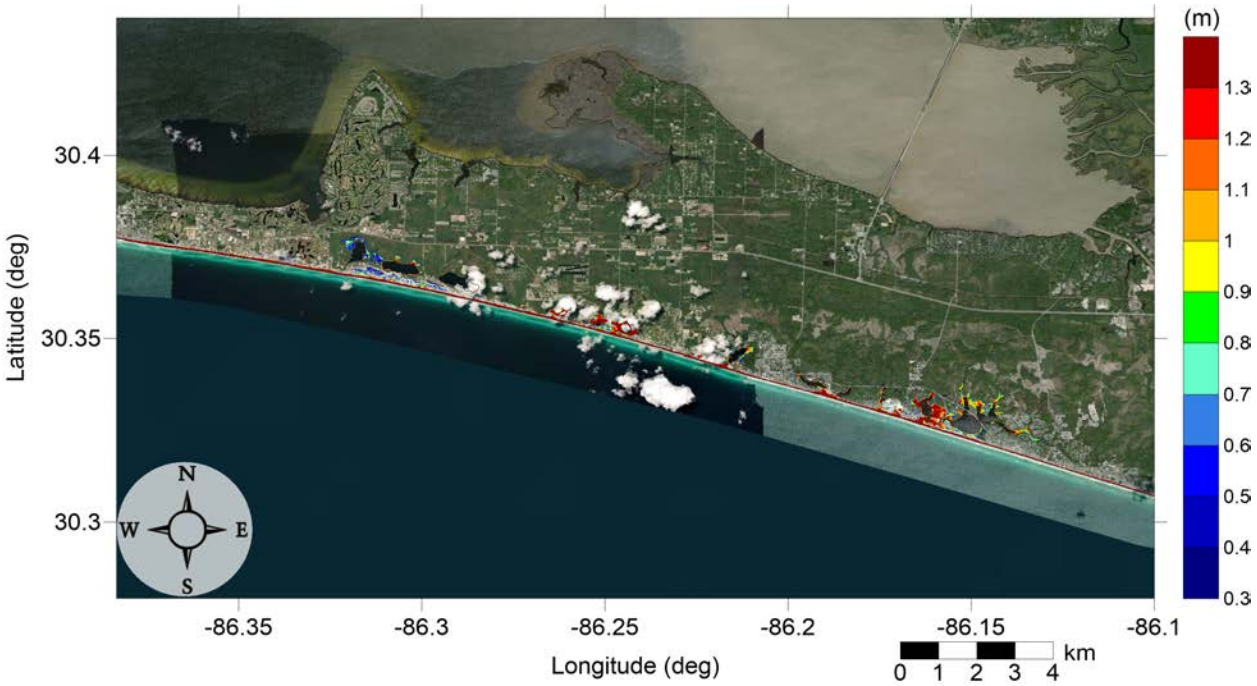

Figure 24: Maximum inundation depth (m) caused by the Probabilistic Submarine Landslide C in Miramar Beach, FL. Contour drawn is the zero-meter contour for land elevation.

RosemaryBeach, FL
Probabilistic Submarine Landslide C
Maximum Inundation Depth

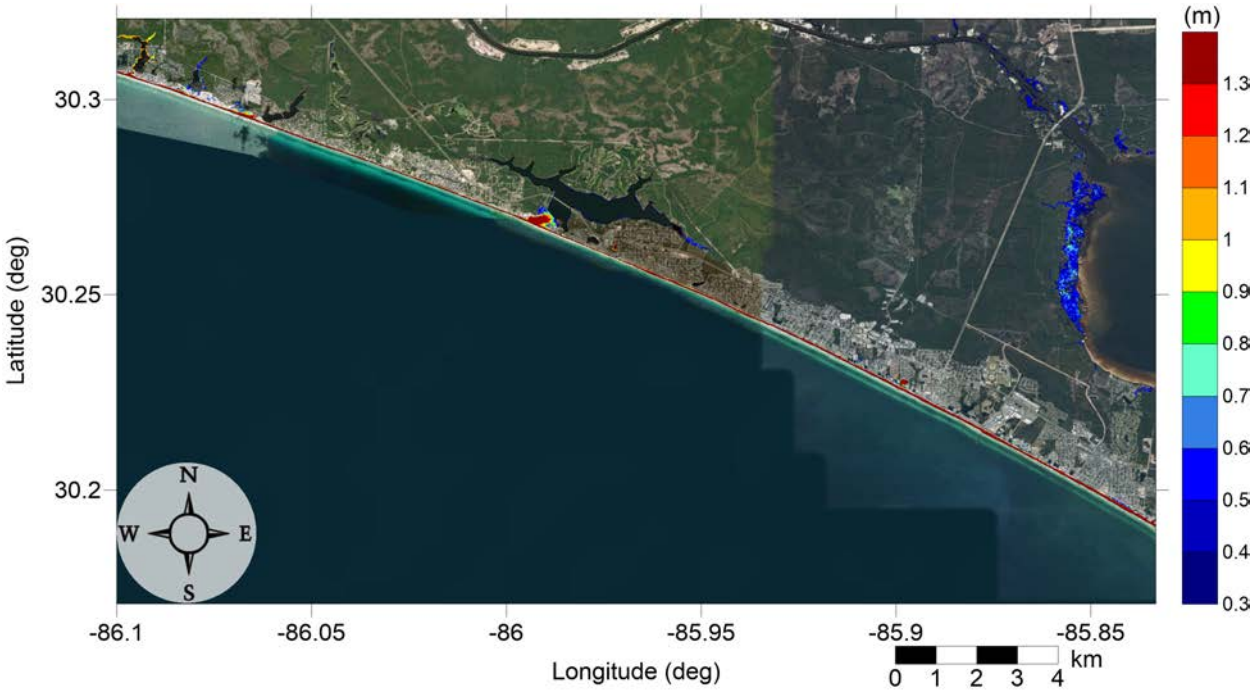

Figure 25: Maximum inundation depth (m) caused by the Probabilistic Submarine Landslide C in Panama City Beach, FL. Contour drawn is the zero-meter contour for land elevation.

RosemaryBeach, FL
West Florida submarine landslide
Maximum Momentum Flux

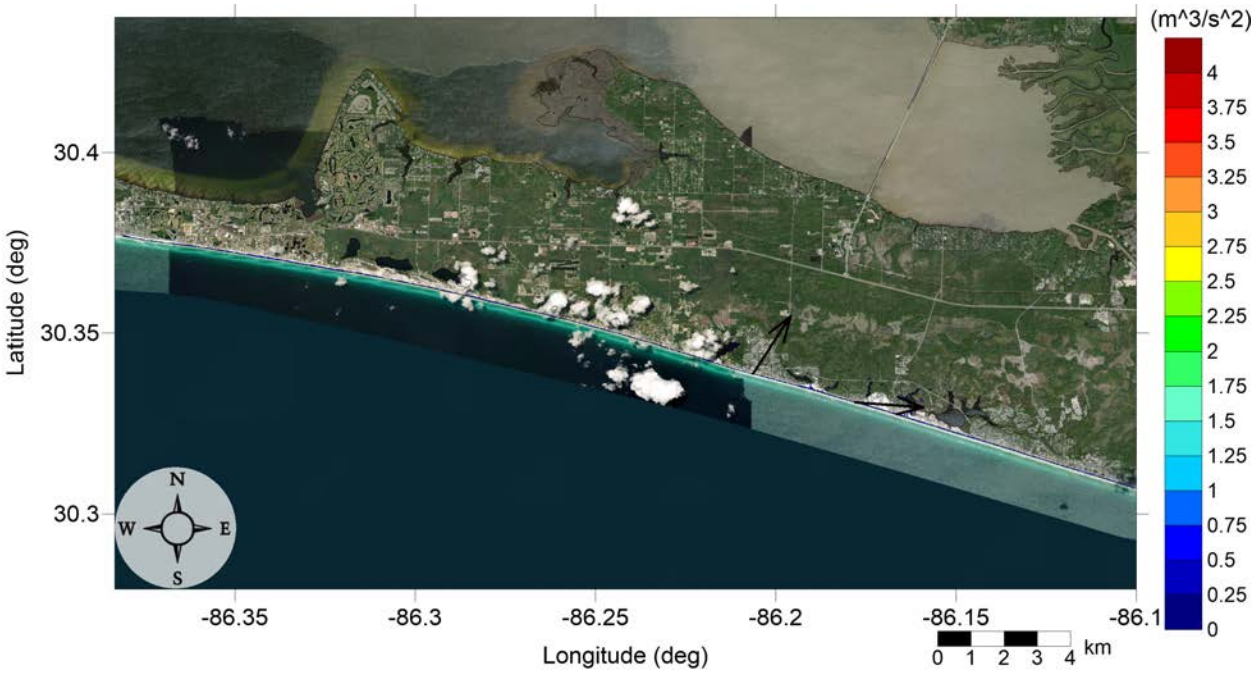

Figure 26: Maximum momentum flux (m^3/s^2) caused by the West Florida submarine landslide in Miramar Beach, FL. Arrows represent direction of maximum momentum flux. Contour drawn is the zero-meter contour for land elevation.

RosemaryBeach, FL
West Florida submarine landslide
Maximum Momentum Flux

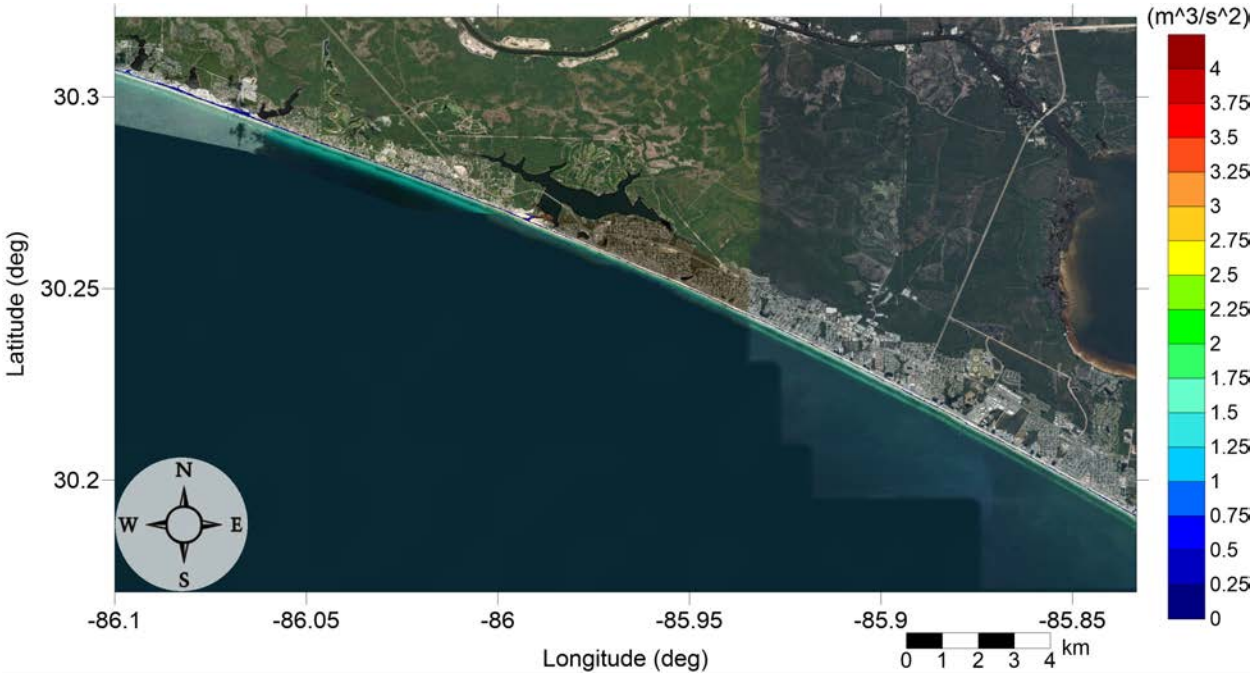

Figure 27: Maximum momentum flux (m^3/s^2) caused by the West Florida submarine landslide in Panama City Beach, FL. Arrows represent direction of maximum momentum flux. Contour drawn is the zero-meter contour for land elevation.

RosemaryBeach, FL
West Florida submarine landslide
Maximum Inundation Depth

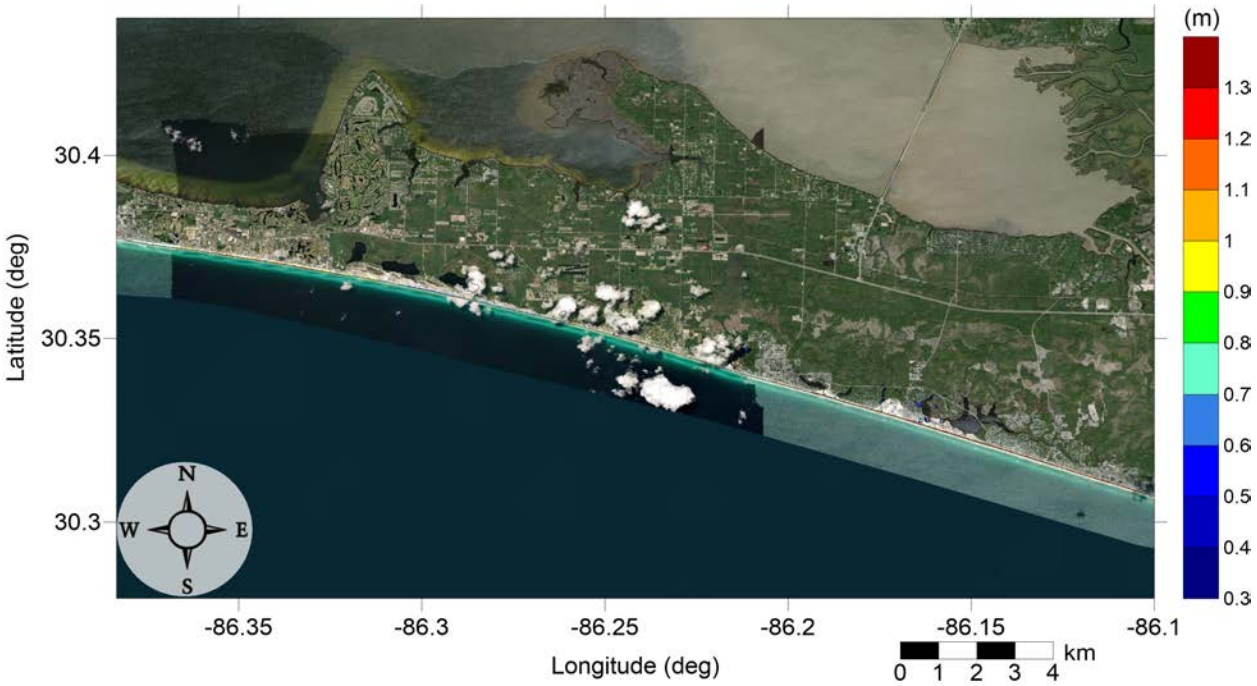

Figure 28: Maximum inundation depth (m) caused by the West Florida submarine landslide in Miramar Beach, FL. Contour drawn is the zero-meter contour for land elevation.

RosemaryBeach, FL
West Florida submarine landslide
Maximum Inundation Depth

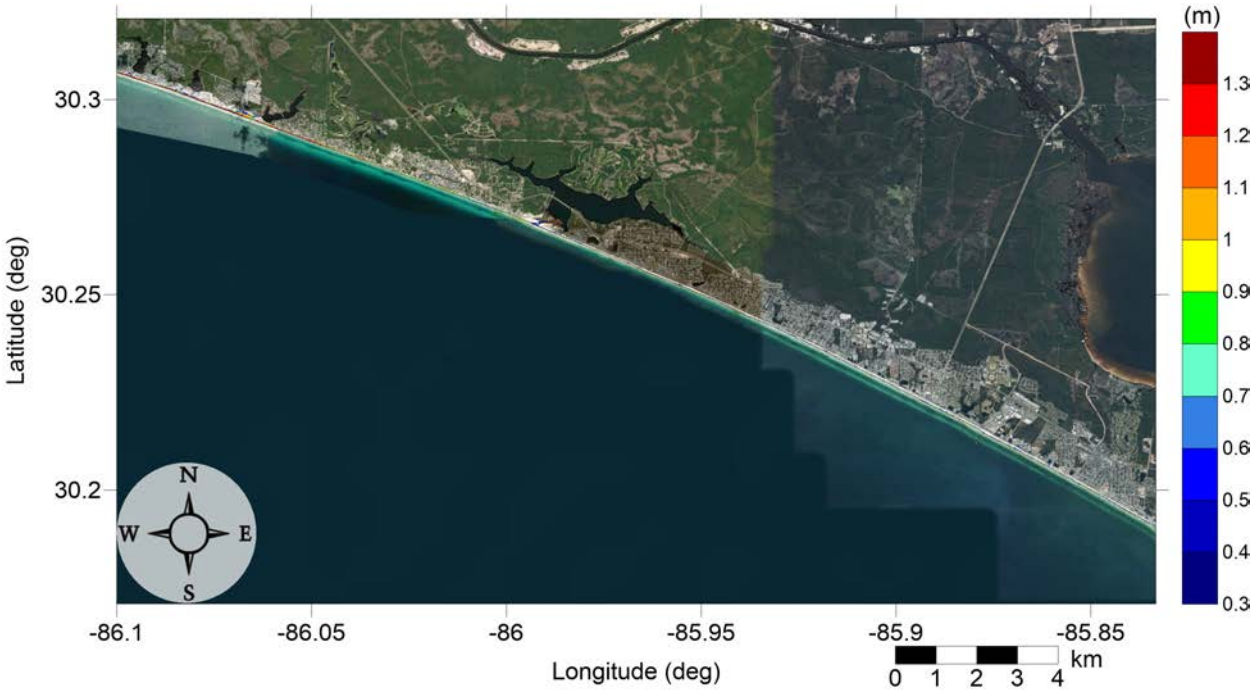

Figure 29: Maximum inundation depth (m) caused by the West Florida submarine landslide in Panama City Beach, FL. Contour drawn is the zero-meter contour for land elevation.

RosemaryBeach, FL
Yucatán 3 submarine landslide
Maximum Momentum Flux

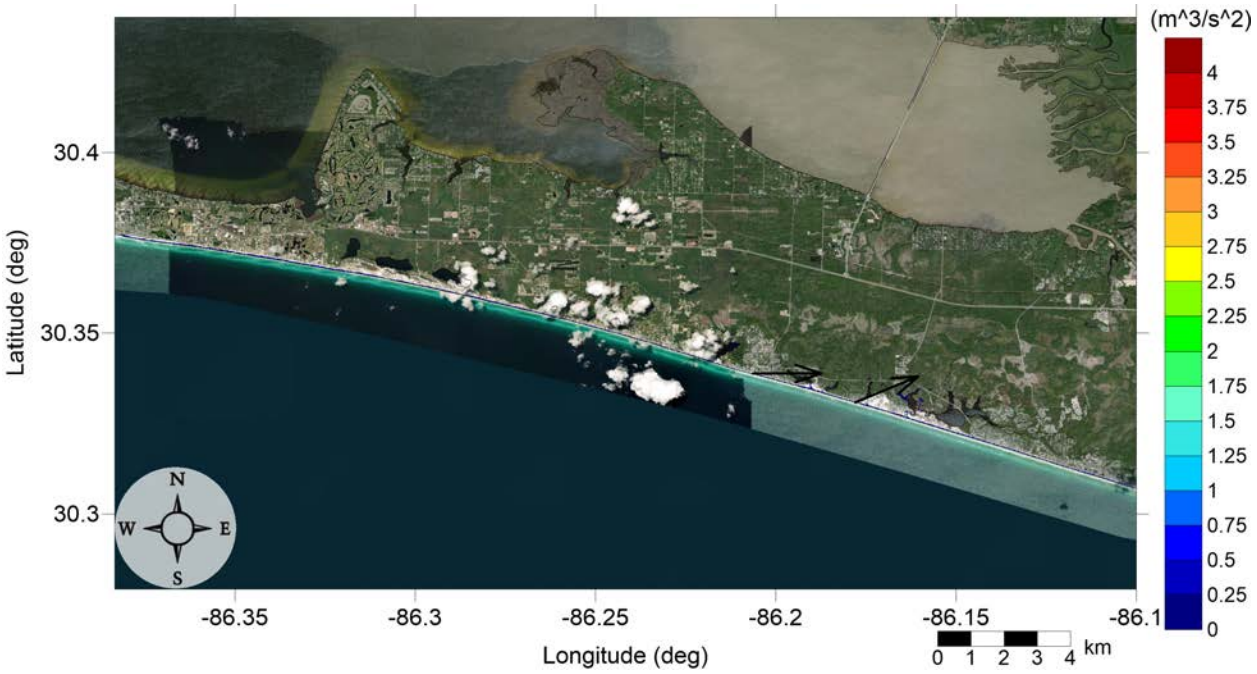

Figure 30: Maximum momentum flux (m^3/s^2) caused by the Yucatán 3 submarine landslide in Miramar Beach, FL. Arrows represent direction of maximum momentum flux. Contour drawn is the zero-meter contour for land elevation.

RosemaryBeach, FL
Yucatán 3 submarine landslide
Maximum Momentum Flux

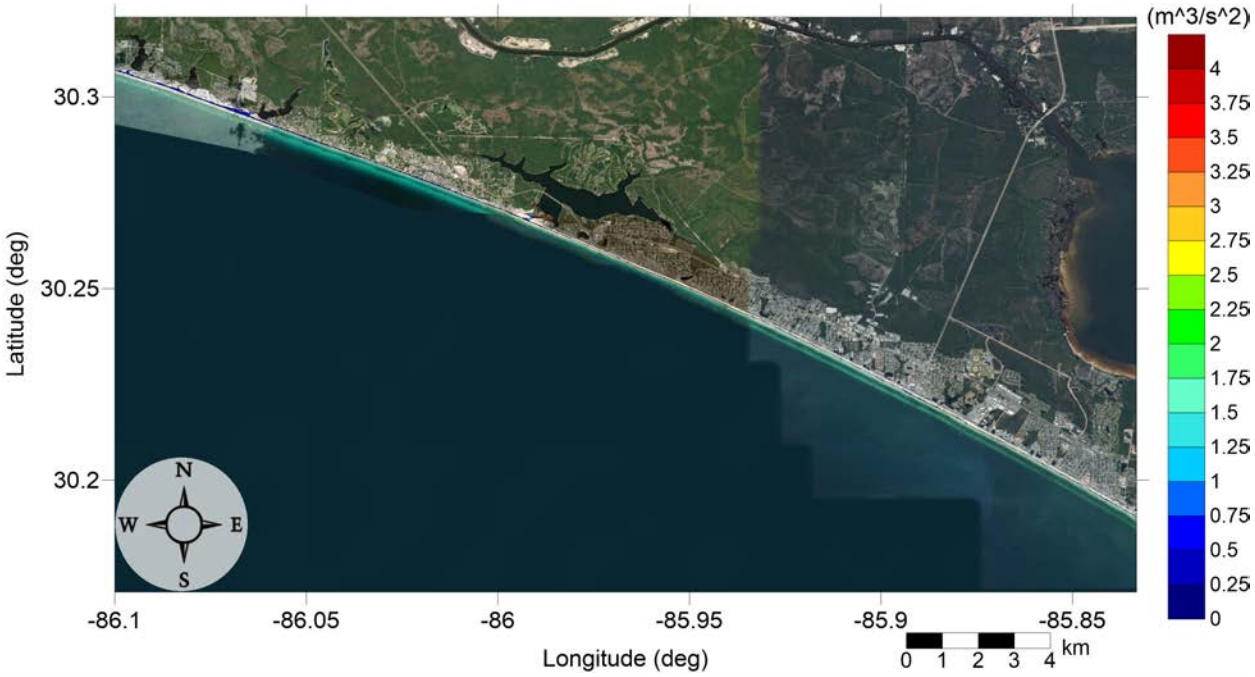

Figure 31: Maximum momentum flux (m^3/s^2) caused by the Yucatán 3 submarine landslide in Panama City Beach, FL. Arrows represent direction of maximum momentum flux. Contour drawn is the zero-meter contour for land elevation.

RosemaryBeach, FL
Yucatán 3 submarine landslide
Maximum Inundation Depth

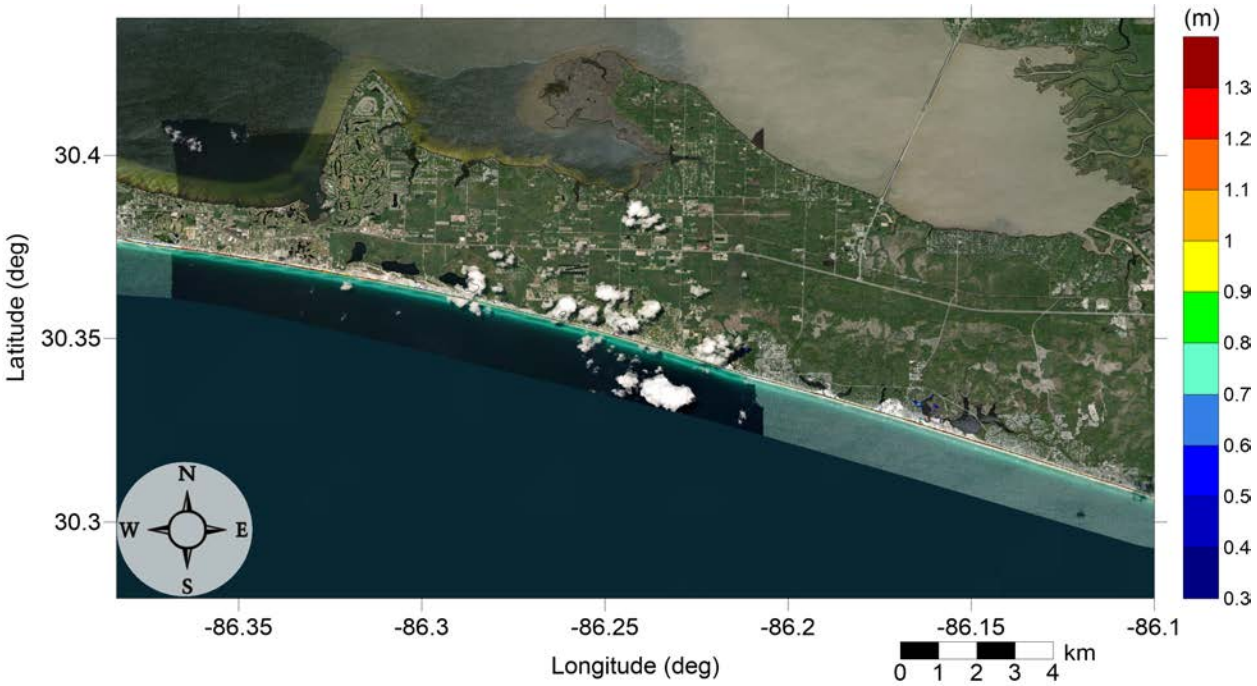

Figure 32: Maximum inundation depth (m) caused by the Yucatán 3 submarine landslide in Miramar Beach, FL. Contour drawn is the zero-meter contour for land elevation.

RosemaryBeach, FL
Yucatán 3 submarine landslide
Maximum Inundation Depth

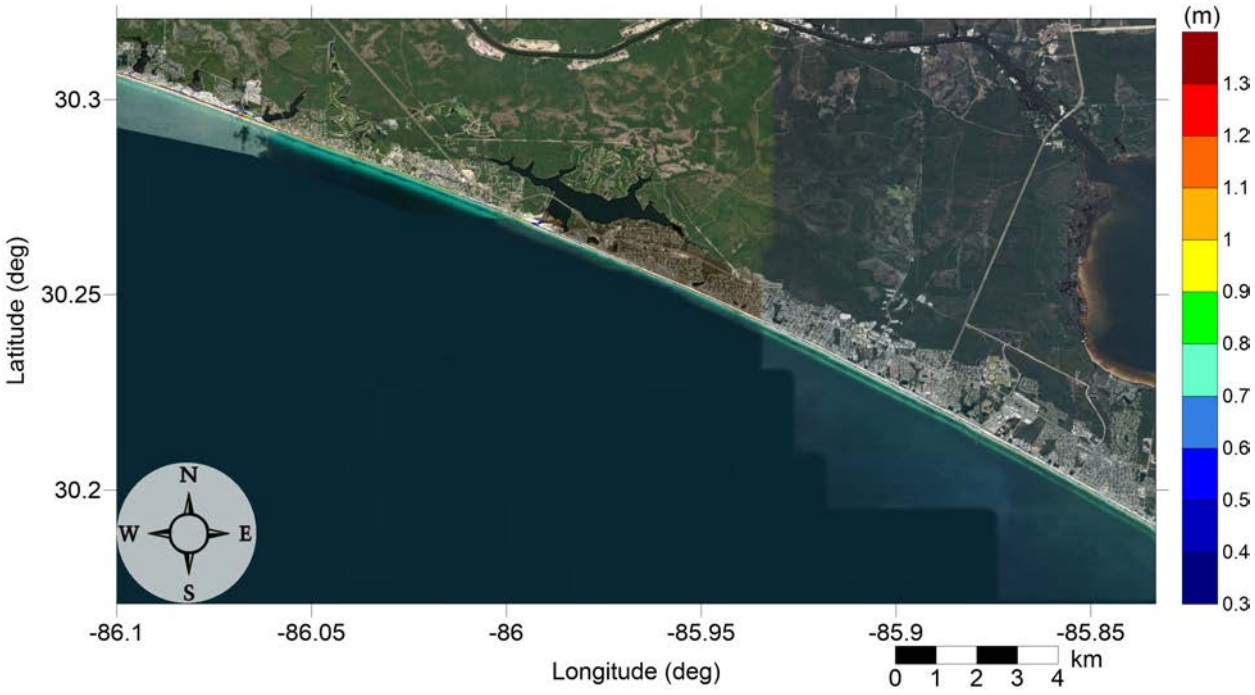

Figure 33: Maximum inundation depth (m) caused by the Yucatán 3 submarine landslide in Panama City Beach, FL. Contour drawn is the zero-meter contour for land elevation.

RosemaryBeach, FL
Yucatán 5 submarine landslide
Maximum Momentum Flux

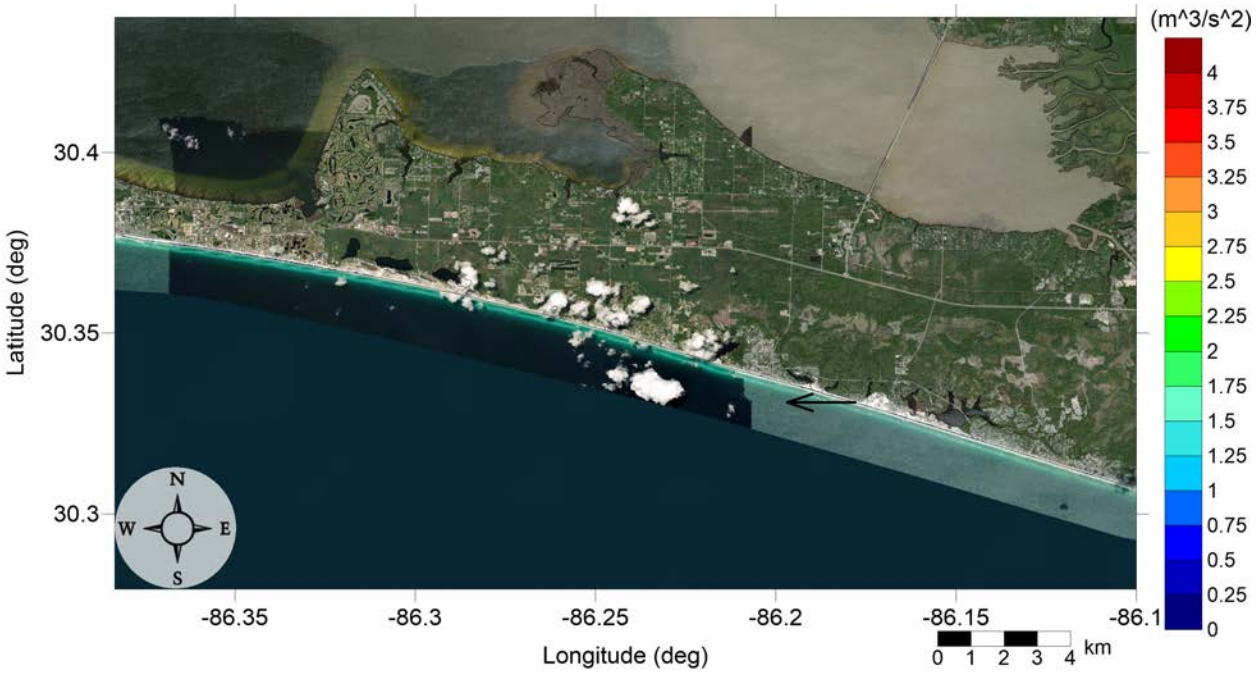

Figure 34: Maximum momentum flux (m^3/s^2) caused by the Yucatán 5 submarine landslide in Miramar Beach, FL. Arrows represent direction of maximum momentum flux. Contour drawn is the zero-meter contour for land elevation.

RosemaryBeach, FL
Yucatán 5 submarine landslide
Maximum Momentum Flux

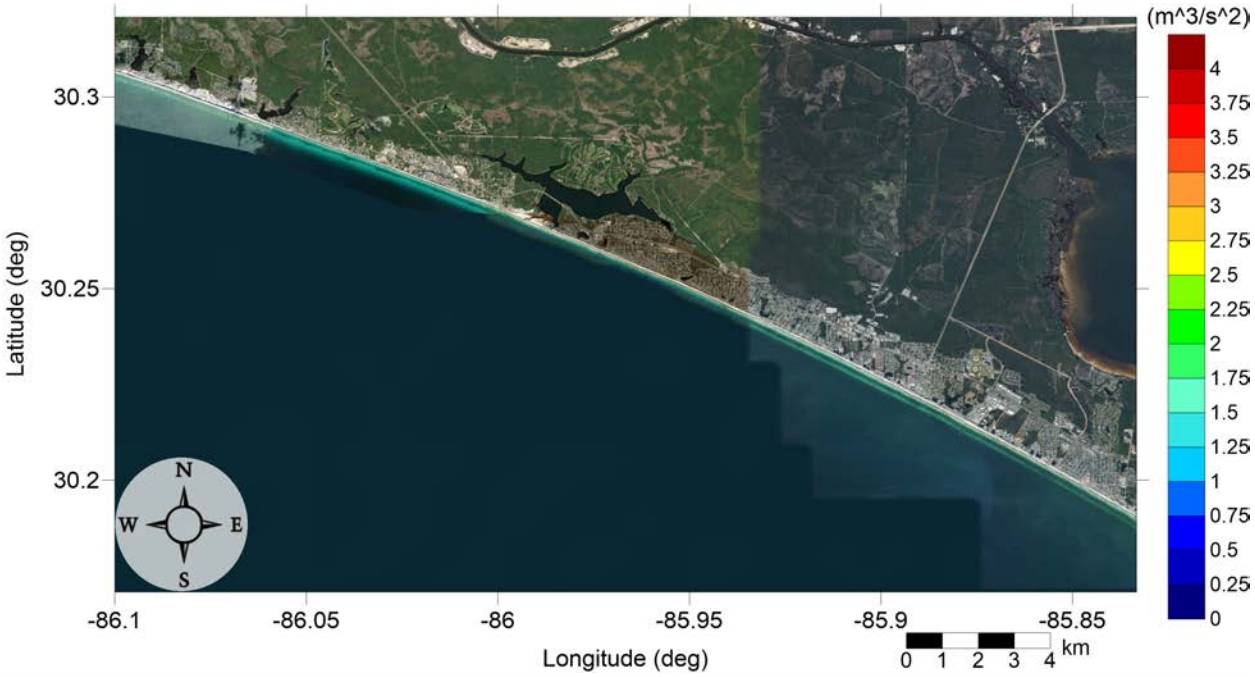

Figure 35: Maximum momentum flux (m^3/s^2) caused by the Yucatán 5 submarine landslide in Panama City Beach, FL. Arrows represent direction of maximum momentum flux. Contour drawn is the zero-meter contour for land elevation.

RosemaryBeach, FL
Yucatán 5 submarine landslide
Maximum Inundation Depth

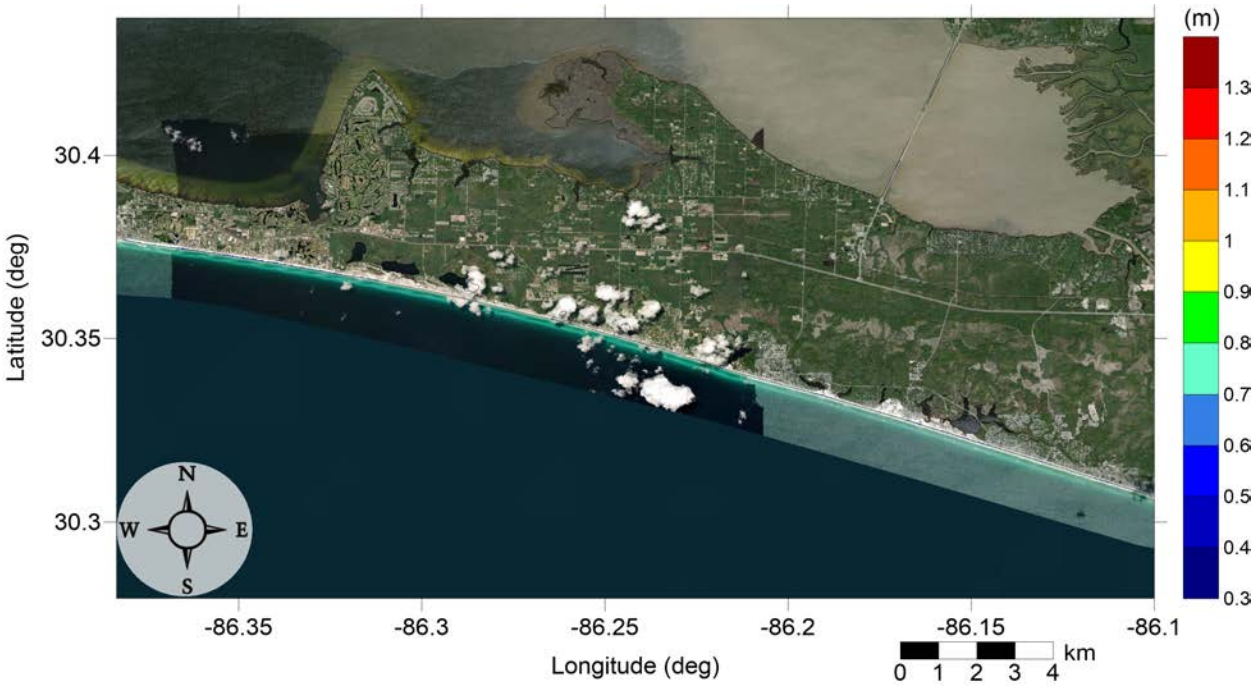

Figure 36: Maximum inundation depth (m) caused by the Yucatán 5 submarine landslide in Miramar Beach, FL. Contour drawn is the zero-meter contour for land elevation.

RosemaryBeach, FL
Yucatán 5 submarine landslide
Maximum Inundation Depth

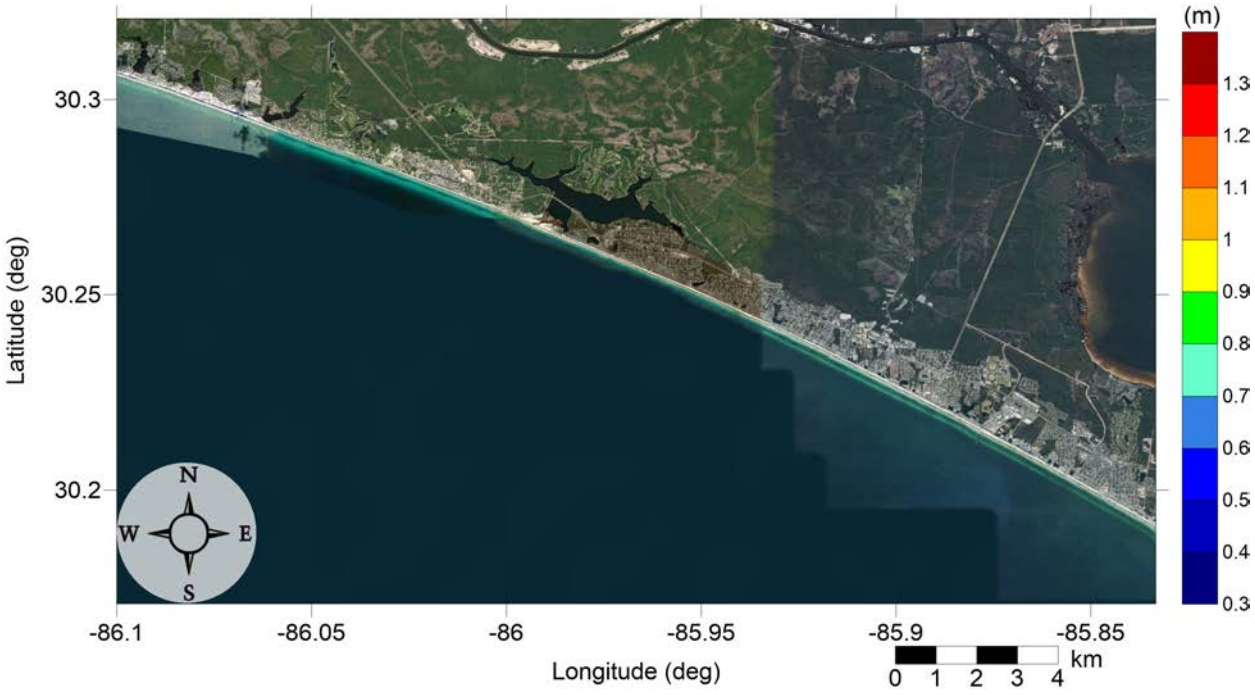

Figure 37: Maximum inundation depth (m) caused by the Yucatán 5 submarine landslide in Panama City Beach, FL. Contour drawn is the zero-meter contour for land elevation.

RosemaryBeach, FL
All Sources
Maximum of Maximum Inundation Depth

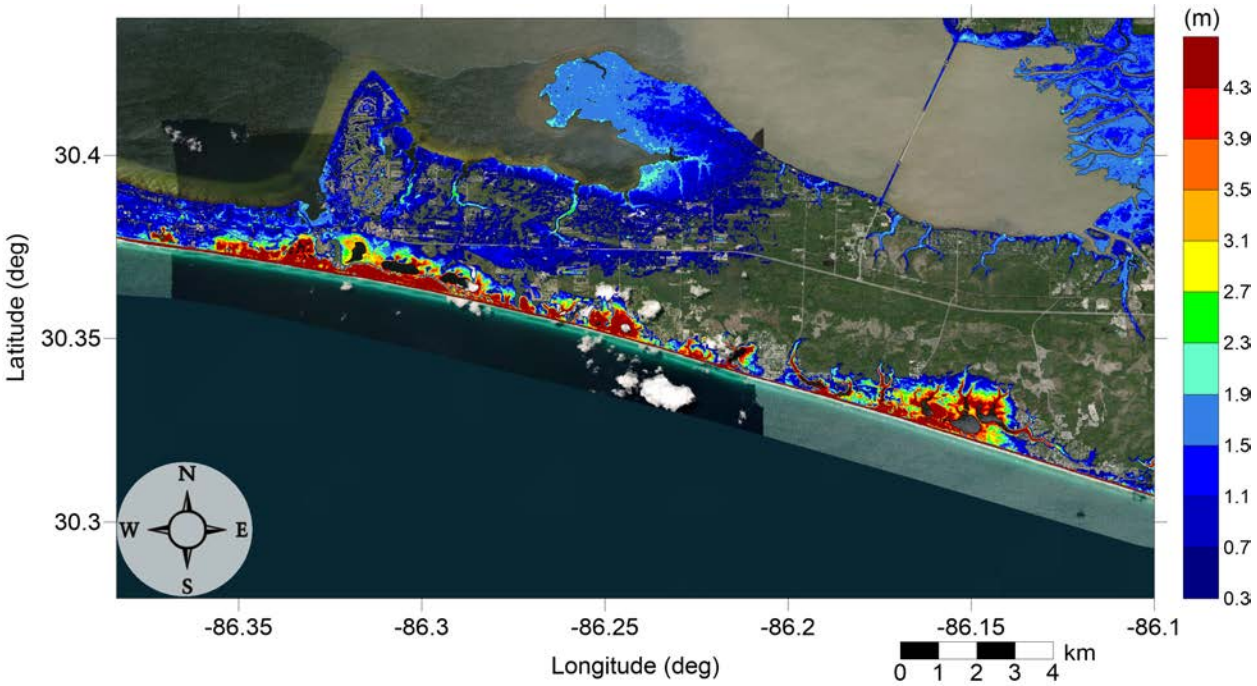

Figure 38: Maximum of maximums inundation depth (m) in Miramar Beach, FL, calculated as the maximum inundation depth in each grid cell from an ensemble of all tsunami sources considered. Contour drawn is the zero-meter contour for land elevation.

RosemaryBeach, FL
All Sources
Maximum of Maximum Inundation Depth

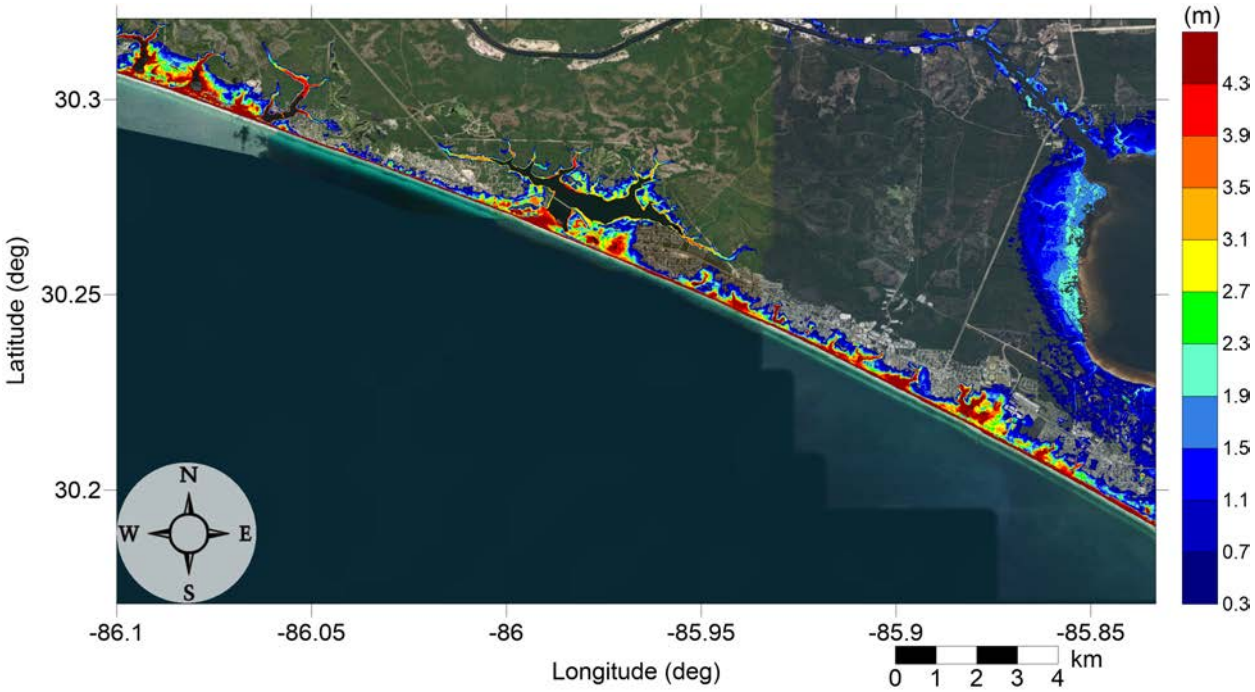

Figure 39: Maximum of maximums inundation depth (m) in Panama City Beach, FL, calculated as the maximum inundation depth in each grid cell from an ensemble of all tsunami sources considered. Contour drawn is the zero-meter contour for land elevation.

RosemaryBeach, FL
All Sources
Maximum Inundation Depth by Source

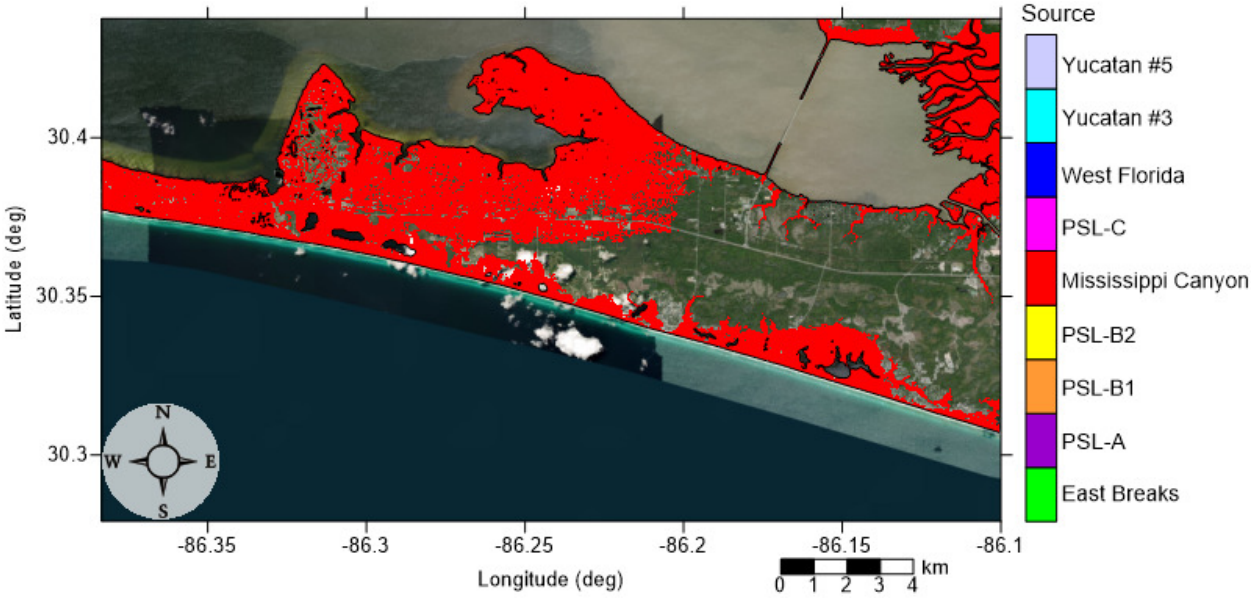

Figure 40: Indication of the tsunami source which causes the maximum of maximums inundation depth (m) in each grid cell from an ensemble of all tsunami sources in Miramar Beach, FL. Contour drawn is the zero-meter contour for land elevation.

RosemaryBeach, FL
All Sources
Maximum Inundation Depth by Source

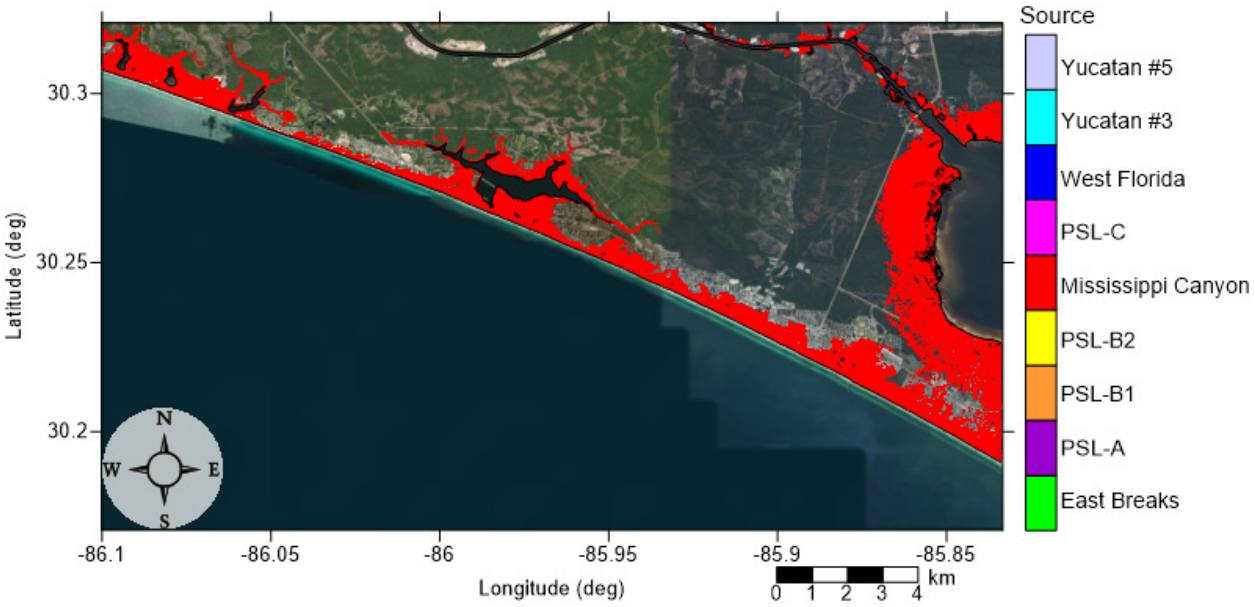

Figure 41: Indication of the tsunami source which causes the maximum of maximums inundation depth (m) in each grid cell from an ensemble of all tsunami sources in Panama City Beach, FL. Contour drawn is the zero-meter contour for land elevation.

4.2 Tampa Bay North, FL

Table 3: Maximum tsunami wave amplitude and corresponding arrival time after landslide failure at Tampa Bay North, FL numerical wave gauge: 30°4'45.0012"N, 85°46'14.9982"W, approximate water depth 20 m.

Tsunami Source	Maximum Wave Amplitude (m)	Arrival Time After Landslide Failure (hr)
East Breaks	0.44	3.2
PSL-A	0.60	2.8
PSL-B1	0.61	2.0
PSL-B2	0.59	2.2
Mississippi Canyon	4.79	1.5
PSL-C	2.40	1.4
West Florida	1.08	2.1
Yucatán #3	1.42	2.4
Yucatán #5	0.91	2.5

North Tampa Bay, FL
East Breaks submarine landslide
Maximum Momentum Flux

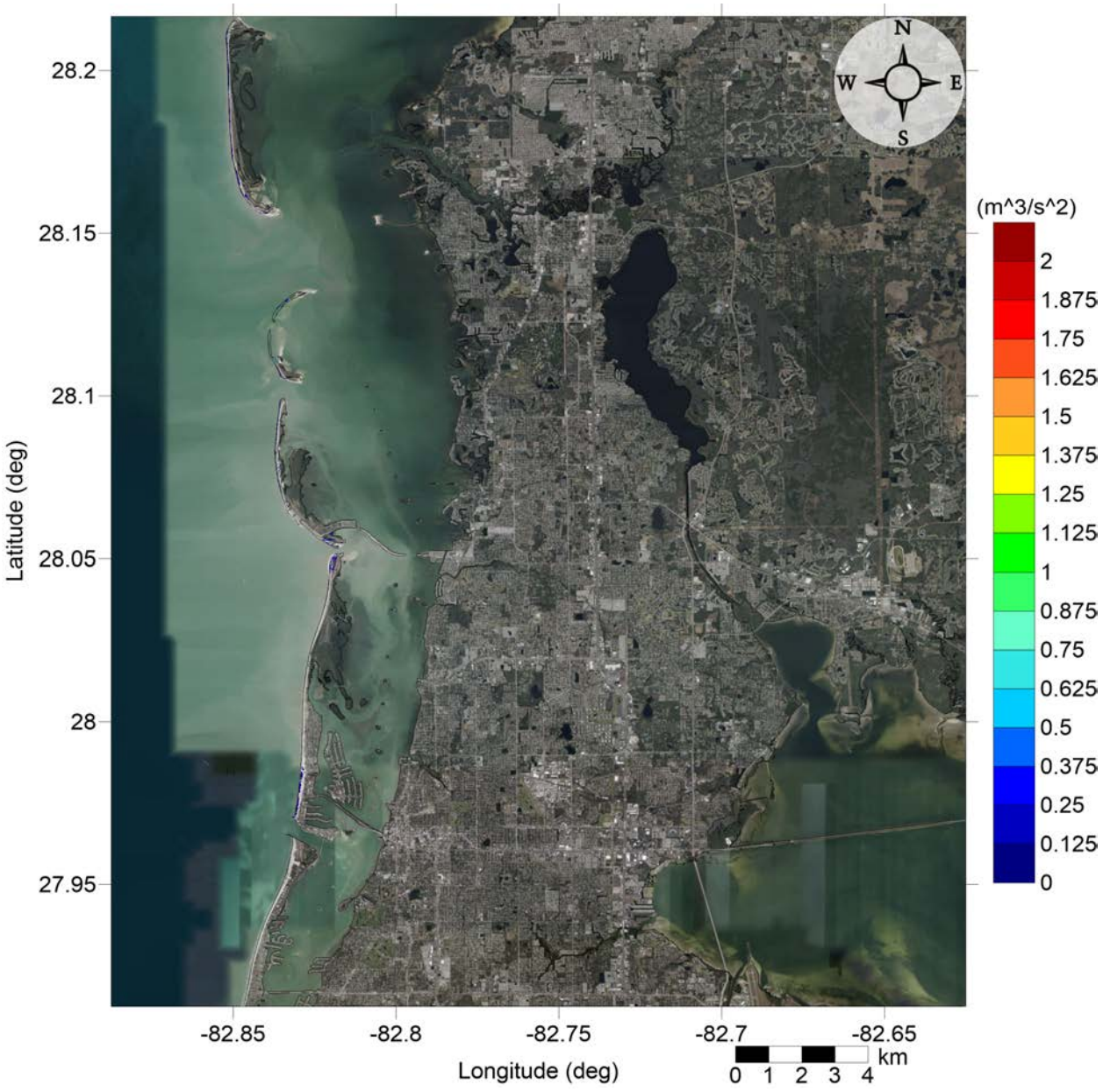

Figure 42: Maximum momentum flux (m^3/s^2) caused by the East Breaks submarine landslide in Pasco County, FL. Arrows represent direction of maximum momentum flux. Contour drawn is the zero-meter contour for land elevation.

North Tampa Bay, FL
East Breaks submarine landslide
Maximum Momentum Flux

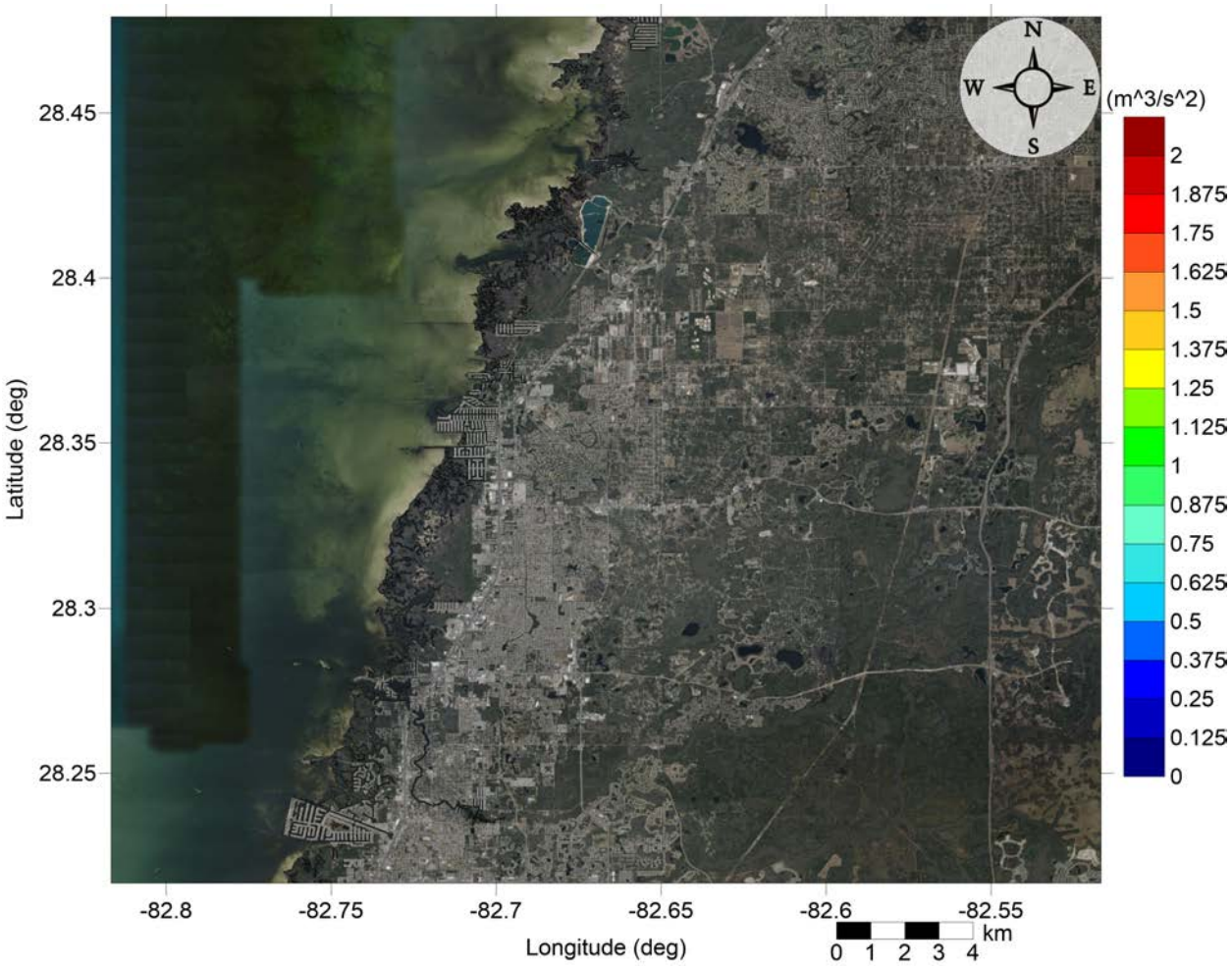

Figure 43: Maximum momentum flux (m^3/s^2) caused by the East Breaks submarine landslide in North Pinellas County, FL. Arrows represent direction of maximum momentum flux. Contour drawn is the zero-meter contour for land elevation.

North Tampa Bay, FL
East Breaks submarine landslide
Maximum Inundation Depth

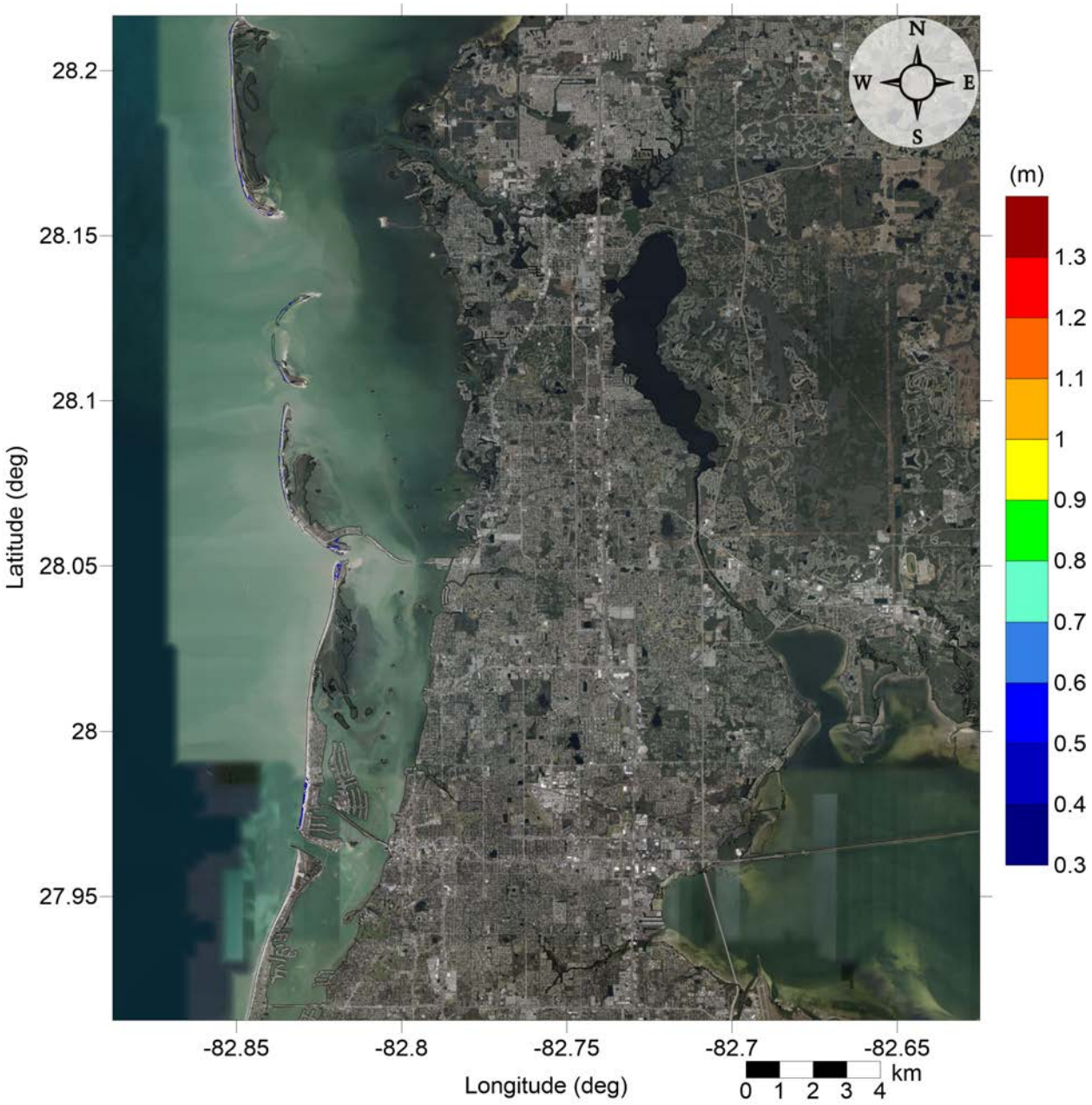

Figure 44: Maximum inundation depth (m) caused by the East Breaks submarine landslide in Pasco County, FL. Contour drawn is the zero-meter contour for land elevation.

North Tampa Bay, FL
East Breaks submarine landslide
Maximum Inundation Depth

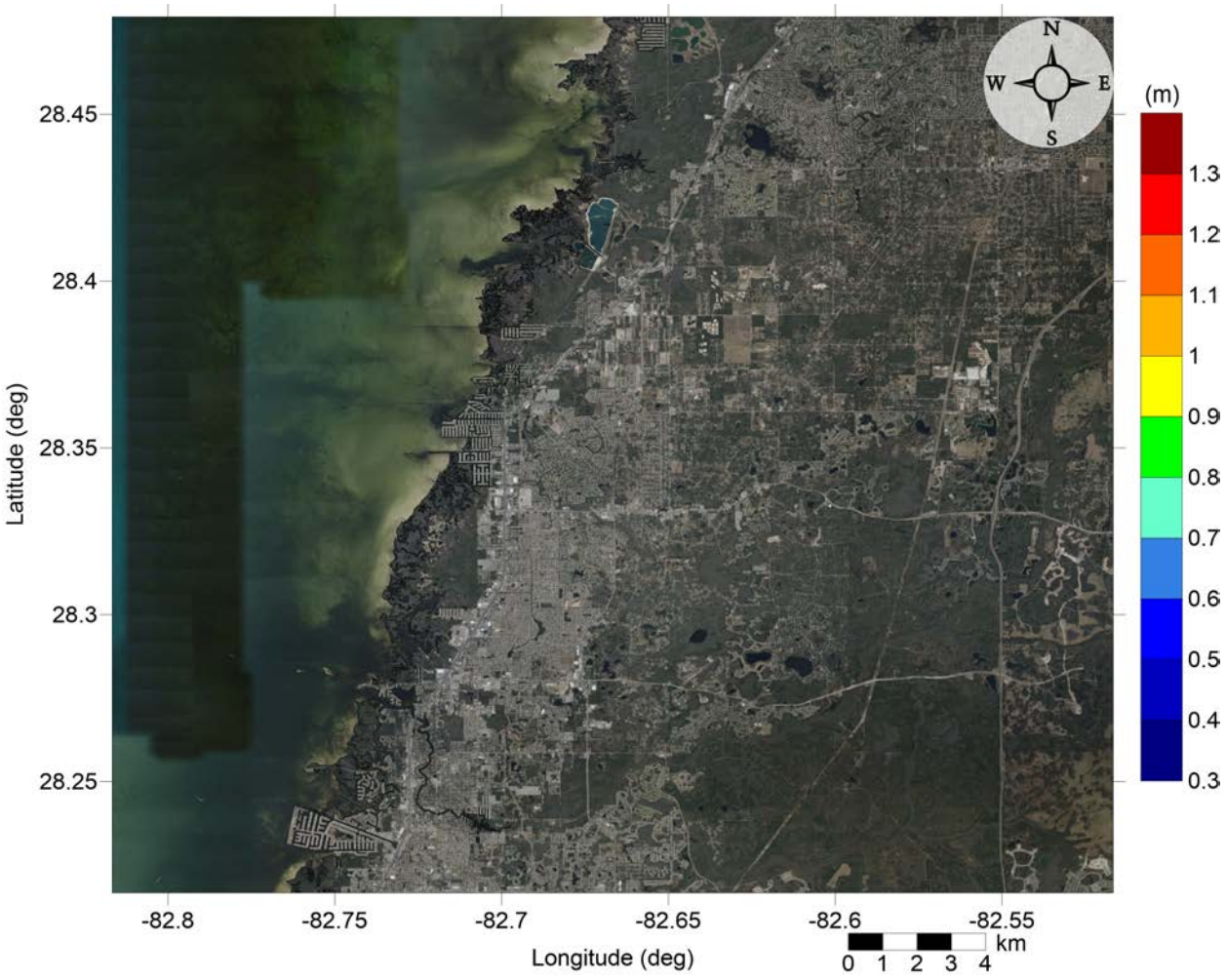

Figure 45: Maximum inundation depth (m) caused by the East Breaks submarine landslide in North Pinellas County, FL. Contour drawn is the zero-meter contour for land elevation.

North Tampa Bay, FL
Probabilistic Submarine Landslide A
Maximum Momentum Flux

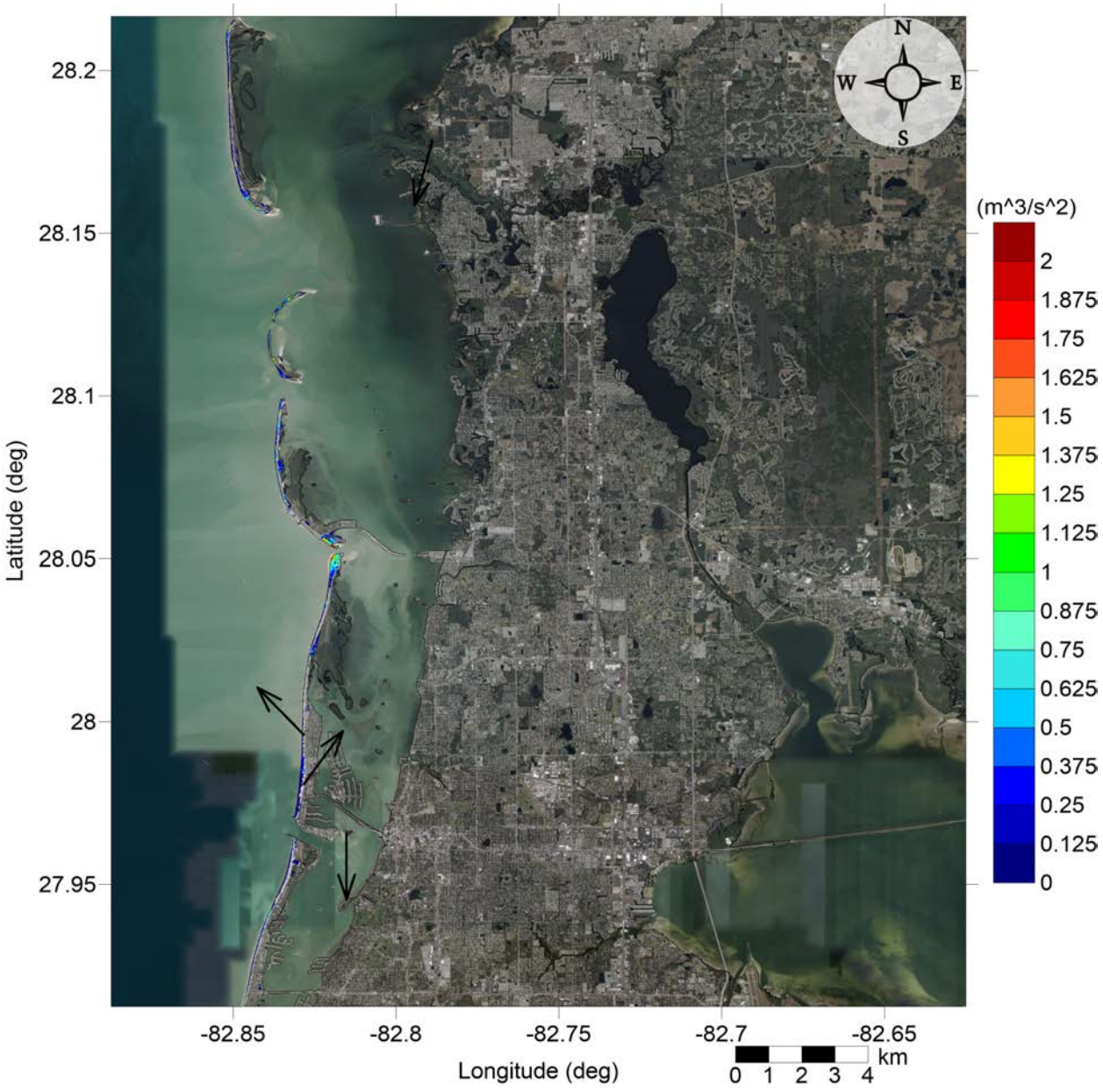

Figure 46: Maximum momentum flux (m^3/s^2) caused by the Probabilistic Submarine Landslide A in Pasco County, FL. Arrows represent direction of maximum momentum flux. Contour drawn is the zero-meter contour for land elevation.

North Tampa Bay, FL
Probabilistic Submarine Landslide A
Maximum Momentum Flux

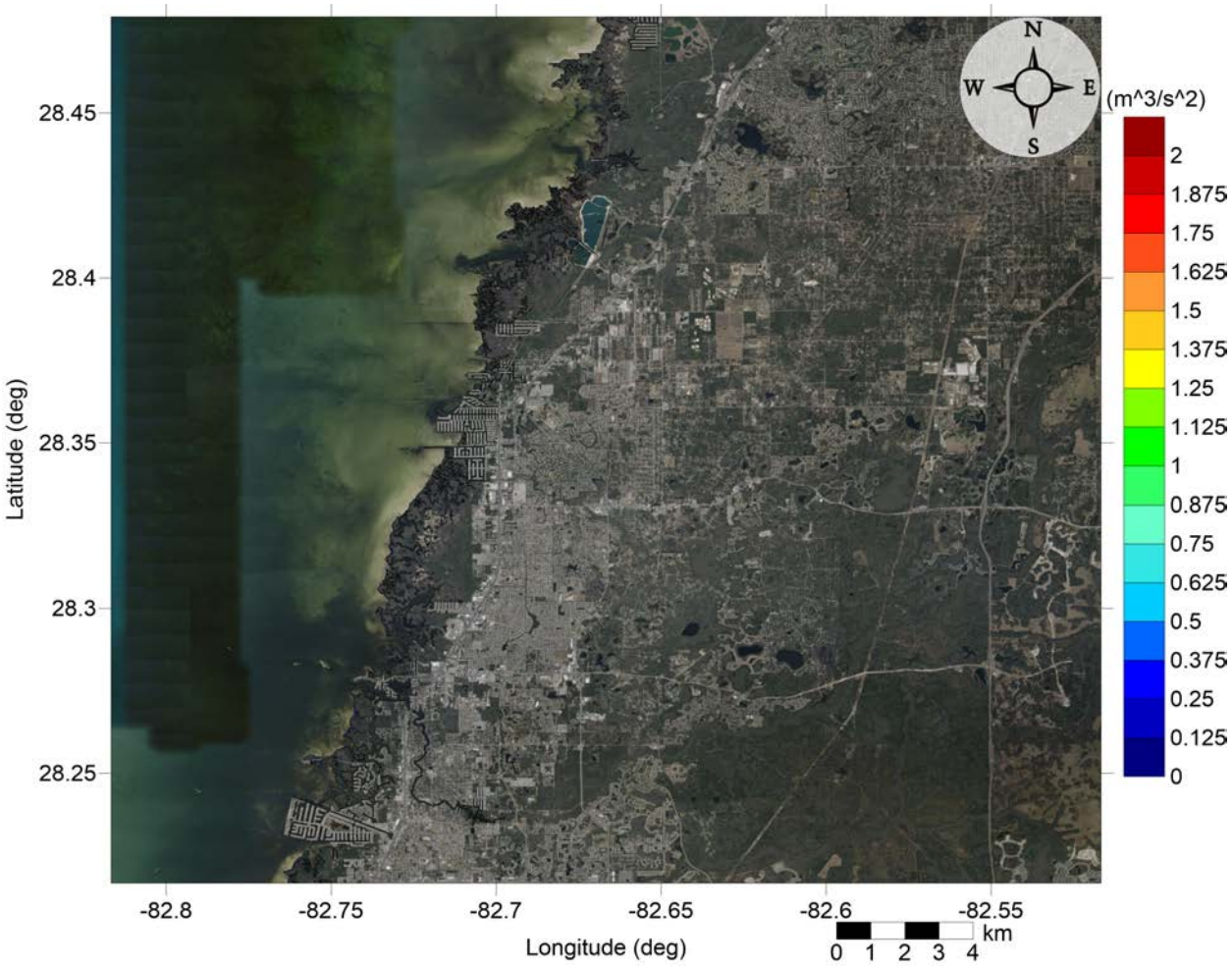

Figure 47: Maximum momentum flux (m^3/s^2) caused by the Probabilistic Submarine Landslide A in North Pinellas County, FL. Arrows represent direction of maximum momentum flux. Contour drawn is the zero-meter contour for land elevation.

North Tampa Bay, FL
Probabilistic Submarine Landslide A
Maximum Inundation Depth

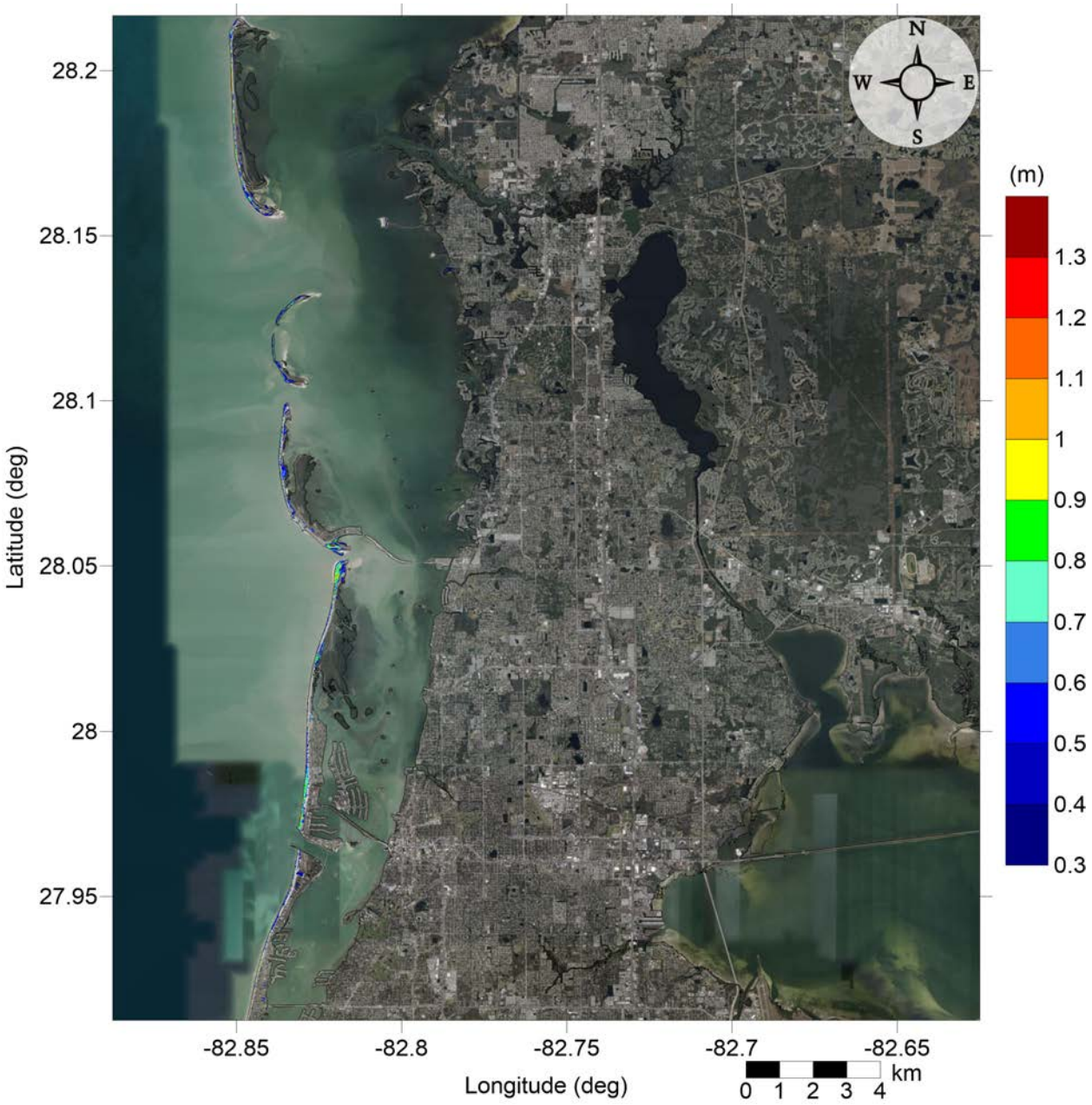

Figure 48: Maximum inundation depth (m) caused by the Probabilistic Submarine Landslide A in Pasco County, FL. Contour drawn is the zero-meter contour for land elevation.

North Tampa Bay, FL
Probabilistic Submarine Landslide A
Maximum Inundation Depth

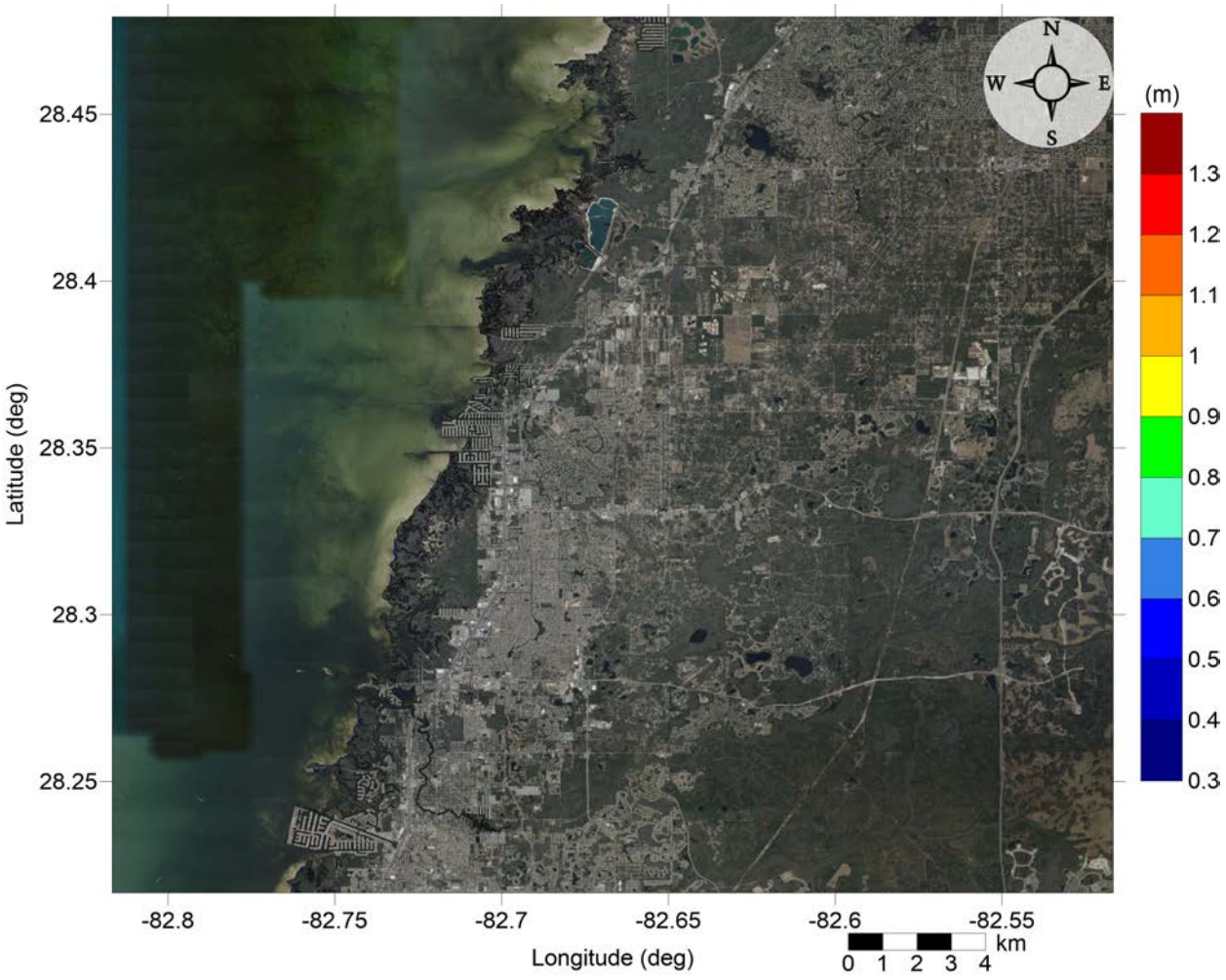

Figure 49: Maximum inundation depth (m) caused by the Probabilistic Submarine Landslide A in North Pinellas County, FL. Contour drawn is the zero-meter contour for land elevation.

North Tampa Bay, FL
Probabilistic Submarine Landslide B1
Maximum Momentum Flux

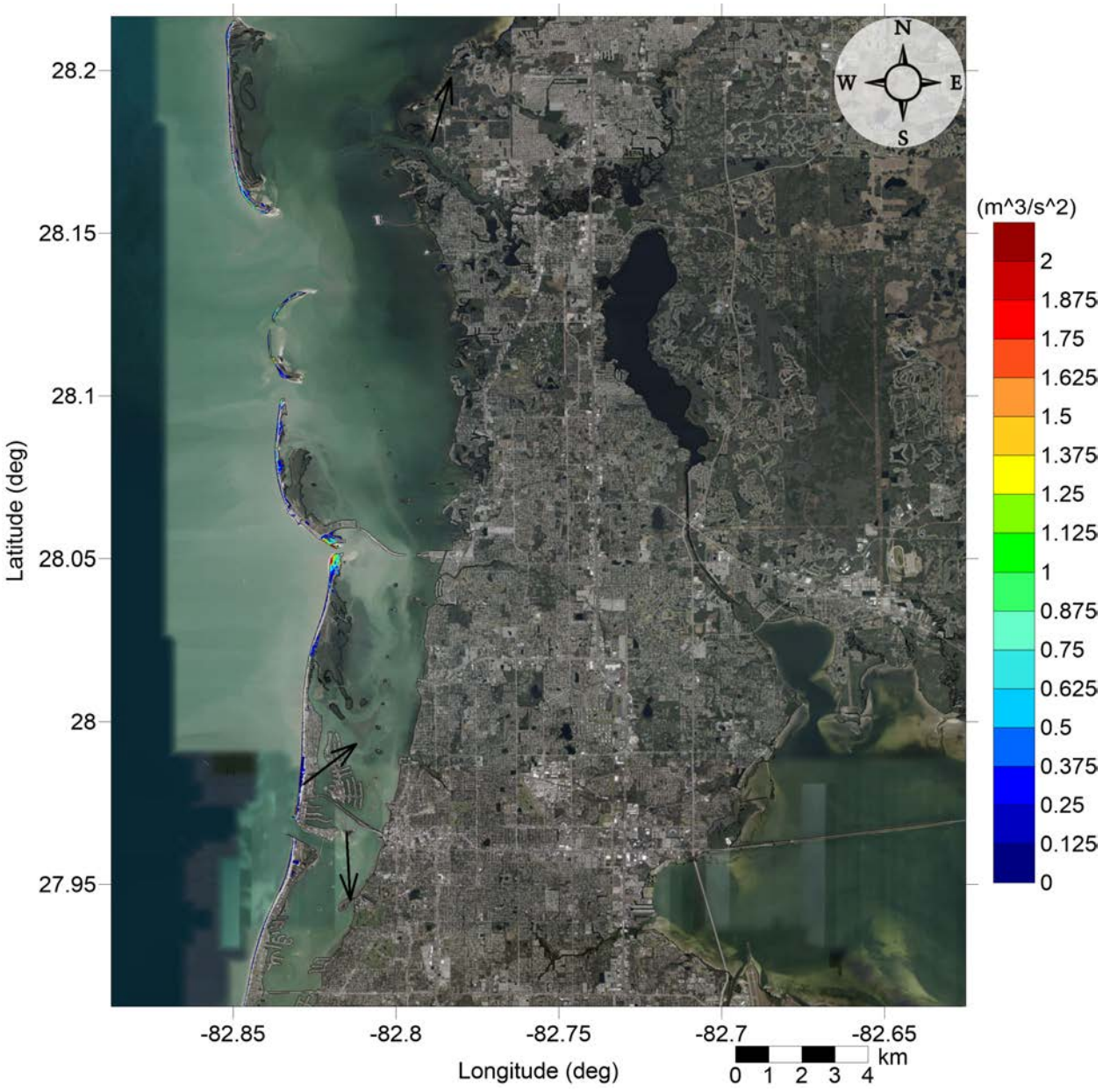

Figure 50: Maximum momentum flux (m^3/s^2) caused by the Probabilistic Submarine Landslide B1 in Pasco County, FL. Arrows represent direction of maximum momentum flux. Contour drawn is the zero-meter contour for land elevation.

North Tampa Bay, FL
Probabilistic Submarine Landslide B1
Maximum Momentum Flux

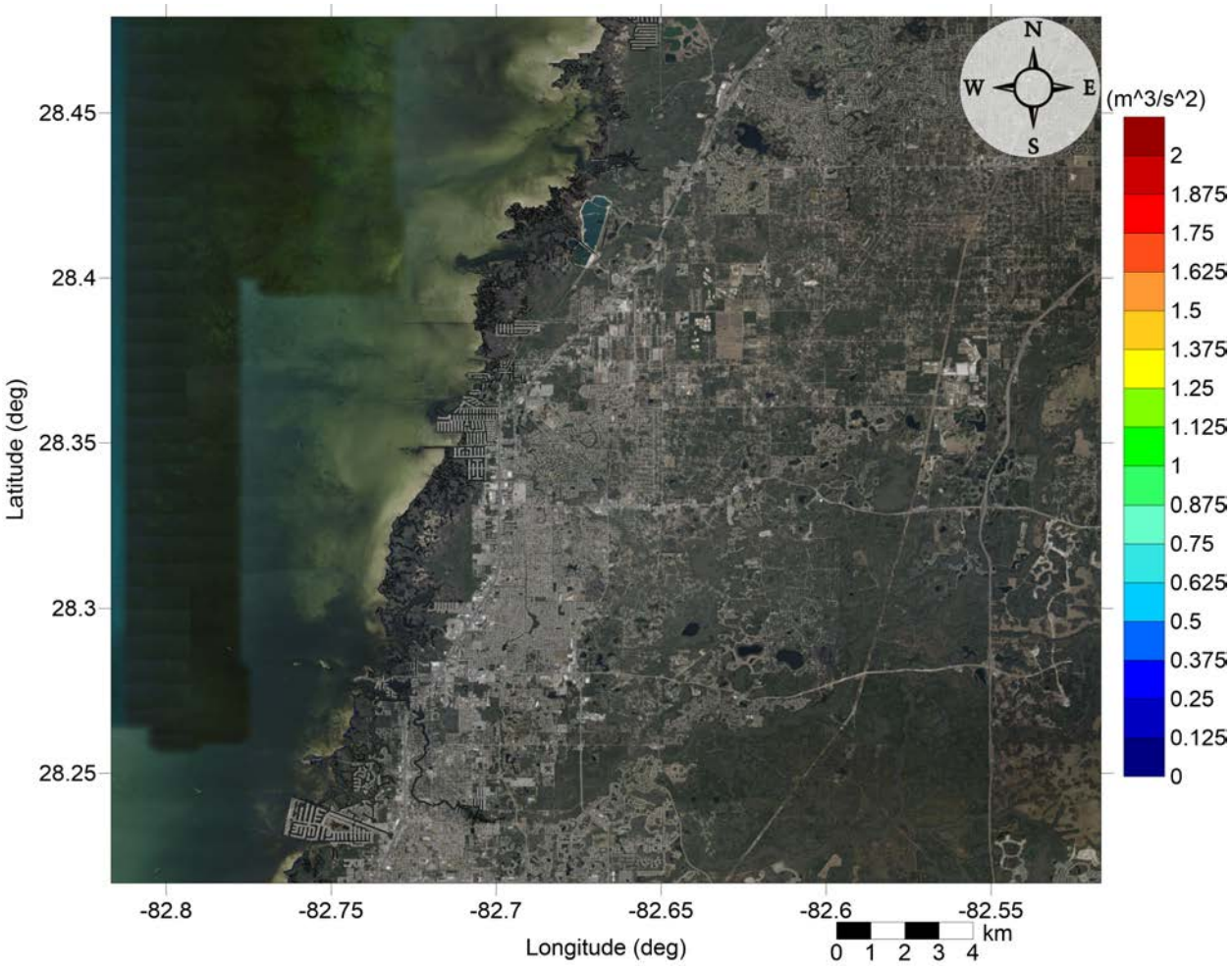

Figure 51: Maximum momentum flux (m^3/s^2) caused by the Probabilistic Submarine Landslide B1 in North Pinellas County, FL. Arrows represent direction of maximum momentum flux. Contour drawn is the zero-meter contour for land elevation.

North Tampa Bay, FL
Probabilistic Submarine Landslide B1
Maximum Inundation Depth

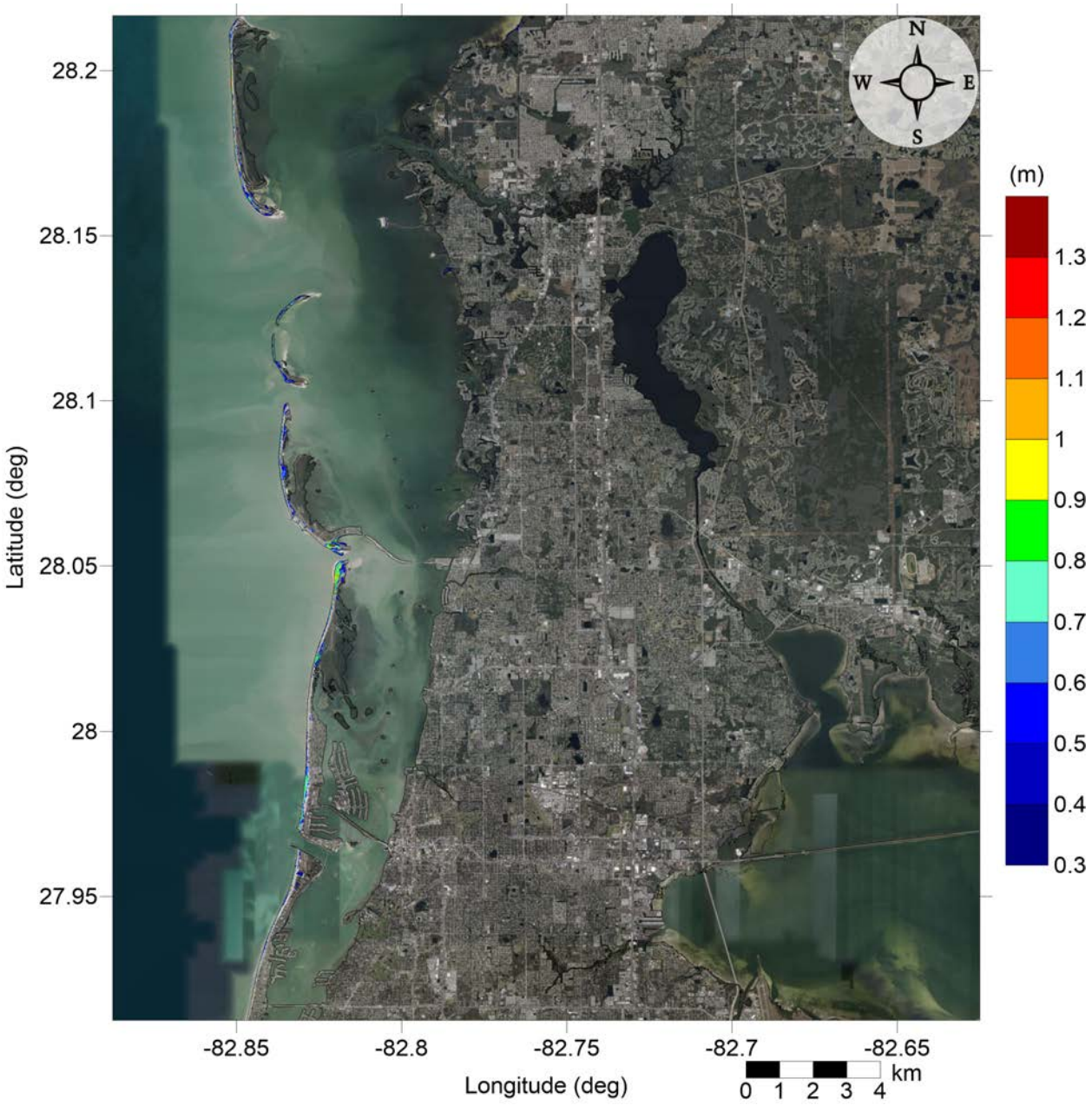

Figure 52: Maximum inundation depth (m) caused by the Probabilistic Submarine Landslide B1 in Pasco County, FL. Contour drawn is the zero-meter contour for land elevation.

North Tampa Bay, FL
Probabilistic Submarine Landslide B1
Maximum Inundation Depth

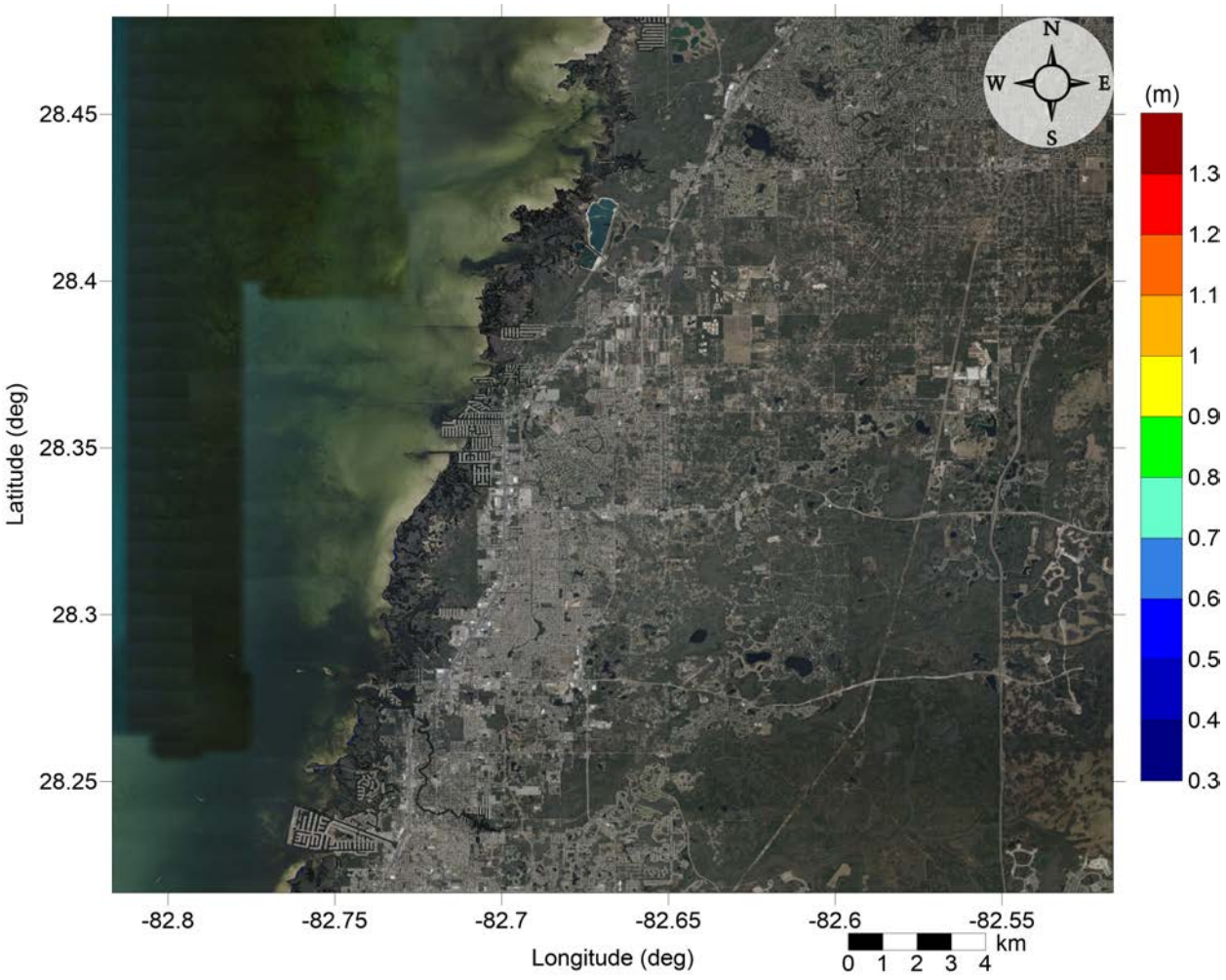

Figure 53: Maximum inundation depth (m) caused by the Probabilistic Submarine Landslide B1 in North Pinellas County, FL. Contour drawn is the zero-meter contour for land elevation.

North Tampa Bay, FL
Probabilistic Submarine Landslide B2
Maximum Momentum Flux

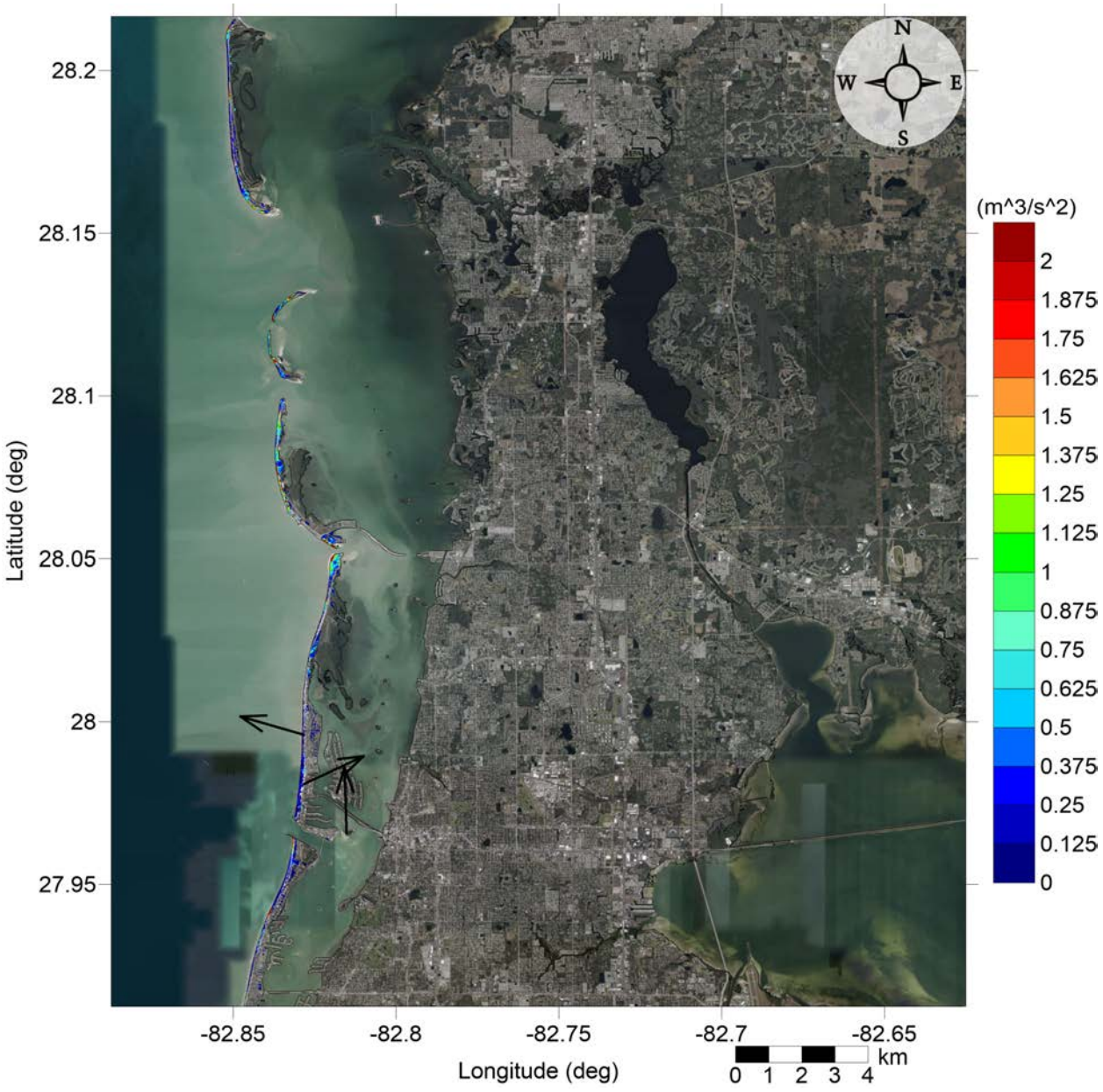

Figure 54: Maximum momentum flux (m^3/s^2) caused by the Probabilistic Submarine Landslide B2 in Pasco County, FL. Arrows represent direction of maximum momentum flux. Contour drawn is the zero-meter contour for land elevation.

North Tampa Bay, FL
Probabilistic Submarine Landslide B2
Maximum Momentum Flux

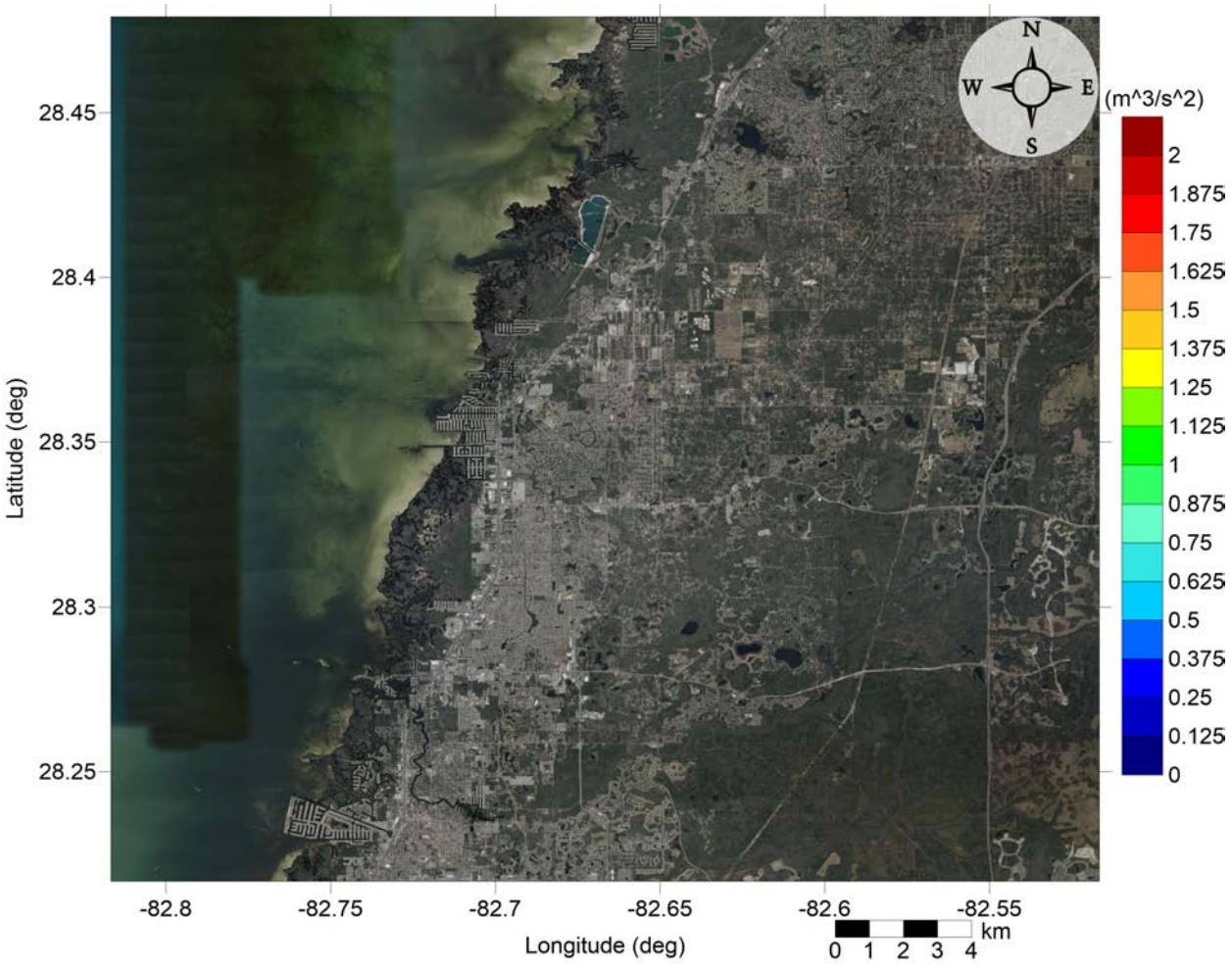

Figure 55: Maximum momentum flux (m^3/s^2) caused by the Probabilistic Submarine Landslide B2 in North Pinellas County, FL. Arrows represent direction of maximum momentum flux. Contour drawn is the zero-meter contour for land elevation.

North Tampa Bay, FL
Probabilistic Submarine Landslide B2
Maximum Inundation Depth

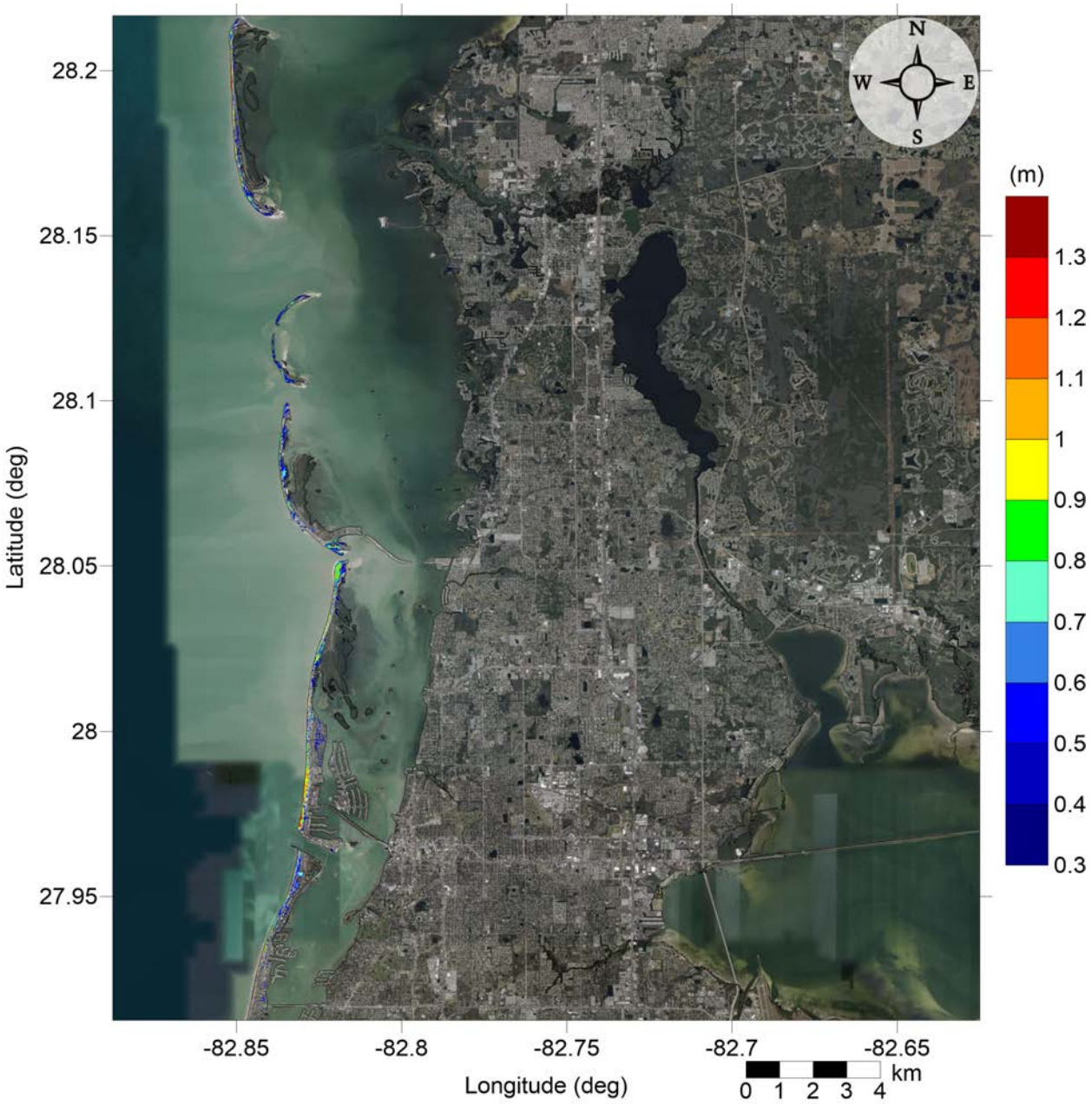

Figure 56: Maximum inundation depth (m) caused by the Probabilistic Submarine Landslide B2 in Pasco County, FL. Contour drawn is the zero-meter contour for land elevation.

North Tampa Bay, FL
Probabilistic Submarine Landslide B2
Maximum Inundation Depth

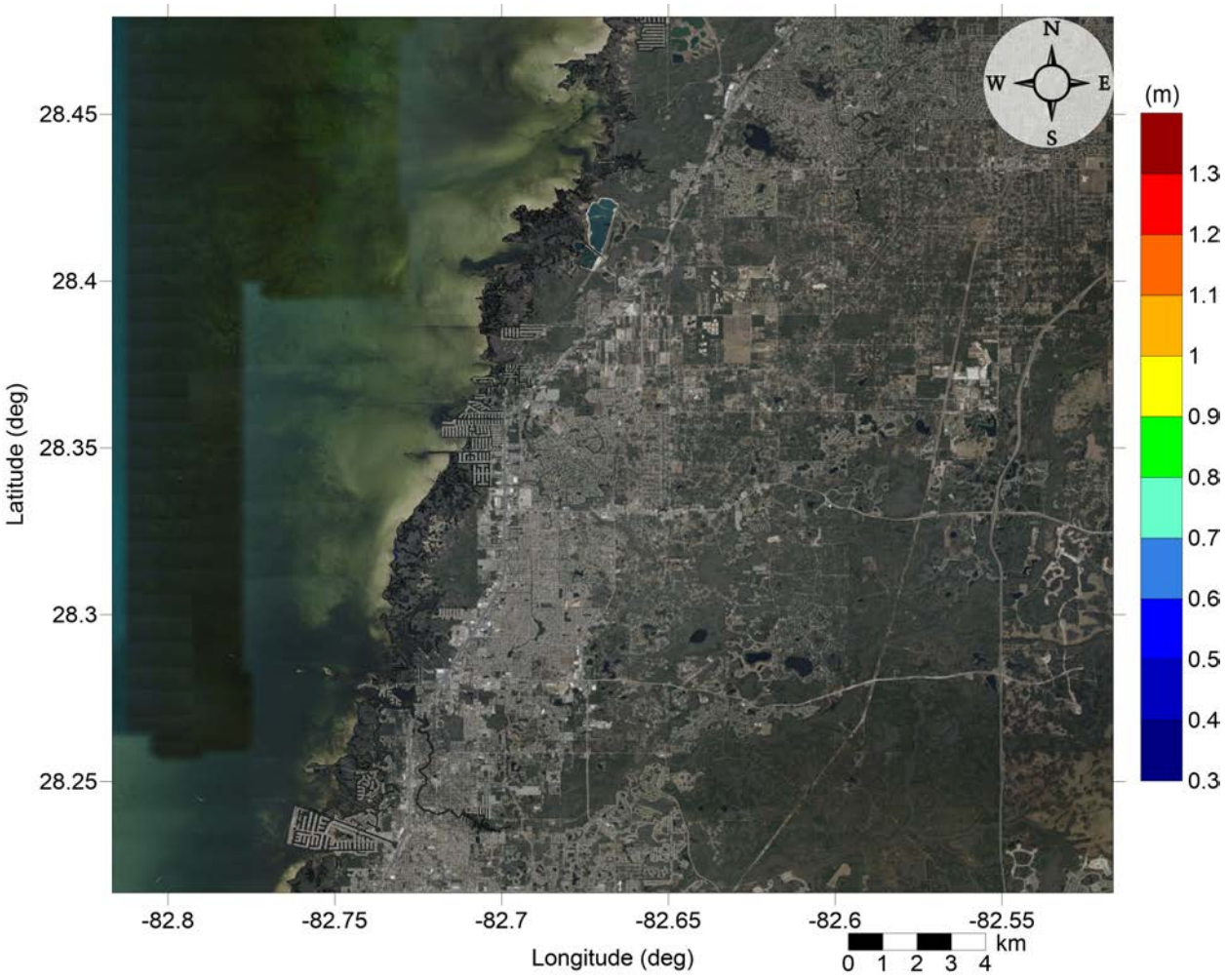

Figure 57: Maximum inundation depth (m) caused by the Probabilistic Submarine Landslide B2 in North Pinellas County, FL. Contour drawn is the zero-meter contour for land elevation.

North Tampa Bay, FL
Mississippi Canyon submarine landslide
Maximum Momentum Flux

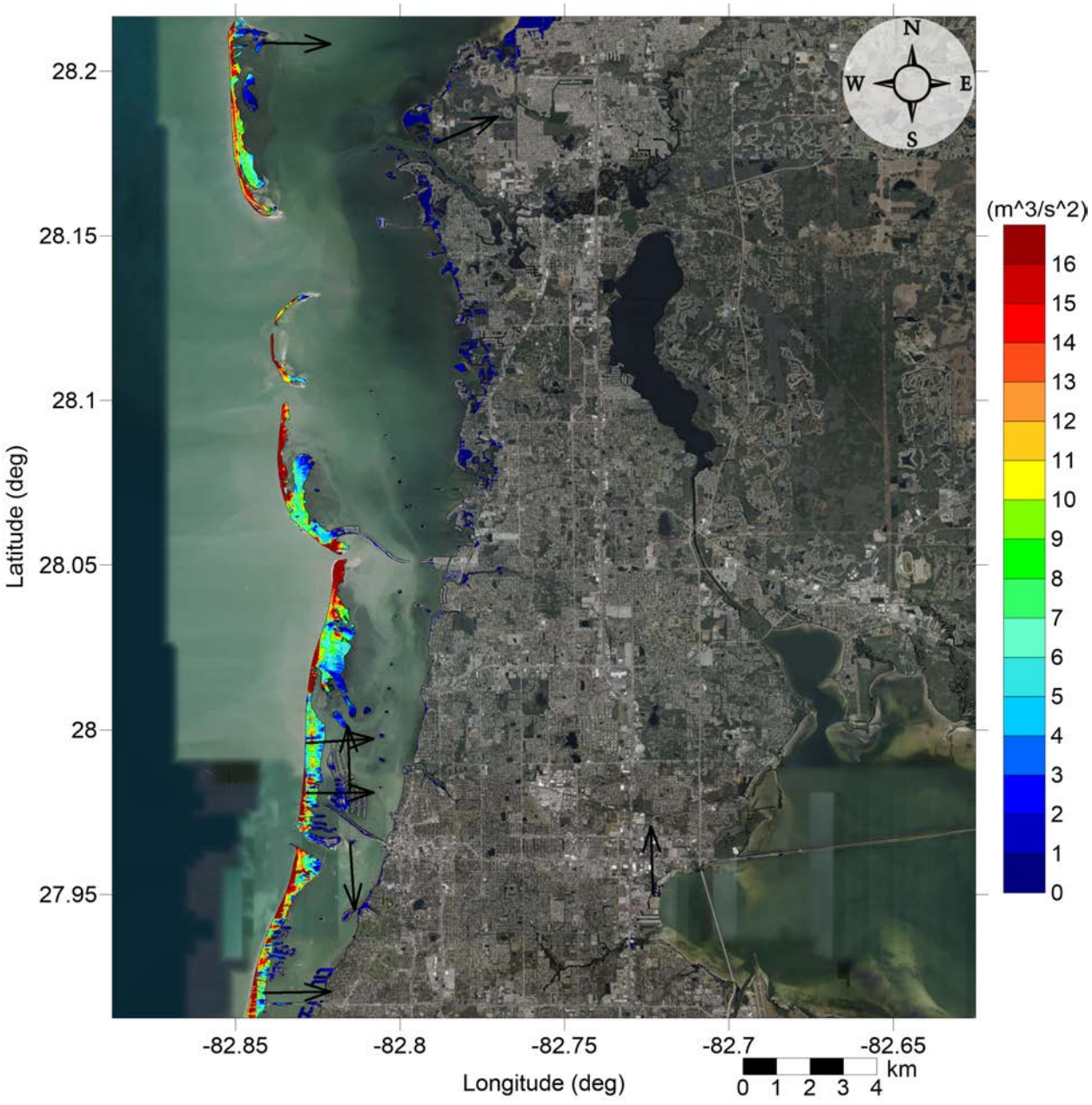

Figure 58: Maximum momentum flux (m^3/s^2) caused by the Mississippi Canyon submarine landslide in Pasco County, FL. Arrows represent direction of maximum momentum flux. Contour drawn is the zero-meter contour for land elevation.

North Tampa Bay, FL
Mississippi Canyon submarine landslide
Maximum Momentum Flux

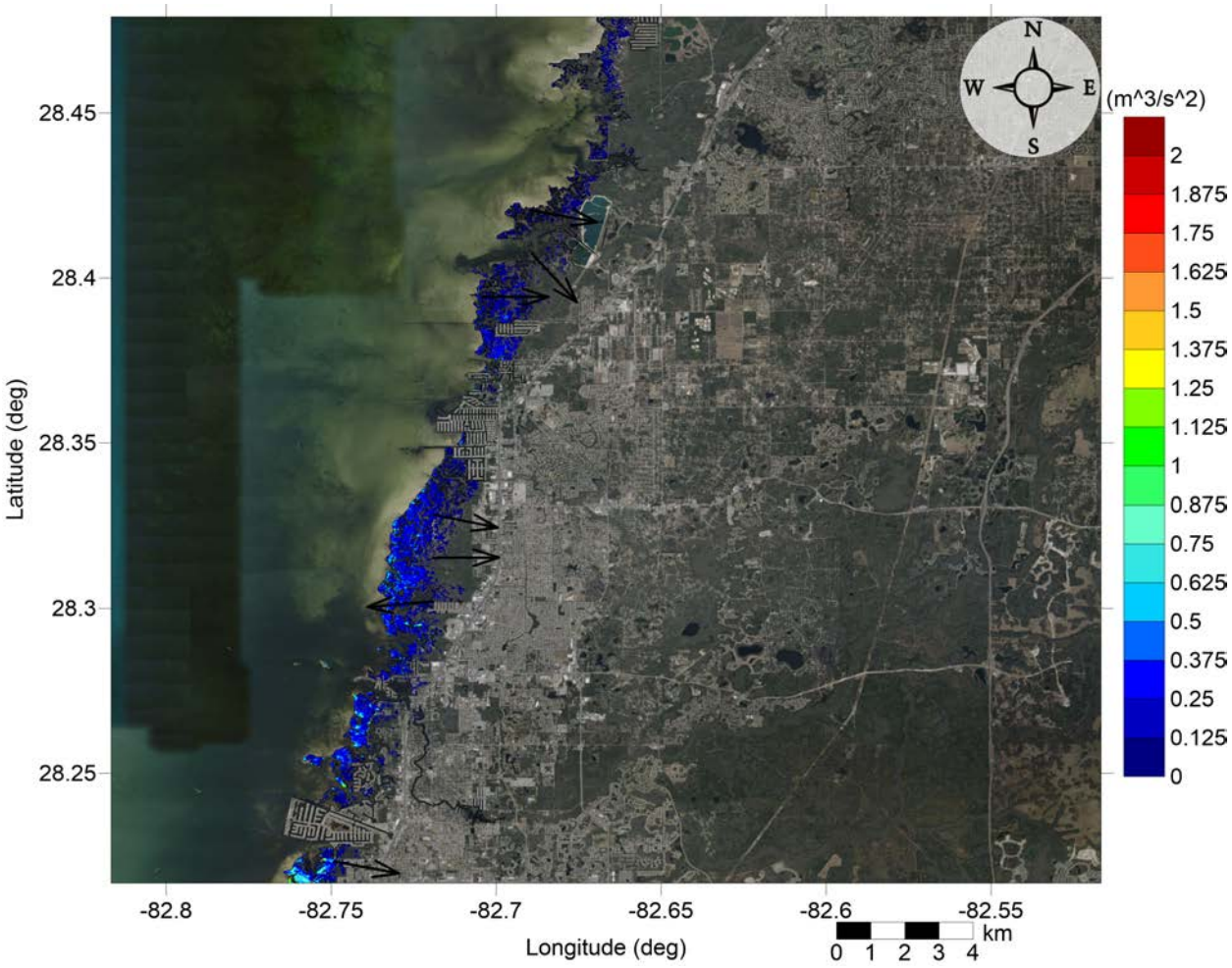

Figure 59: Maximum momentum flux (m^3/s^2) caused by the Mississippi Canyon submarine landslide in North Pinellas County, FL. Arrows represent direction of maximum momentum flux. Contour drawn is the zero-meter contour for land elevation.

North Tampa Bay, FL
Mississippi Canyon submarine landslide
Maximum Inundation Depth

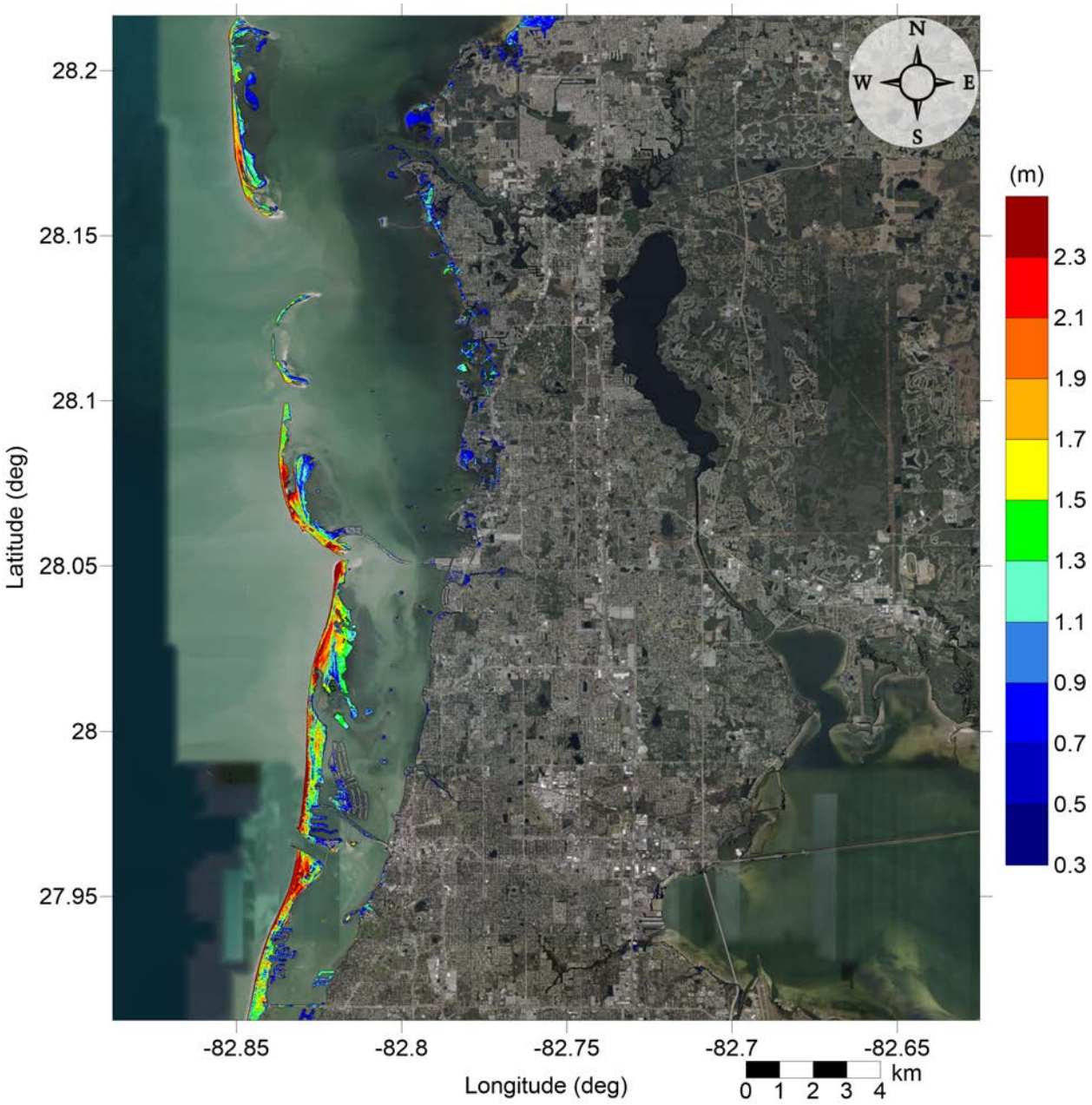

Figure 60: Maximum inundation depth (m) caused by the Mississippi Canyon submarine landslide in Pasco County, FL. Contour drawn is the zero-meter contour for land elevation.

North Tampa Bay, FL
Mississippi Canyon submarine landslide
Maximum Inundation Depth

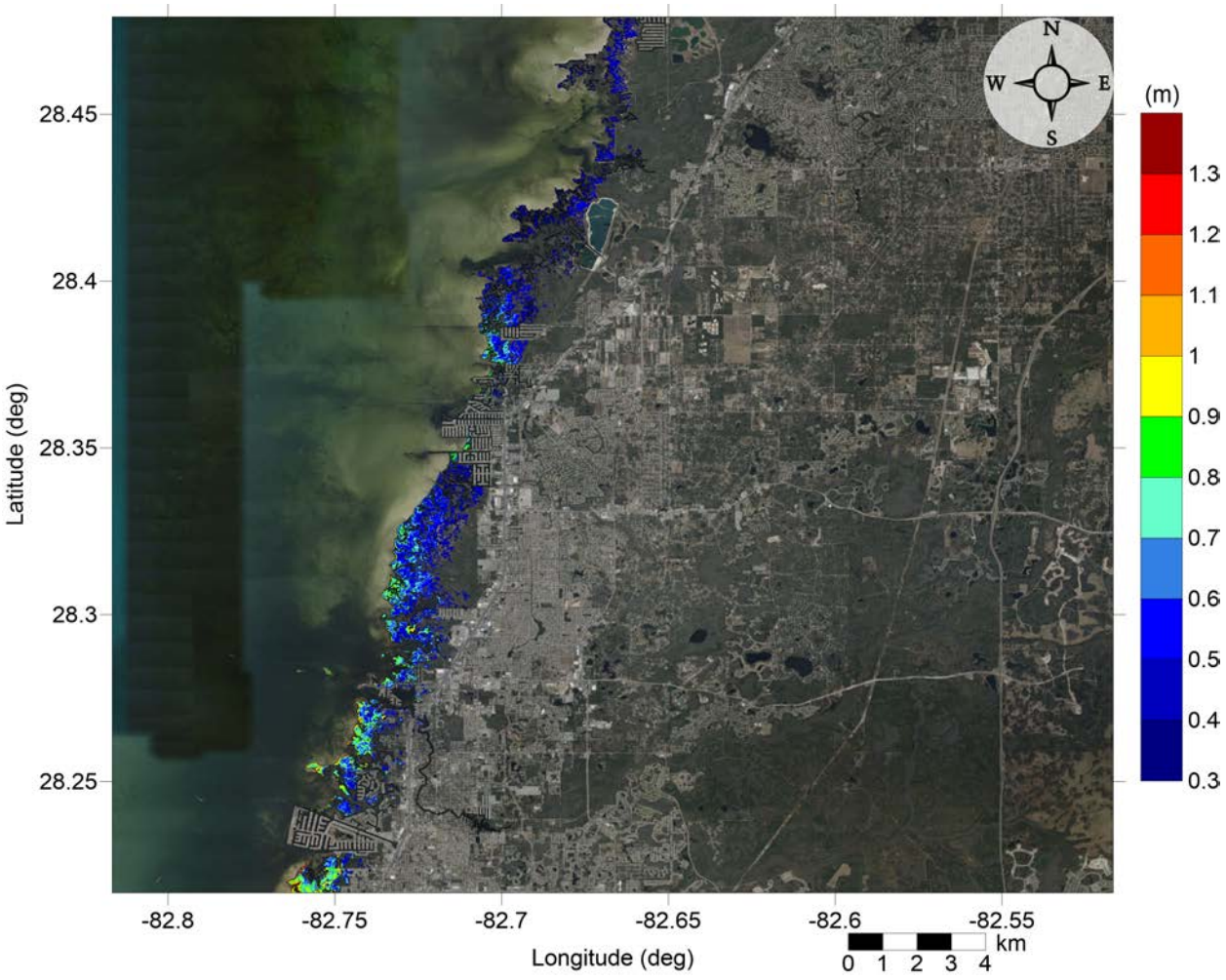

Figure 61: Maximum inundation depth (m) caused by the Mississippi Canyon submarine landslide in North Pinellas County, FL. Contour drawn is the zero-meter contour for land elevation.

North Tampa Bay, FL
Probabilistic Submarine Landslide C
Maximum Momentum Flux

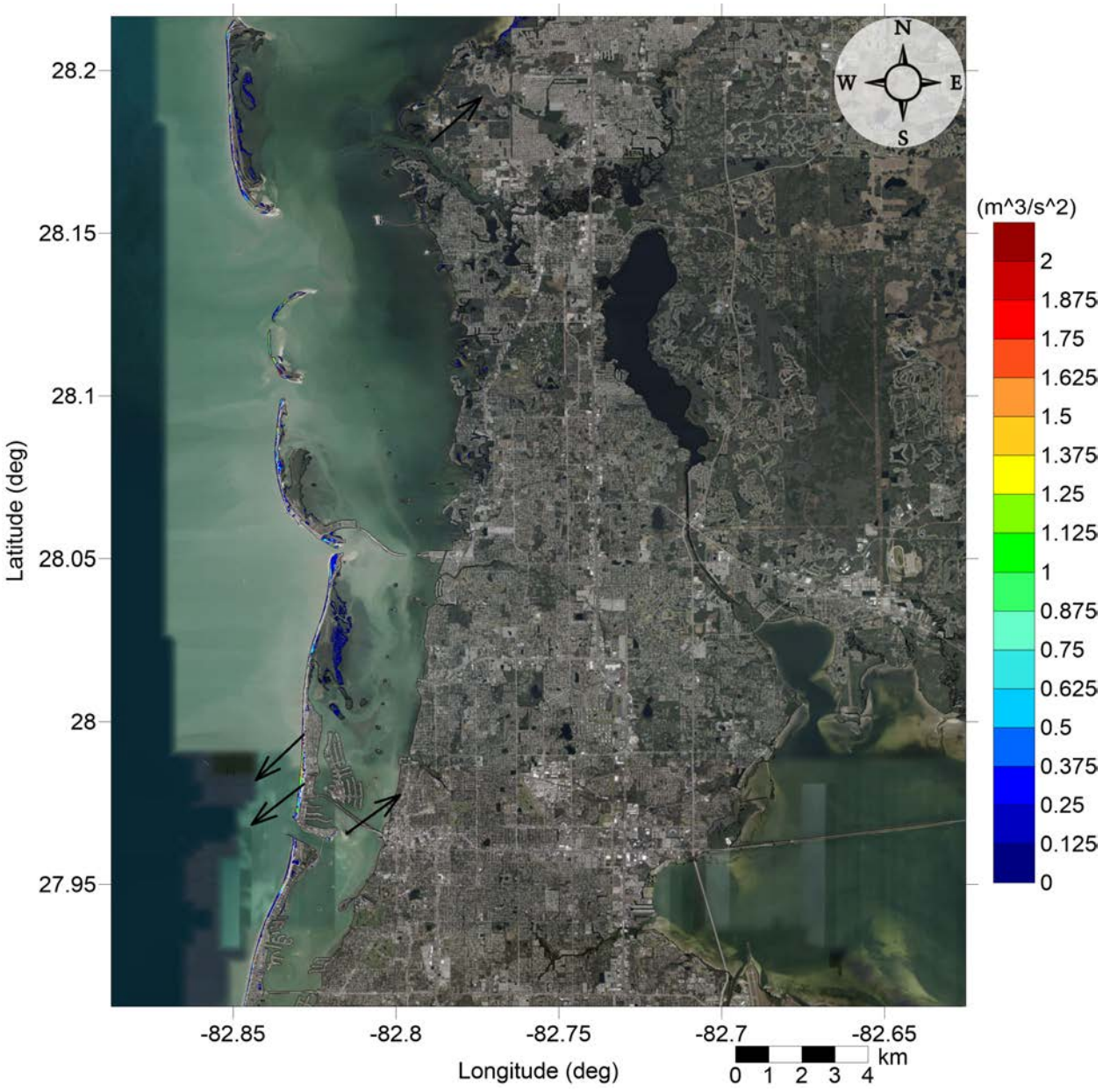

Figure 62: Maximum momentum flux (m^3/s^2) caused by the Probabilistic Submarine Landslide C in Pasco County, FL. Arrows represent direction of maximum momentum flux. Contour drawn is the zero-meter contour for land elevation.

North Tampa Bay, FL
Probabilistic Submarine Landslide C
Maximum Momentum Flux

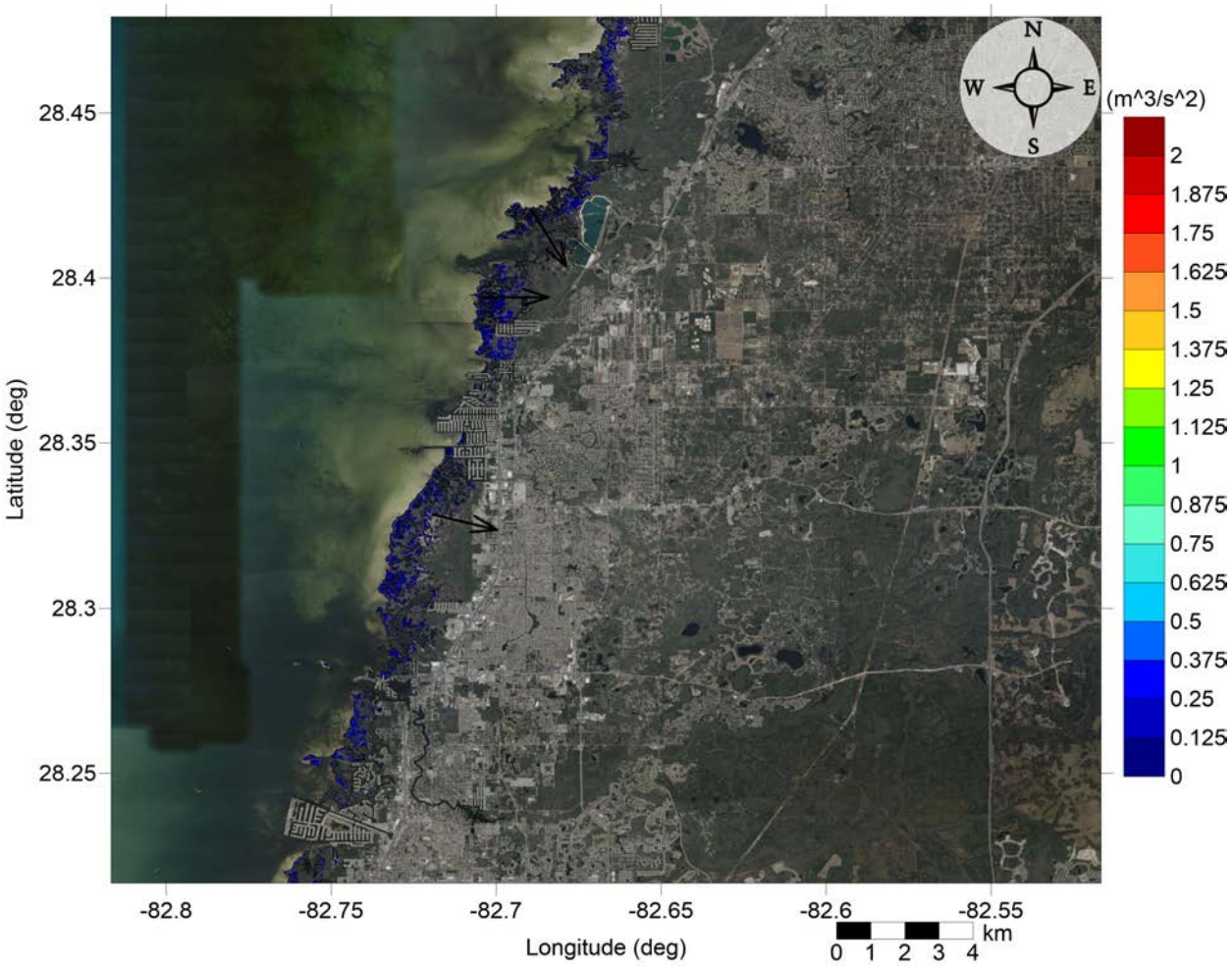

Figure 63: Maximum momentum flux (m^3/s^2) caused by the Probabilistic Submarine Landslide C in North Pinellas County, FL. Arrows represent direction of maximum momentum flux. Contour drawn is the zero-meter contour for land elevation.

North Tampa Bay, FL
Probabilistic Submarine Landslide C
Maximum Inundation Depth

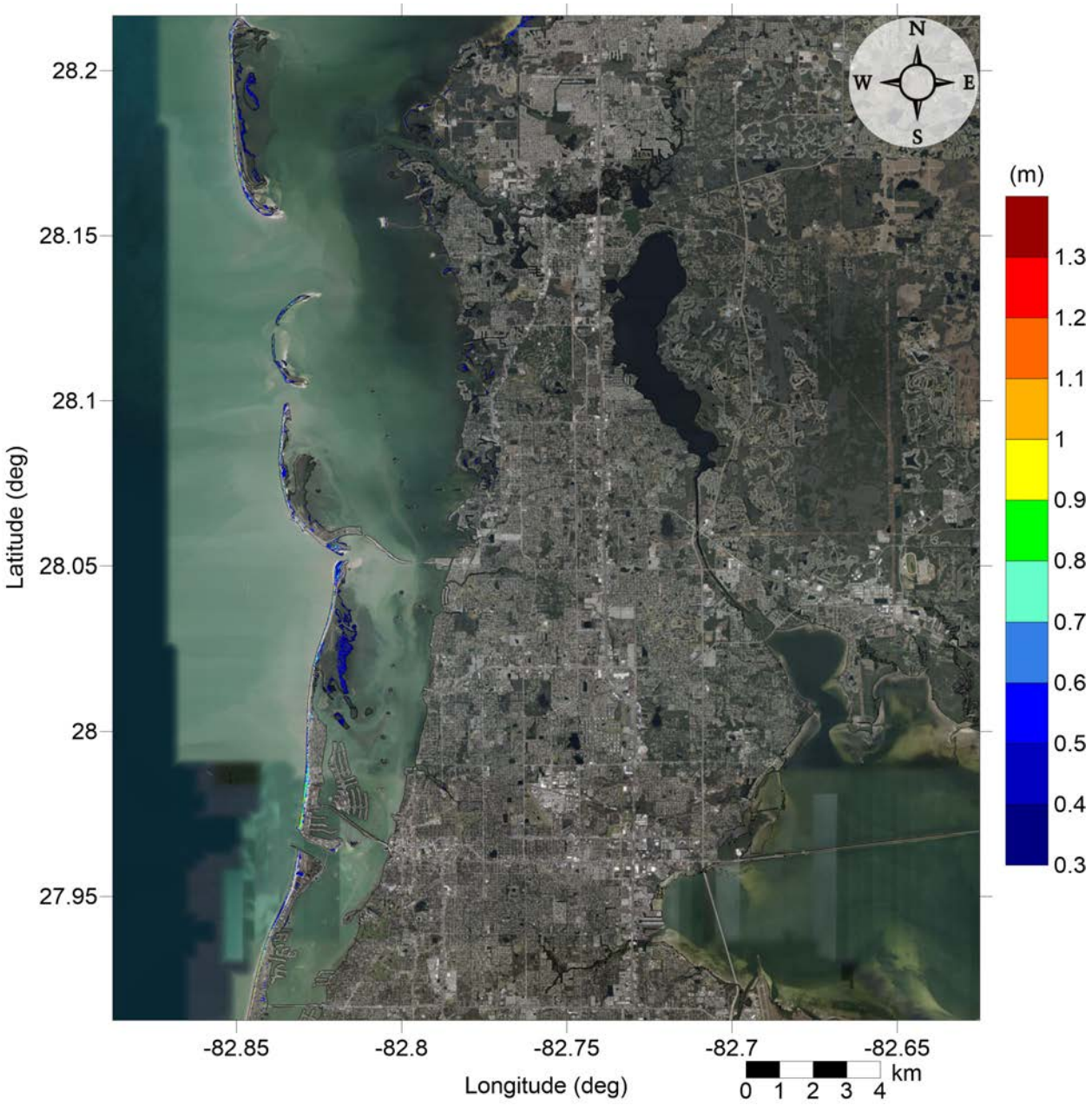

Figure 64: Maximum inundation depth (m) caused by the Probabilistic Submarine Landslide C in Pasco County, FL. Contour drawn is the zero-meter contour for land elevation.

North Tampa Bay, FL
Probabilistic Submarine Landslide C
Maximum Inundation Depth

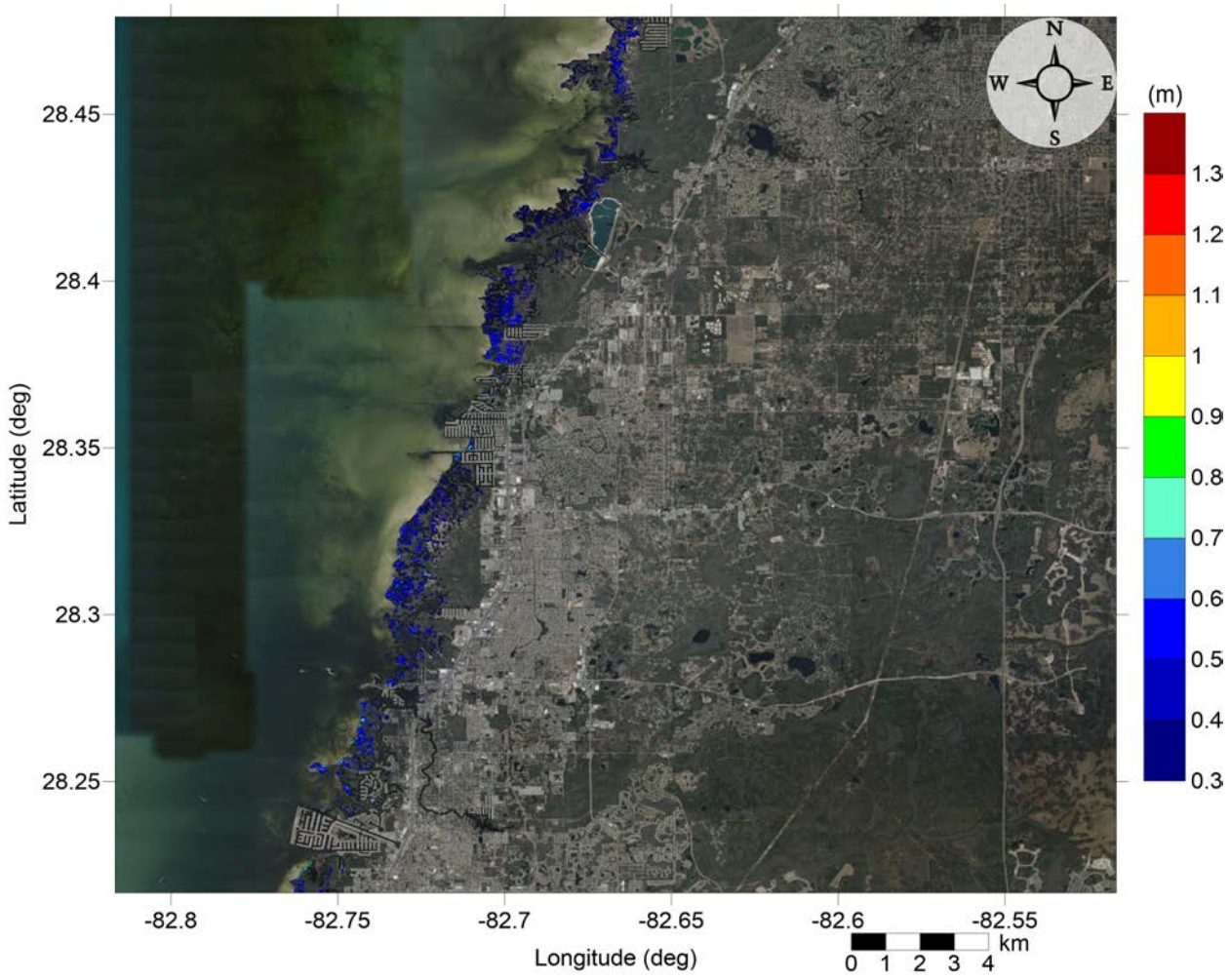

Figure 65: Maximum inundation depth (m) caused by the Probabilistic Submarine Landslide C in North Pinellas County, FL. Contour drawn is the zero-meter contour for land elevation.

North Tampa Bay, FL
West Florida submarine landslide
Maximum Momentum Flux

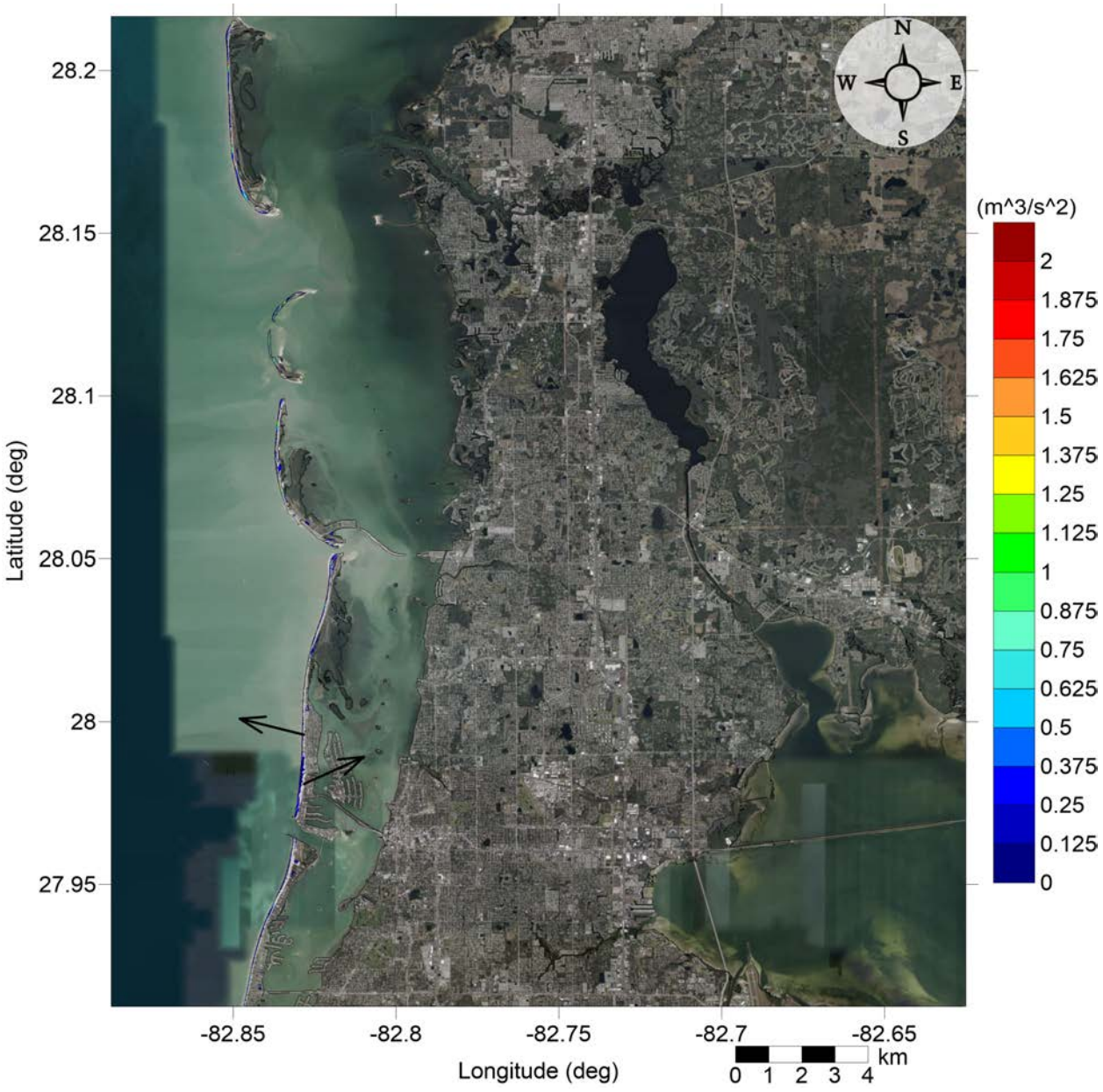

Figure 66: Maximum momentum flux (m^3/s^2) caused by the West Florida submarine landslide in Pasco County, FL. Arrows represent direction of maximum momentum flux. Contour drawn is the zero-meter contour for land elevation.

North Tampa Bay, FL
West Florida submarine landslide
Maximum Momentum Flux

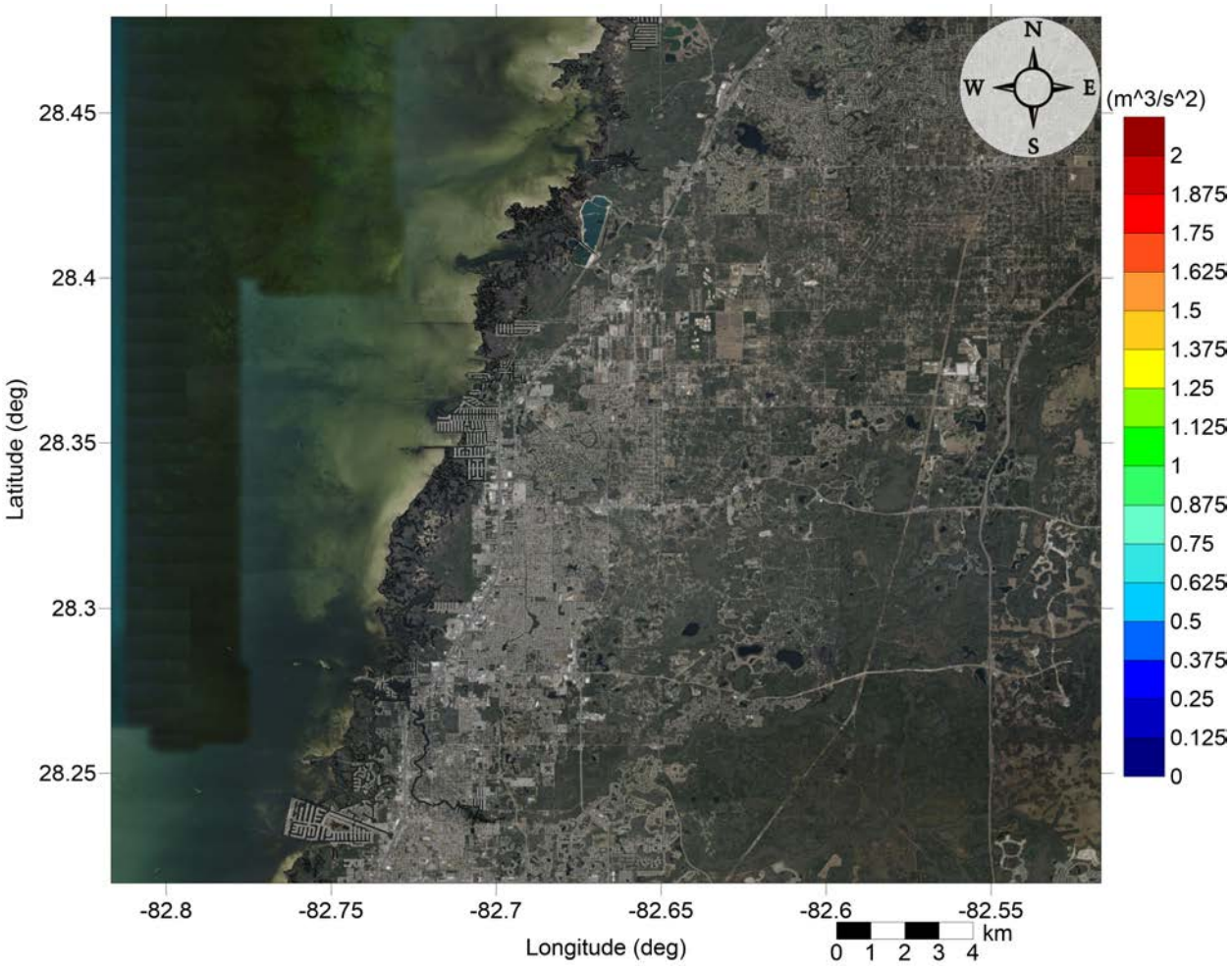

Figure 67: Maximum momentum flux (m^3/s^2) caused by the West Florida submarine landslide in North Pinellas County, FL. Arrows represent direction of maximum momentum flux. Contour drawn is the zero-meter contour for land elevation.

North Tampa Bay, FL
West Florida submarine landslide
Maximum Inundation Depth

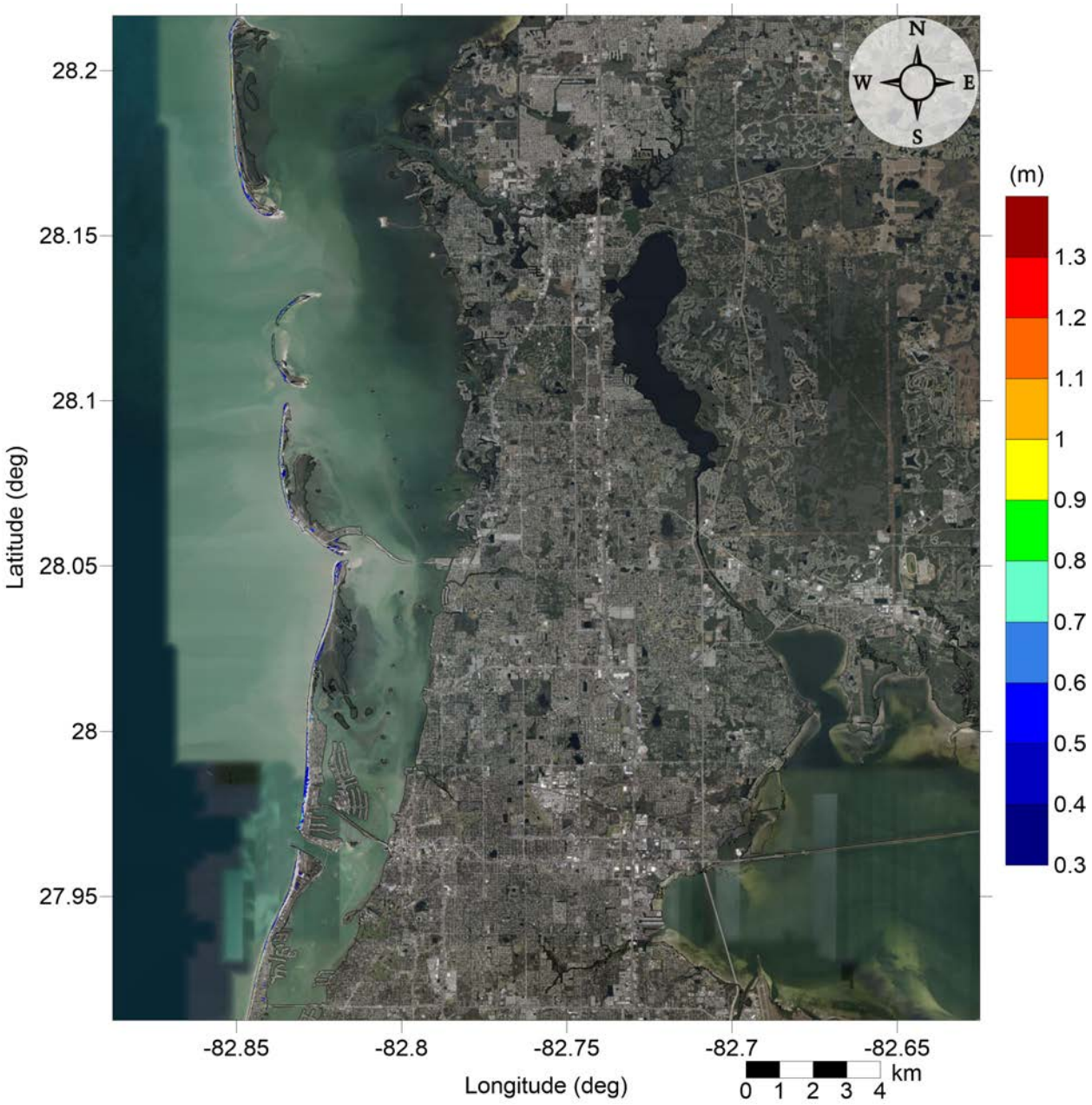

Figure 68: Maximum inundation depth (m) caused by the West Florida submarine landslide in Pasco County, FL. Contour drawn is the zero-meter contour for land elevation.

North Tampa Bay, FL
West Florida submarine landslide
Maximum Inundation Depth

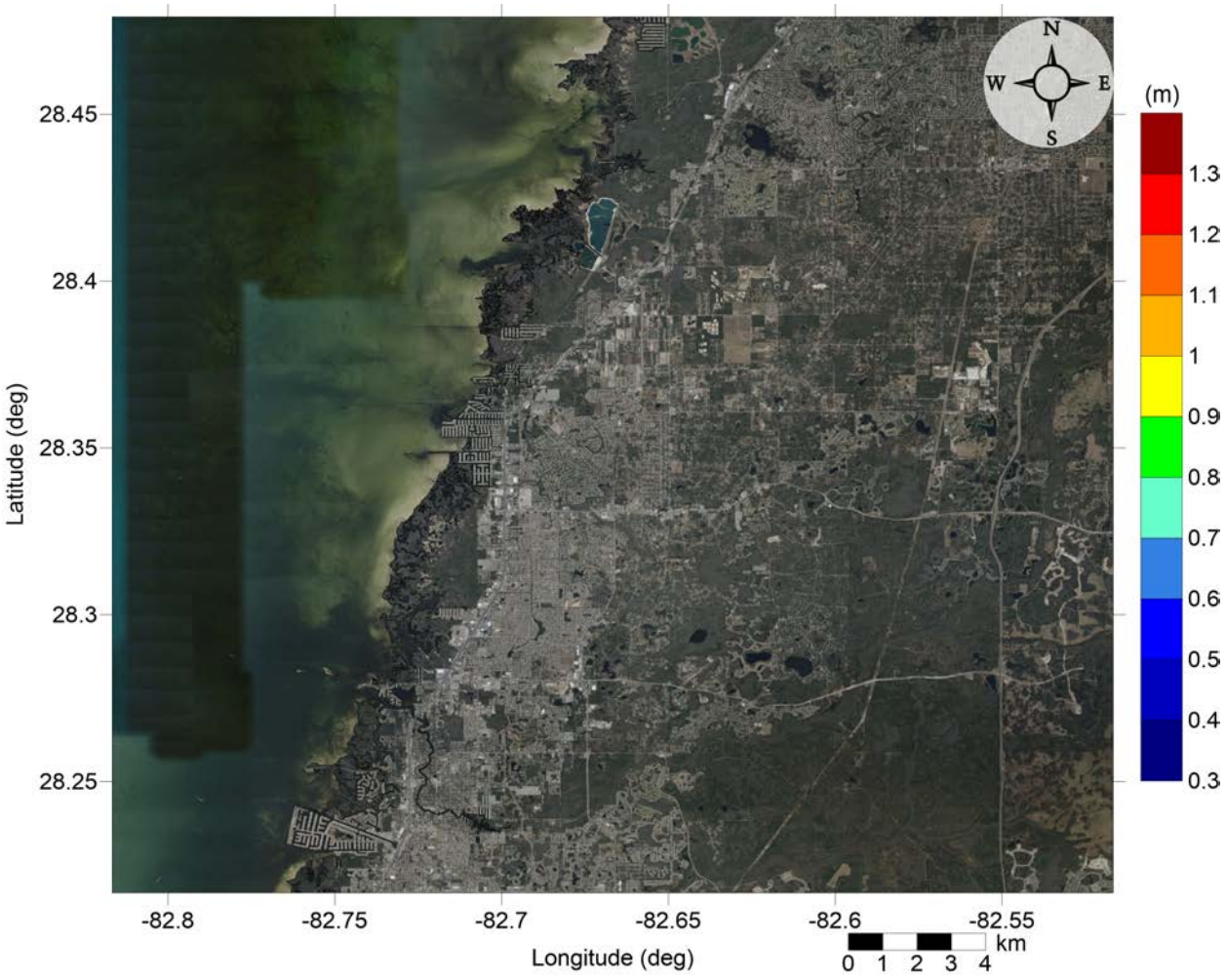

Figure 69: Maximum inundation depth (m) caused by the West Florida submarine landslide in North Pinellas County, FL. Contour drawn is the zero-meter contour for land elevation.

North Tampa Bay, FL
Yucatán 3 submarine landslide
Maximum Momentum Flux

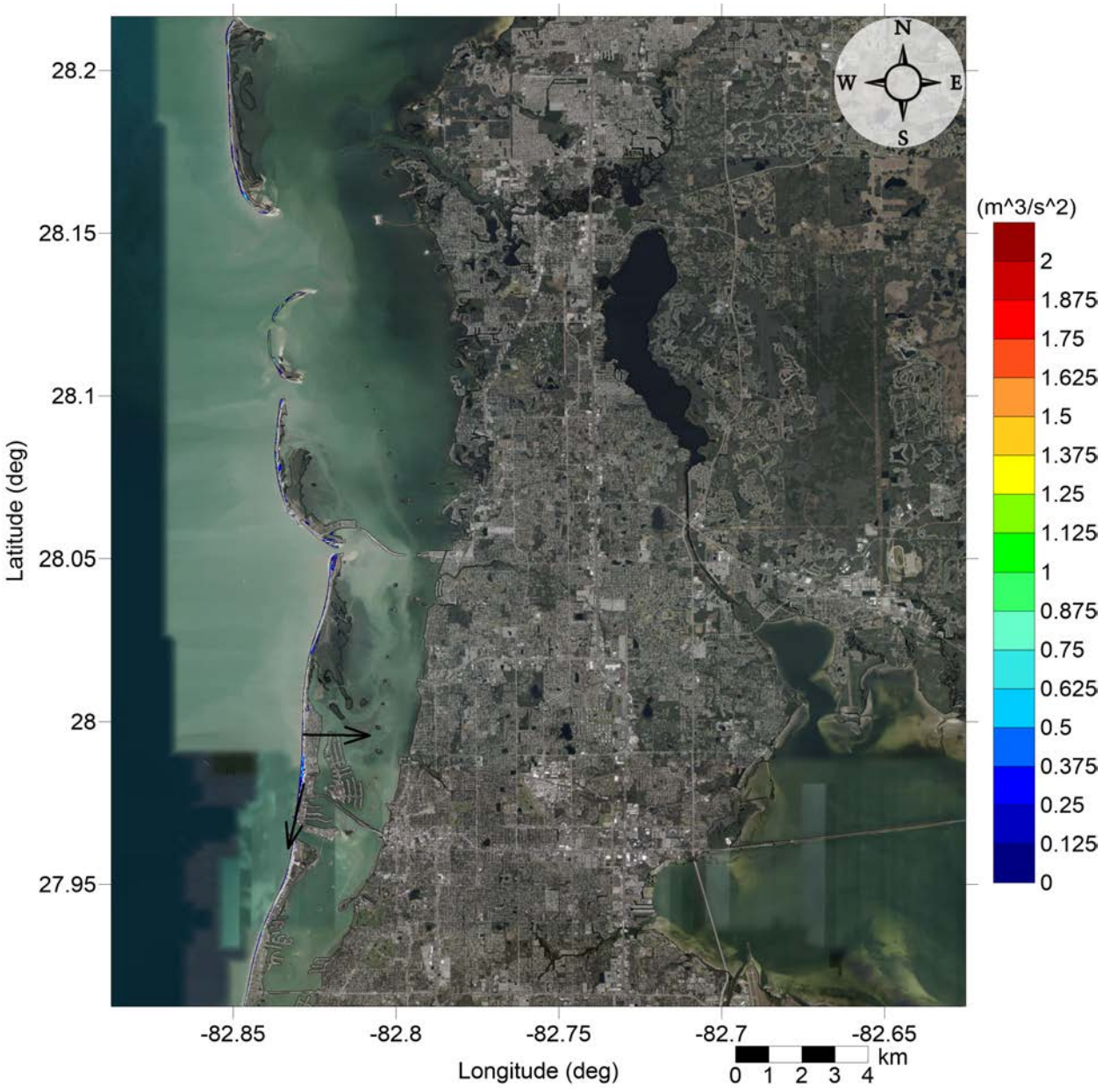

Figure 70: Maximum momentum flux (m^3/s^2) caused by the Yucatán 3 submarine landslide in Pasco County, FL. Arrows represent direction of maximum momentum flux. Contour drawn is the zero-meter contour for land elevation.

North Tampa Bay, FL
Yucatán 3 submarine landslide
Maximum Momentum Flux

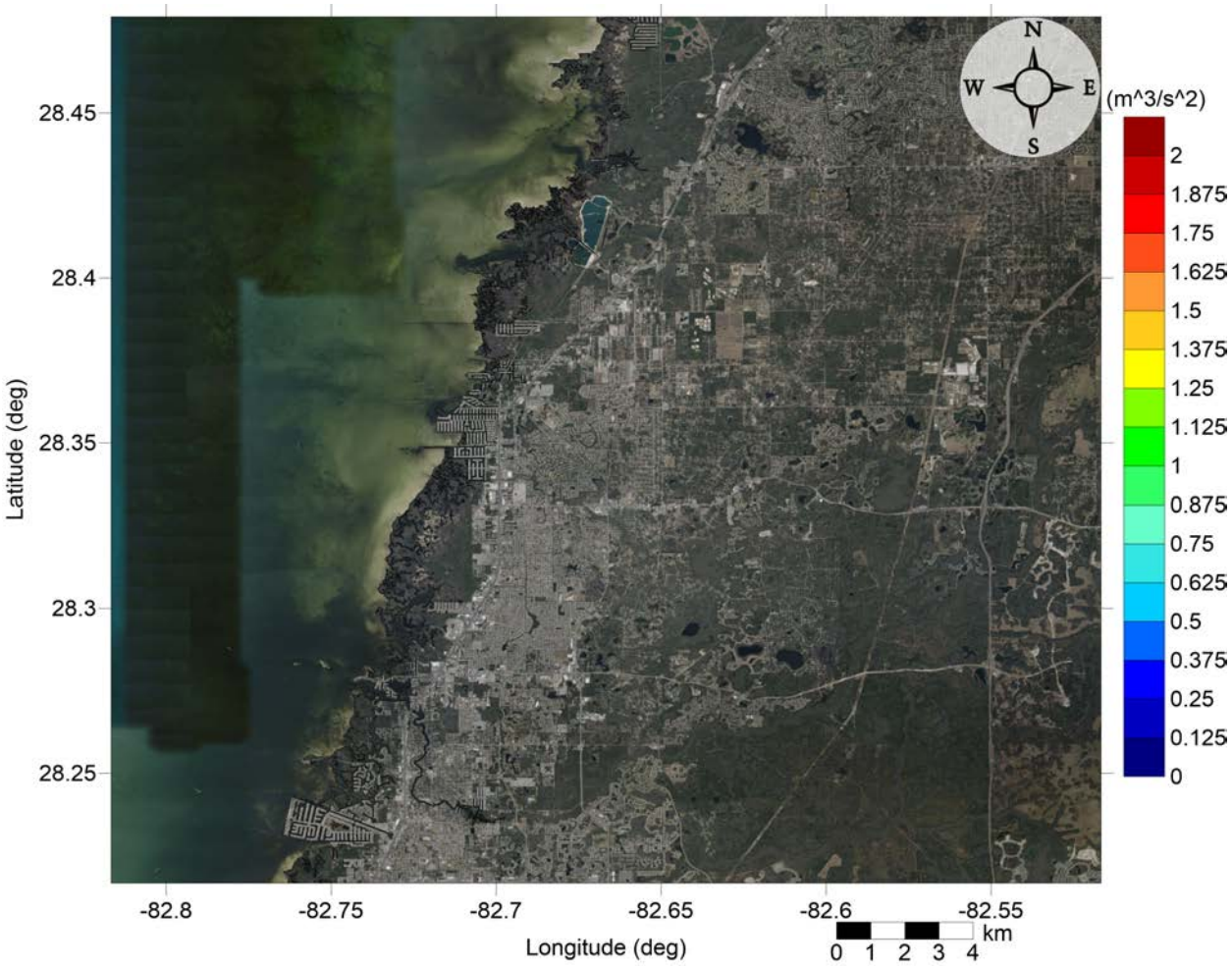

Figure 71: Maximum momentum flux (m^3/s^2) caused by the Yucatán 3 submarine landslide in North Pinellas County, FL. Arrows represent direction of maximum momentum flux. Contour drawn is the zero-meter contour for land elevation.

North Tampa Bay, FL
Yucatán 3 submarine landslide
Maximum Inundation Depth

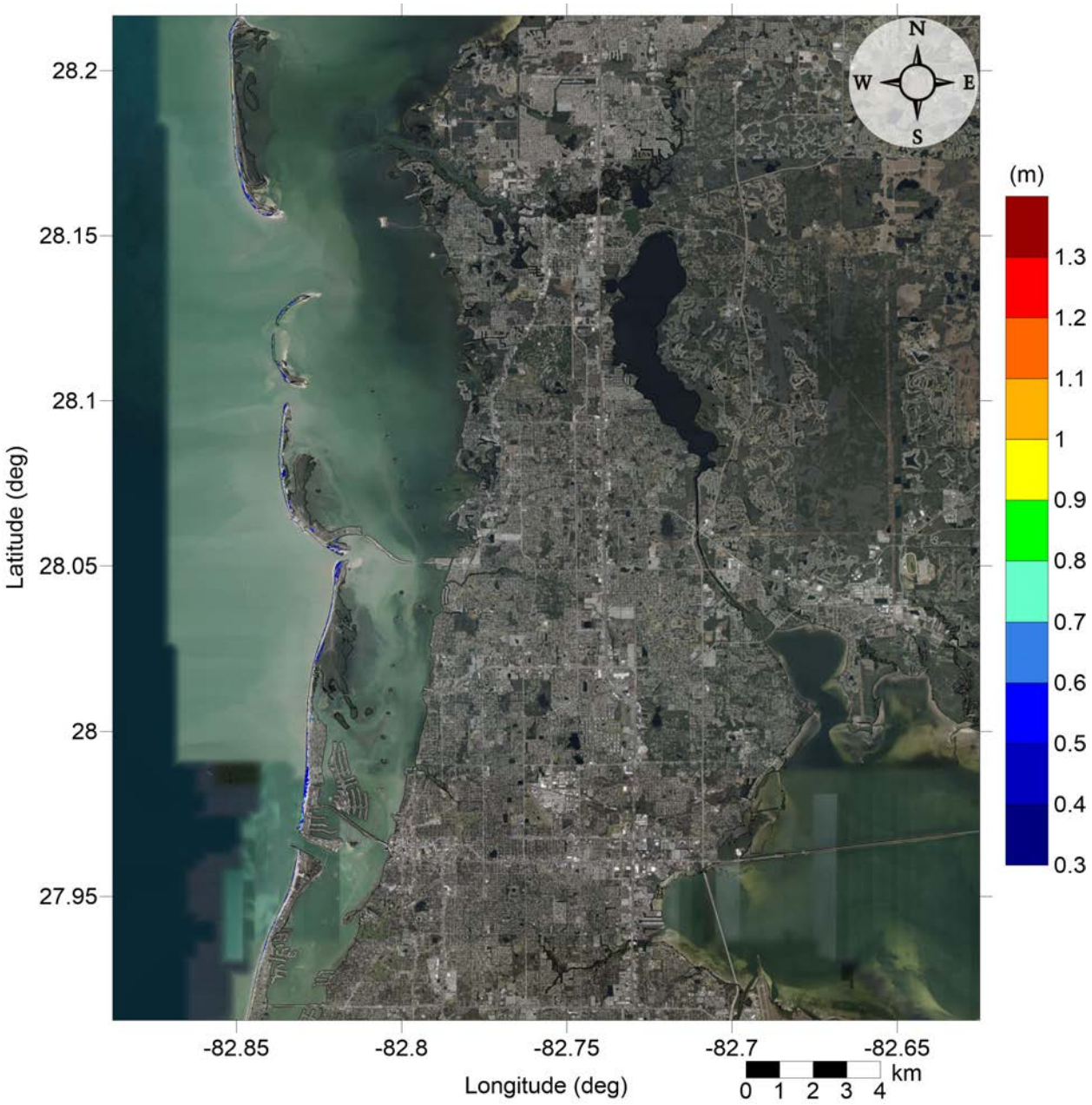

Figure 72: Maximum inundation depth (m) caused by the Yucatán 3 submarine landslide in Pasco County, FL. Contour drawn is the zero-meter contour for land elevation.

North Tampa Bay, FL
Yucatán 3 submarine landslide
Maximum Inundation Depth

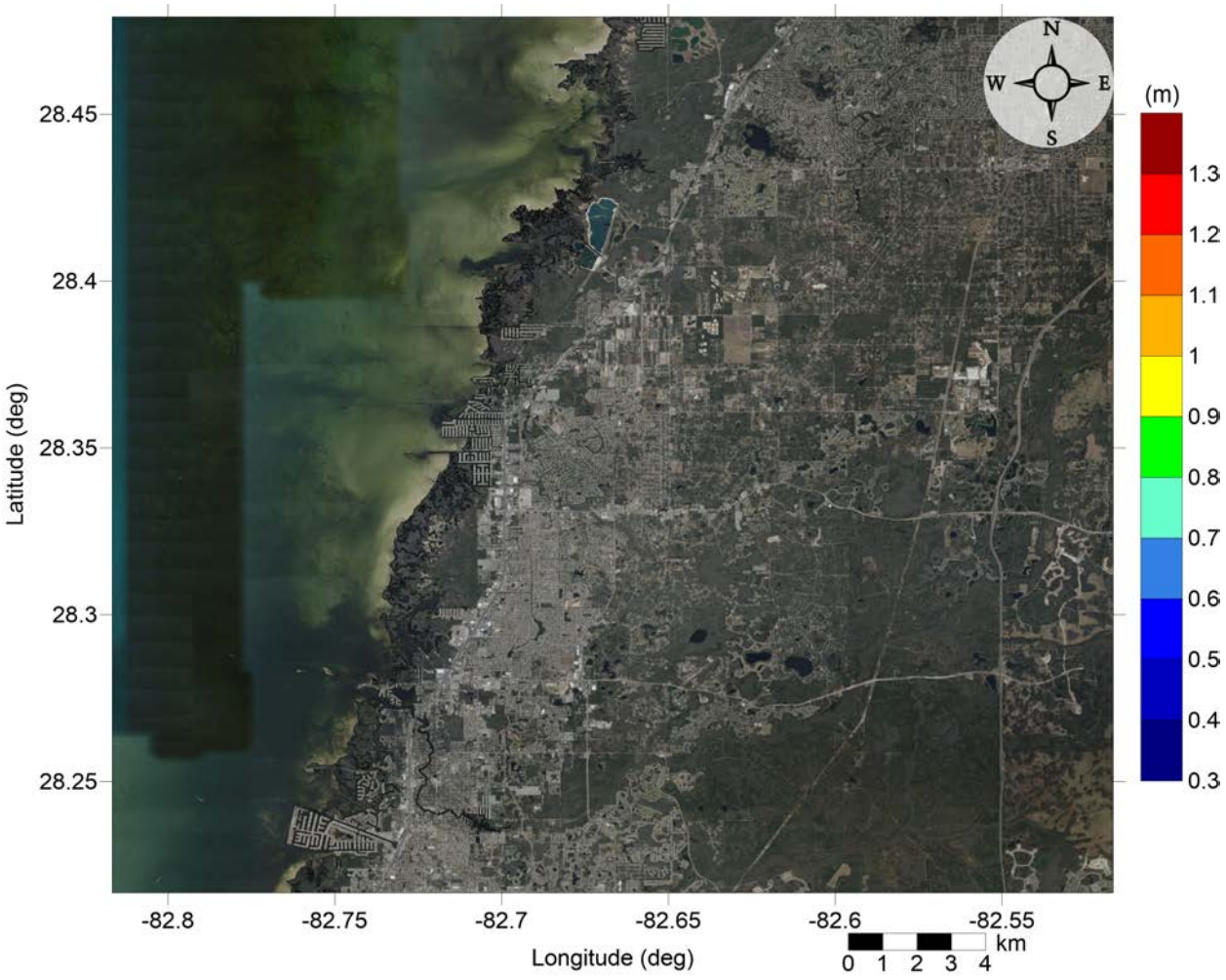

Figure 73: Maximum inundation depth (m) caused by the Yucatán 3 submarine landslide in North Pinellas County, FL. Contour drawn is the zero-meter contour for land elevation.

North Tampa Bay, FL
Yucatán 5 submarine landslide
Maximum Momentum Flux

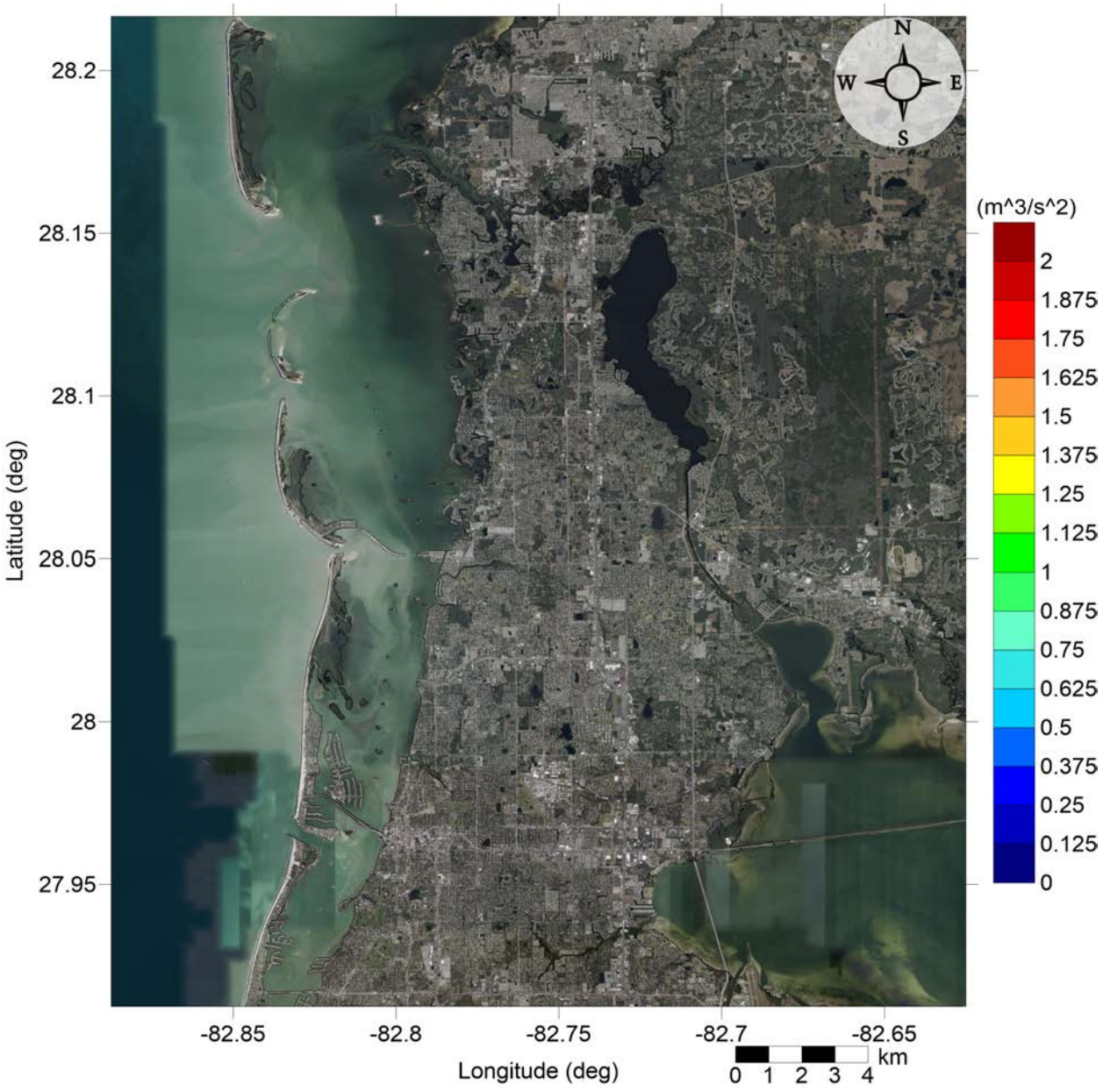

Figure 74: Maximum momentum flux (m^3/s^2) caused by the Yucatán 5 submarine landslide in Pasco County, FL. Arrows represent direction of maximum momentum flux. Contour drawn is the zero-meter contour for land elevation.

North Tampa Bay, FL
Yucatán 5 submarine landslide
Maximum Momentum Flux

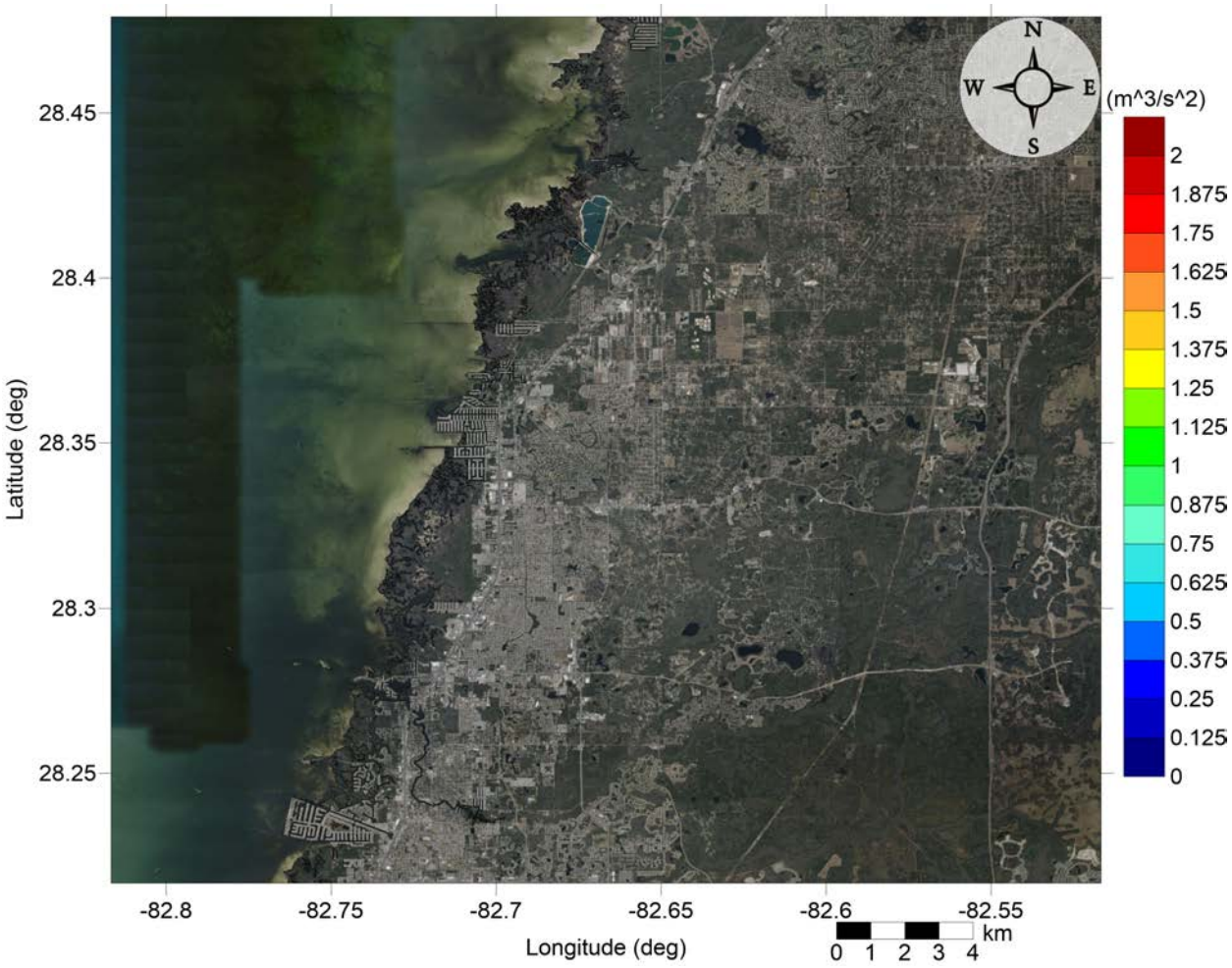

Figure 75: Maximum momentum flux (m^3/s^2) caused by the Yucatán 5 submarine landslide in North Pinellas County, FL. Arrows represent direction of maximum momentum flux. Contour drawn is the zero-meter contour for land elevation.

North Tampa Bay, FL
Yucatán 5 submarine landslide
Maximum Inundation Depth

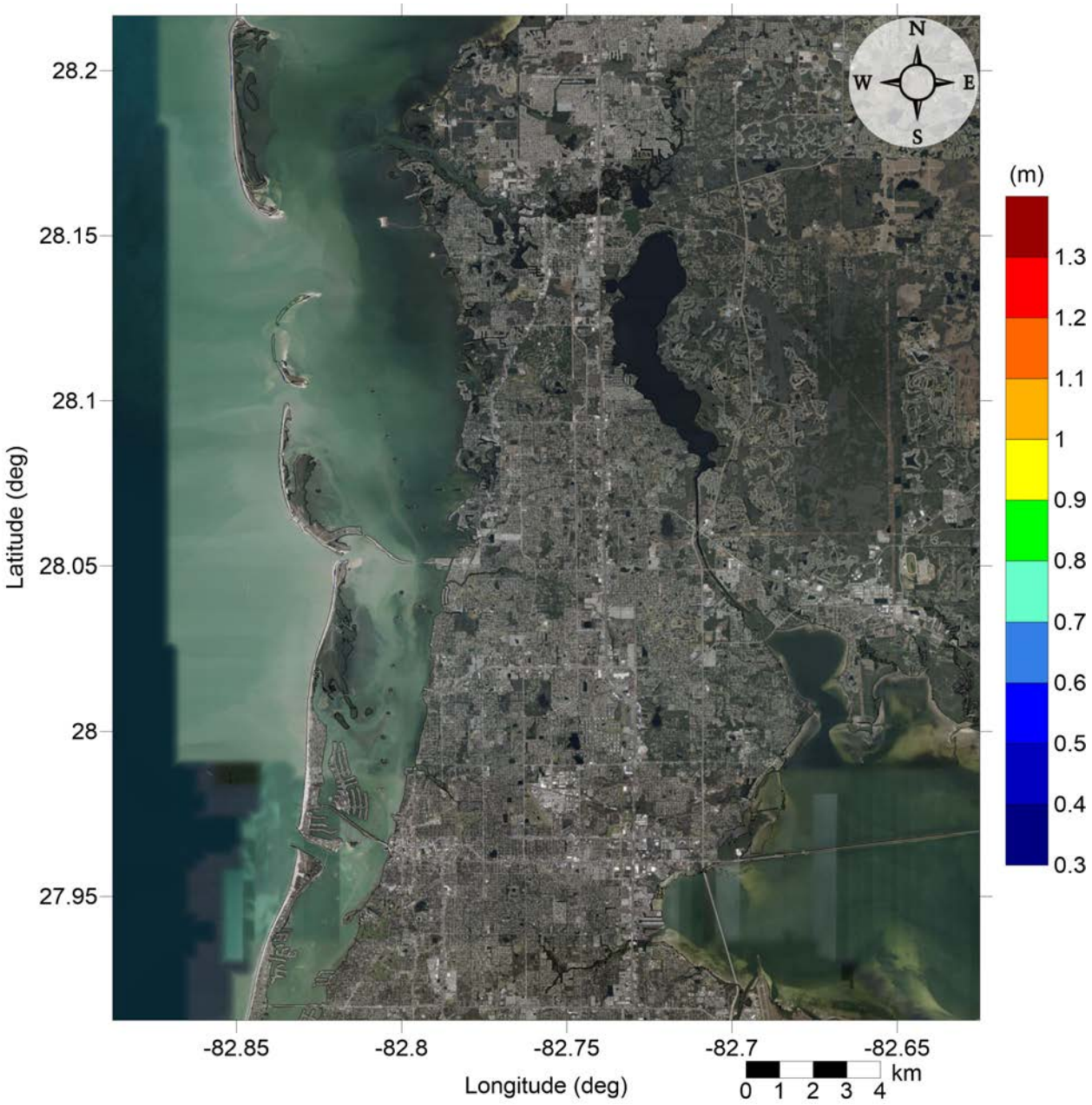

Figure 76: Maximum inundation depth (m) caused by the Yucatán 5 submarine landslide in Pasco County, FL. Contour drawn is the zero-meter contour for land elevation.

North Tampa Bay, FL
Yucatán 5 submarine landslide
Maximum Inundation Depth

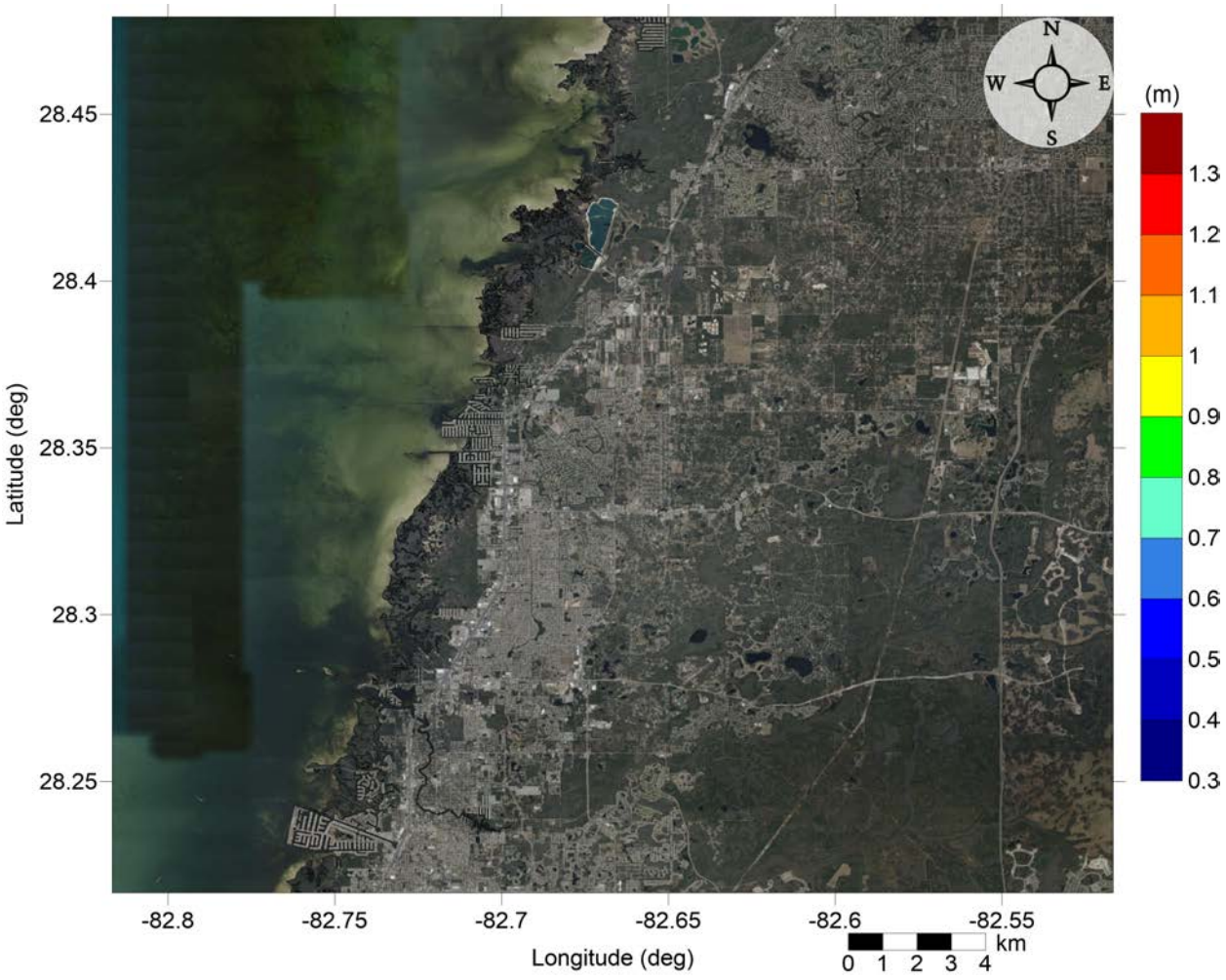

Figure 77: Maximum inundation depth (m) caused by the Yucatán 5 submarine landslide in North Pinellas County, FL. Contour drawn is the zero-meter contour for land elevation.

North Tampa Bay, FL
All Sources
Maximum of Maximum Inundation Depth

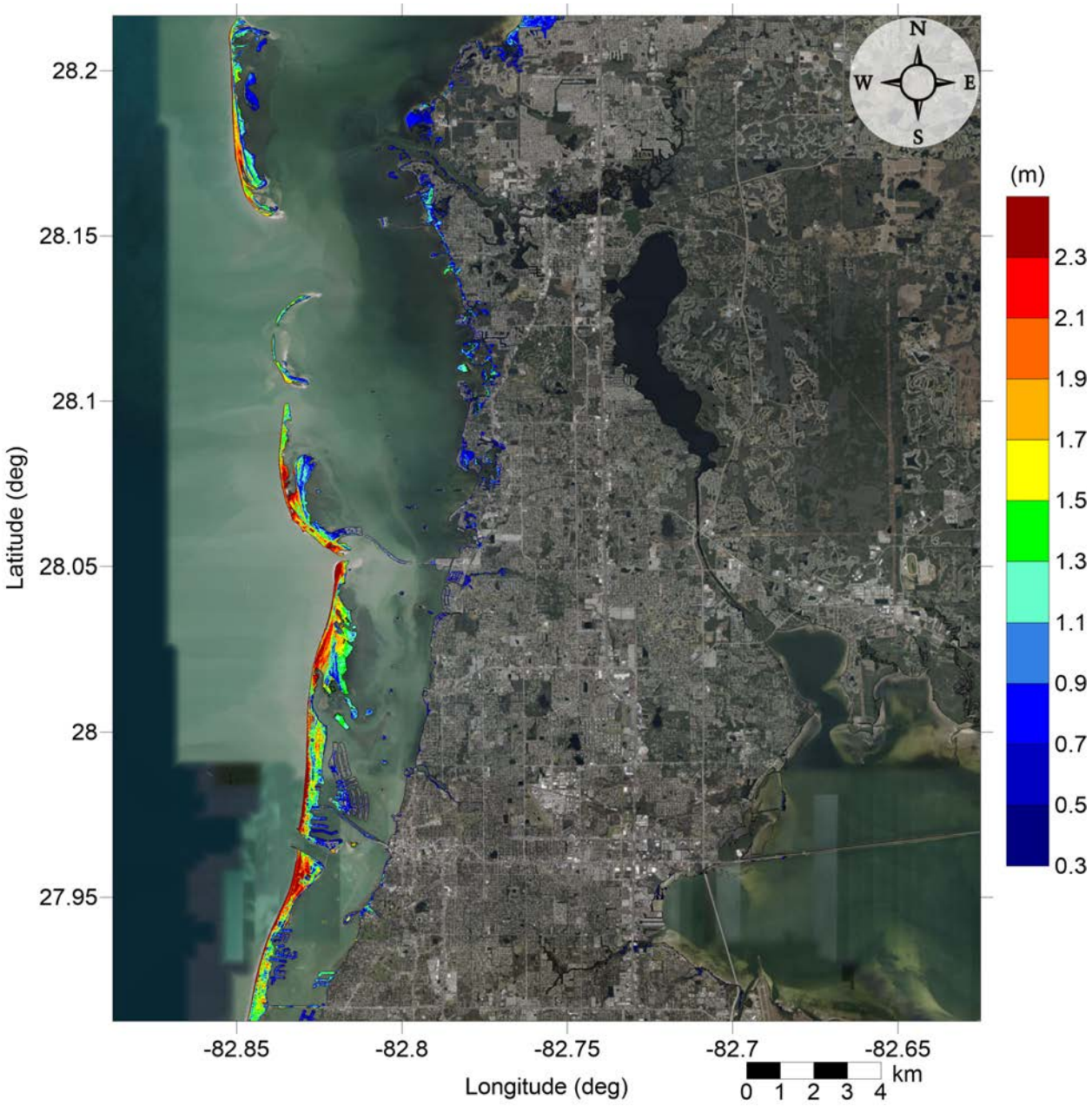

Figure 78: Maximum of maximums inundation depth (m) in Pasco County, FL, calculated as the maximum inundation depth in each grid cell from an ensemble of all tsunami sources considered. Contour drawn is the zero-meter contour for land elevation.

North Tampa Bay, FL
All Sources
Maximum of Maximum Inundation Depth

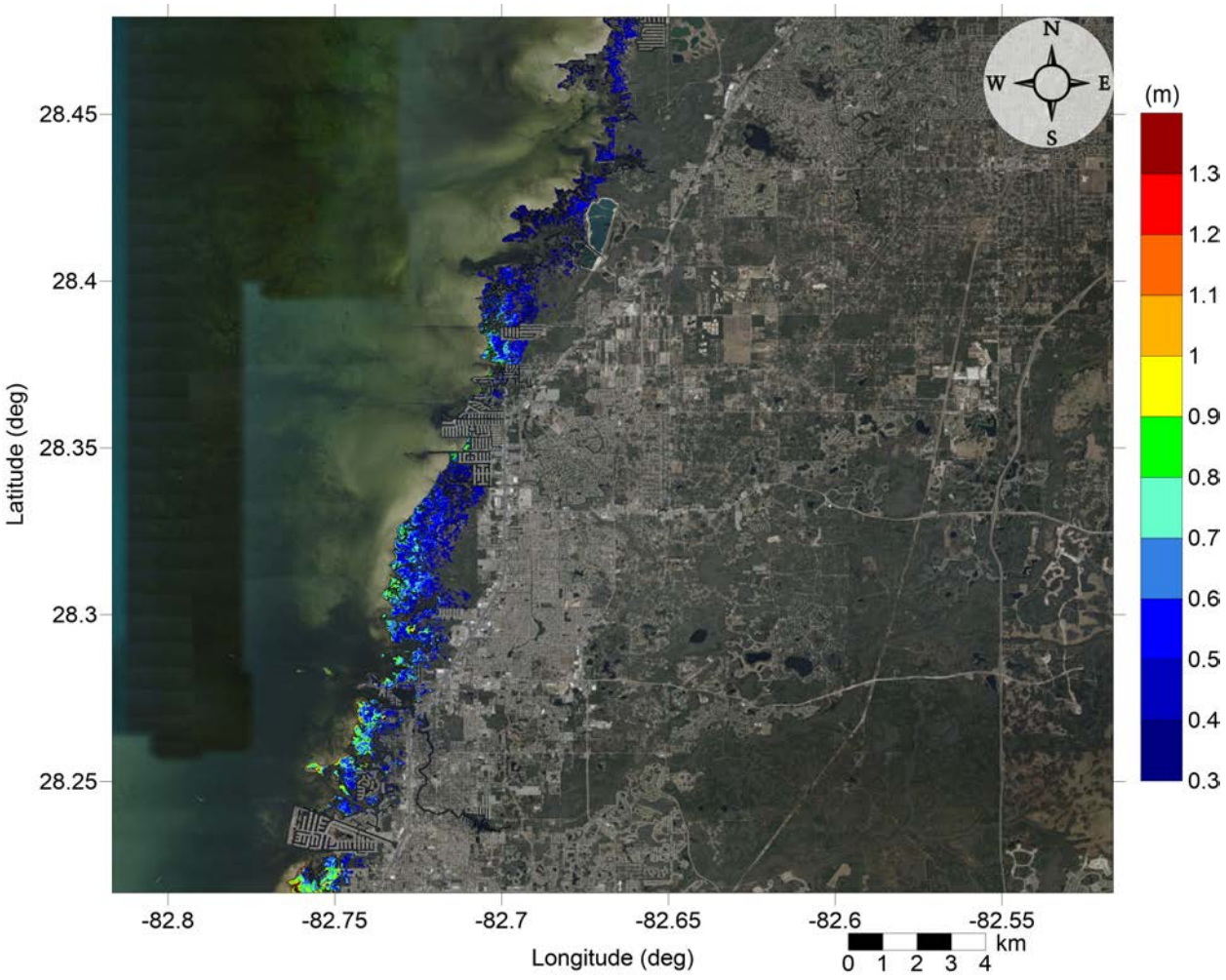

Figure 79: Maximum of maximums inundation depth (m) in North Pinellas County, FL, calculated as the maximum inundation depth in each grid cell from an ensemble of all tsunami sources considered. Contour drawn is the zero-meter contour for land elevation.

North Tampa Bay, FL
All Sources
Maximum Inundation Depth by Source

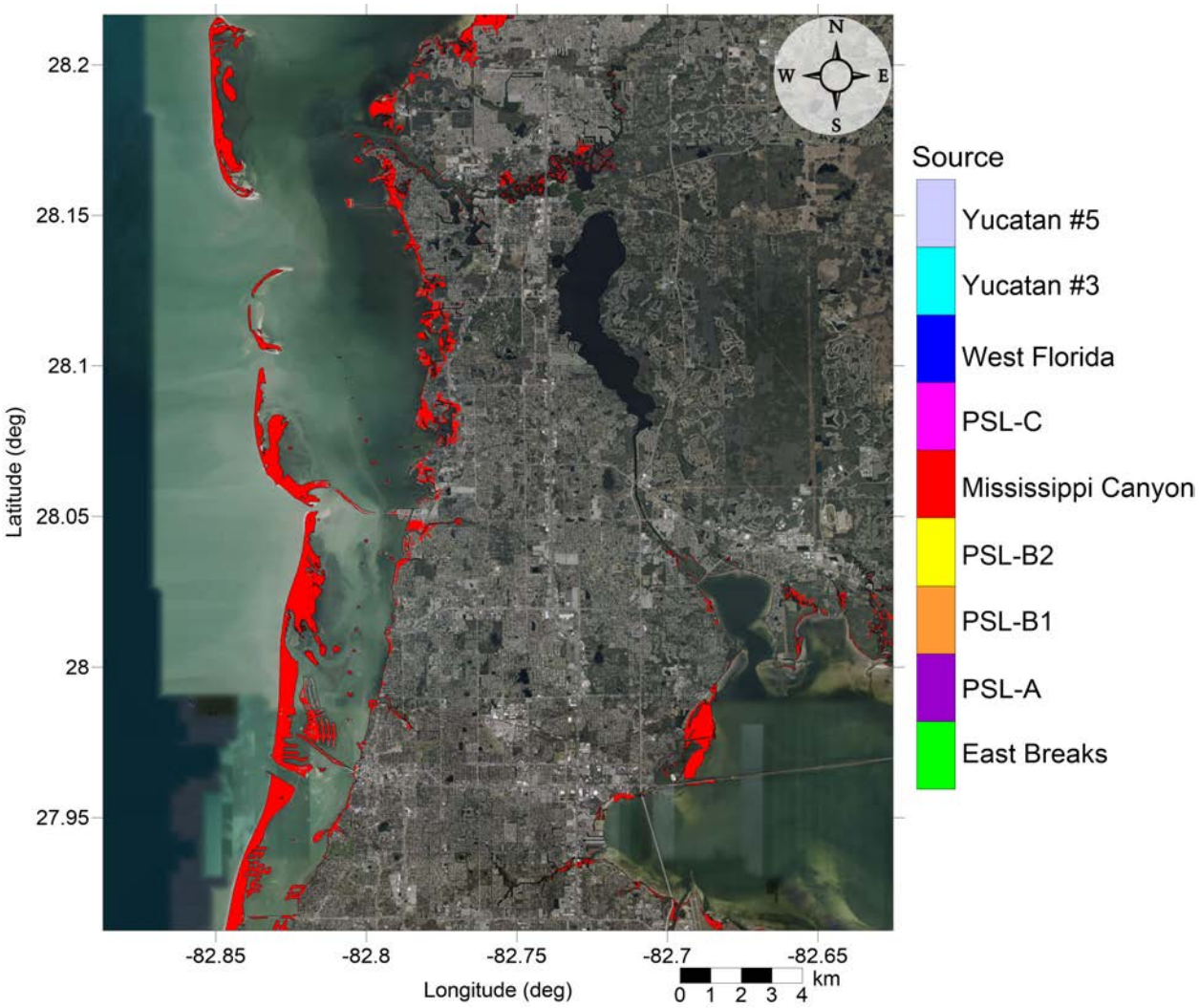

Figure 80: Indication of the tsunami source which causes the maximum of maximums inundation depth (m) in each grid cell from an ensemble of all tsunami sources in Pasco County, FL. Contour drawn is the zero-meter contour for land elevation.

North Tampa Bay, FL
All Sources
Maximum Inundation Depth by Source

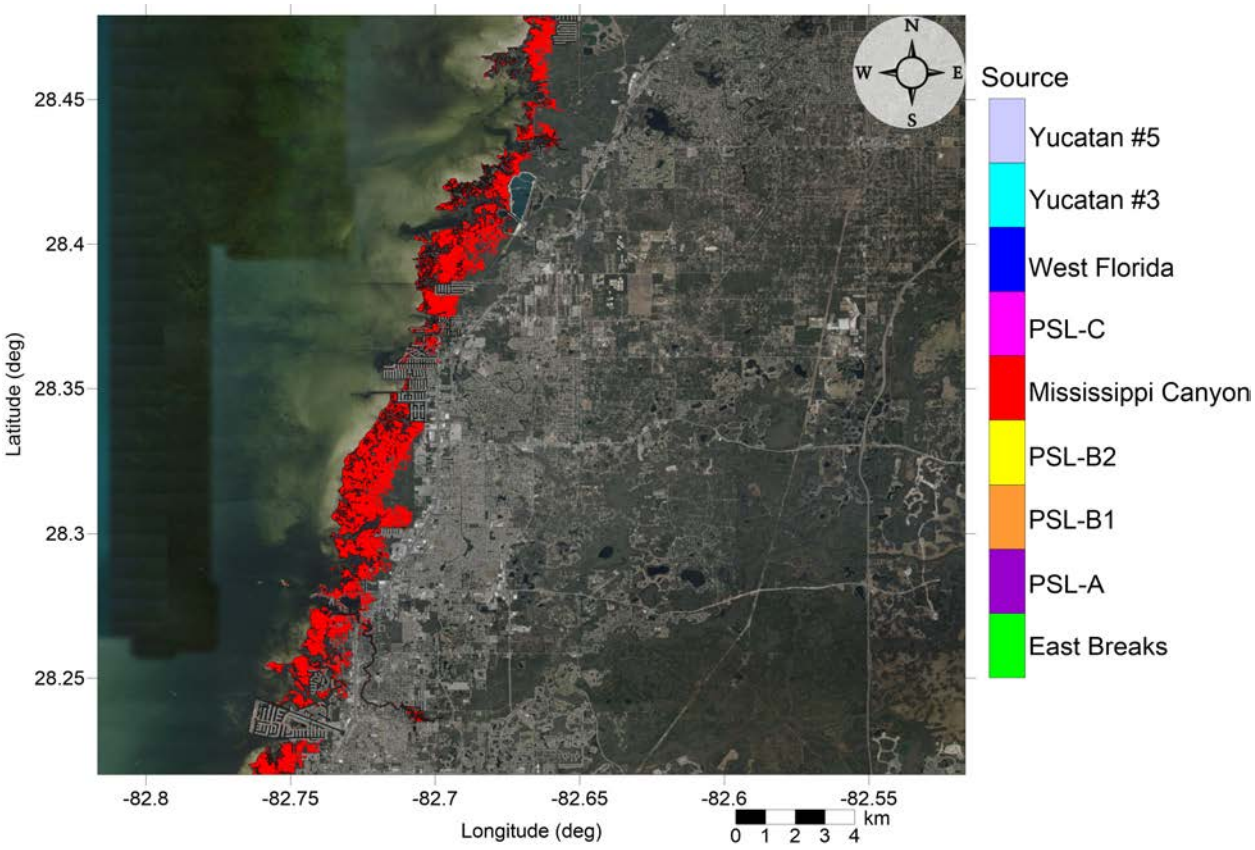

Figure 81: Indication of the tsunami source which causes the maximum of maximums inundation depth (m) in each grid cell from an ensemble of all tsunami sources in North Pinellas County, FL. Contour drawn is the zero-meter contour for land elevation.

5 Tsunami and Hurricane Storm Surge Inundation

Due to the limitations on availability of high-resolution (1/3 arcsecond) DEMs, detailed inundation maps for all communities along the Gulf Coast are not yet possible. In an effort to develop a first-order estimate of potential tsunami inundation for those locations where detailed inundation maps have not yet been developed, we compare tsunami inundation modeled for the communities mentioned above to hurricane storm surge modeled data. The motivation for and implications of this approach are twofold. It provides a way to assess tsunami inundation in unmapped communities based on existing storm surge flood data and also relates the level of tsunami hazard to that of another hazard that is better defined in this region. Tsunamis are not well-understood as a threat along the Gulf Coast, making tsunami hazard mitigation efforts somewhat difficult. However, hurricane is a relatively well-understood threat in this region, and hurricane preparedness approaches are well-developed. As a result, comparisons of tsunami and hurricane storm surge inundation levels provide a more understandable and accessible idea of the level of hazard presented by potential tsunami events and can serve as a basis for tsunami preparedness efforts.

The hurricane storm surge data used here is available from the Sea, Lake, and Overland Surges from Hurricanes (SLOSH) model (http://www.nhc.noaa.gov/surge/slosh.php). The SLOSH model was developed by the National Weather Service (NWS) to provide estimates of storm surge heights caused by historical, predicted, or hypothetical hurricanes based on different values for atmospheric pressure, hurricane size, forward speed, and track. It uses a polar, elliptical, or hyperbolic grid for computations, leading to higher resolutions near coastal areas of interest. Some limitations of the SLOSH model should be acknowledged. Resolution of the model varies from tens of meters to a kilometer or more. Near the coastal communities of interest here, resolution is on the order of 1 km. Sub-grid scale water and topographic features such as channels, rivers, levees, and roads, are parameterized instead of being explicitly modeled. Despite these limitations, the hurricane storm surge data from the SLOSH model is currently the best data publicly available for our purposes, and efforts have been made to ensure the validity of the SLOSH data in performing comparisons with tsunami inundation.

The SLOSH MOM results provide the worst-case storm surge for a given hurricane category and initial tide level based on a set of model runs with various combinations of parameters such as forward speed, trajectory, and landfall location. To perform the storm surge and tsunami comparisons, SLOSH storm surge elevation data was first converted to meters and adjusted from the NAVD88 to the MHW vertical datum using NOAA's VDatum tool (http://vdatum.noaa.gov/). Due to the relatively low resolution of the SLOSH data as compared to the DEMs used for tsunami modeling, the SLOSH data was interpolated to 1/3 arcsecond (10 m) resolution using a kriging method. Inundation was then determined by subtracting land elevation from the storm surge elevation.

Here, an initial high tide level is used for the SLOSH MOM results in order to compare the worst-case tsunami inundation with a worst-case storm surge scenario. The high tide SLOSH MOM data includes effects of the highest predicted tide level at each location. In comparison, water elevations in the tsunami modeling are based on the MHW datum, which averages the high water levels over the National Tidal Datum Epoch (NTDE). Within the

GOM, tidal ranges are relatively small, with diurnal ranges on the order of 1.5 ft (0.5 m) for most of the communities studied here, and slightly higher at around 2.5 ft (0.8 m) for the west coast of Florida. Thus, differences between highest tide levels and the mean of the highest tide levels are expected to be relatively small, though local bathymetric effects combined with tidal effects can still be significant.

It should be noted that the updated Saffir-Simpson Hurricane Wind Scale which delineates hurricane categories 1-5 does not include storm surge as a component of the measure of hurricane intensity and that other methods may capture the physics of hurricane severity and damage in a more appropriate manner (e.g. Kantha [2006], Basco and Klentzman [2006], Irish and Resio [2010]). However, the SLOSH MOM results take into account thousands of scenarios for a given hurricane category, resulting in a composite worst-case storm surge scenario for each Saffir-Simpson hurricane category. Thus, since hurricane preparedness, storm surge evacuation zones, and hazard mitigation efforts are based on hurricane category assignment, we aim to determine the hurricane category which produces MOM storm surge inundation ζ_h that is a best match to the tsunami MOM inundation ζ_t. That is, we determine the hurricane category which satisfies

$$min_c(|\zeta_{h_c} - \zeta_t|), \qquad c = \text{Cat1,..,Cat5} \tag{1}$$

for each grid cell. The inundation level for the best-match category is denoted $\zeta_{h_{min}}$. The actual difference between hurricane and tsunami inundation levels $\Delta\zeta = \zeta_{h_{min}} - \zeta_t$ then indicates how close of a match the best-match category actually is. Thus, positive values of $\Delta\zeta$ indicate where hurricane storm surge inundation is higher than tsunami inundation, and negative values indicate where tsunami inundation is higher. A common local practice in tsunami modeling is to only consider inundation above a threshold of 0.3 m (1 ft) [Horrillo et al., 2011, 2015]. This is due to the extensive flat and low-lying elevation found along the Gulf Coast. All depths are calculated for tsunami inundation modeling, but inundation less than 0.3 m (1 ft) is considered negligible here for inundation mapping purposes. Thus, comparisons are only made where either the tsunami or hurricane MOM inundation is at least 0.3 m (1 ft). Results for the two selected Gulf Coast communities are given in the following subsections. It is possible that tsunami inundation zone has no hurricane flooding, therefore matching with hurricane category cannot be made.

5.1 Rosemary Beach, FL

Miramar Beach, FL

Fig. 38 shows the MOM tsunami inundation affecting from Miramar Beach to Seaside. Under the worst case scenario, the highest inundation (> 4 m) occurs at the immediate ocean front and around the various lakes, and the other potentially at-risk areas would expect less inundation further away from the lakes and the beach. Along the coastline near Miramar Beach, the high inundation appears south of US Highway 98. Around the Choctawhatchee Bay, high inundation (< 2.5 m) mostly appears around the Hogtown Bayou and east of Highway 331 bridge, which are caused by tsunami waves coming in from bay inlet, instead

of overtopping water over the barrier island. The Mississippi Canyon landslide is responsible for the MOM inundation (see Fig. 40).

The hurricane category which best matches the tsunami inundation in Miramar Beach, FL is shown in Fig. 82, and Fig. 83 shows $\Delta\zeta$ for the best-matching hurricane category satisfying Eq. 1. The hurricane category that best matches tsunami inundation closely follows the MOM tsunami inundation trend. Category 5 appears near the beach and around Highway 98. Category 3 appears around the Choctawhatchee Bay and Category 4 mostly appears between Category 3 and 5. The difference between hurricane flooding and tsunami inundation is mostly within ± 1 m for Category 3 and 4, but < 3 m for Category 5, indicating that tsunami inundation greatly exceeds that of the most severe storms.

Panama City Beach, FL

Fig. 39 shows the MOM tsunami inundation affecting Panama City Beach, FL. Overall water depth exhibits decreasing trend from oceanfront toward the inland, with maximum over 4 m. The tsunami inundation is mostly contained south of E County Highway 30A (from Eastern Lake to Rosemary Beach) and Panama City Beach Parkway (from Rosemary Beach to Panama City Beach), while penetrating deeper inland via the various lakes (Eastern Lake, Deer Lake, Camp Creek Lake and the biggest Powell Lake via Philips Inlet). On the west bank of the West Bay, tsunami inundation could reach up to ~ 2 m, which extends upstream the West Bay Creek a few kilometers. The Mississippi Canyon landslide is responsible for the MOM inundation (see Fig. 41).

The hurricane category which best matches the tsunami inundation in Panama City Beach area (grid 5) is shown in Fig. 84, and Fig. 85 shows $\Delta\zeta$ for the best-matching hurricane category satisfying Eq. 1. The hurricane category that best matches tsunami inundation closely follows the MOM tsunami inundation trend. On the coast line, tsunami inundation is mostly comparable to Category 5, while Category 4 only appears around the Powell Lake. Category 3 only appear around the Powell Lake. The difference between hurricane flooding and tsunami inundation is mostly within ± 0.5 m for Category 3 around the Powell Lake and can reach over 1 m for other inundated areas.

RosemaryBeach, FL
All Sources
SLOSH Storm Surge and MOM Tsunami Inundation Comparison

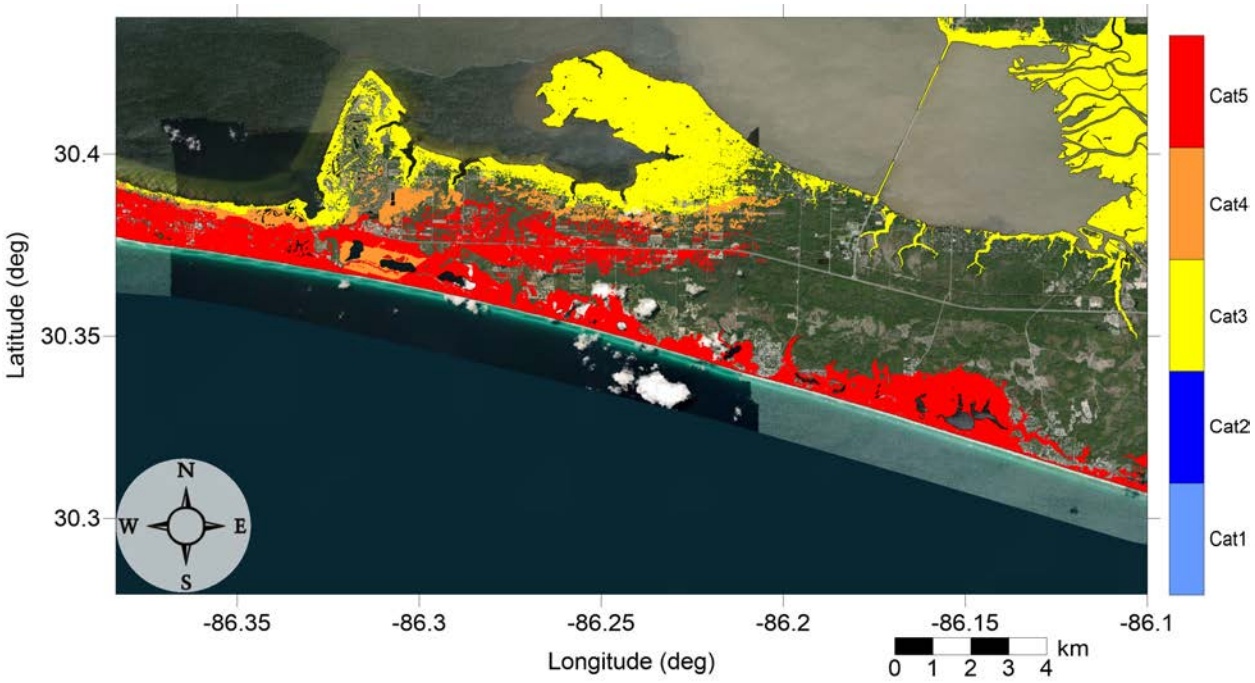

Figure 82: Hurricane category which produces inundation at high tide that best matches the MOM tsunami inundation shown in Figure 83 for Miramar Beach, FL. The contours drawn and labeled are at -5 m, -10 m, and -15 m levels.

RosemaryBeach, FL
All Sources
SLOSH Storm Surge and MOM Tsunami Inundation Comparison

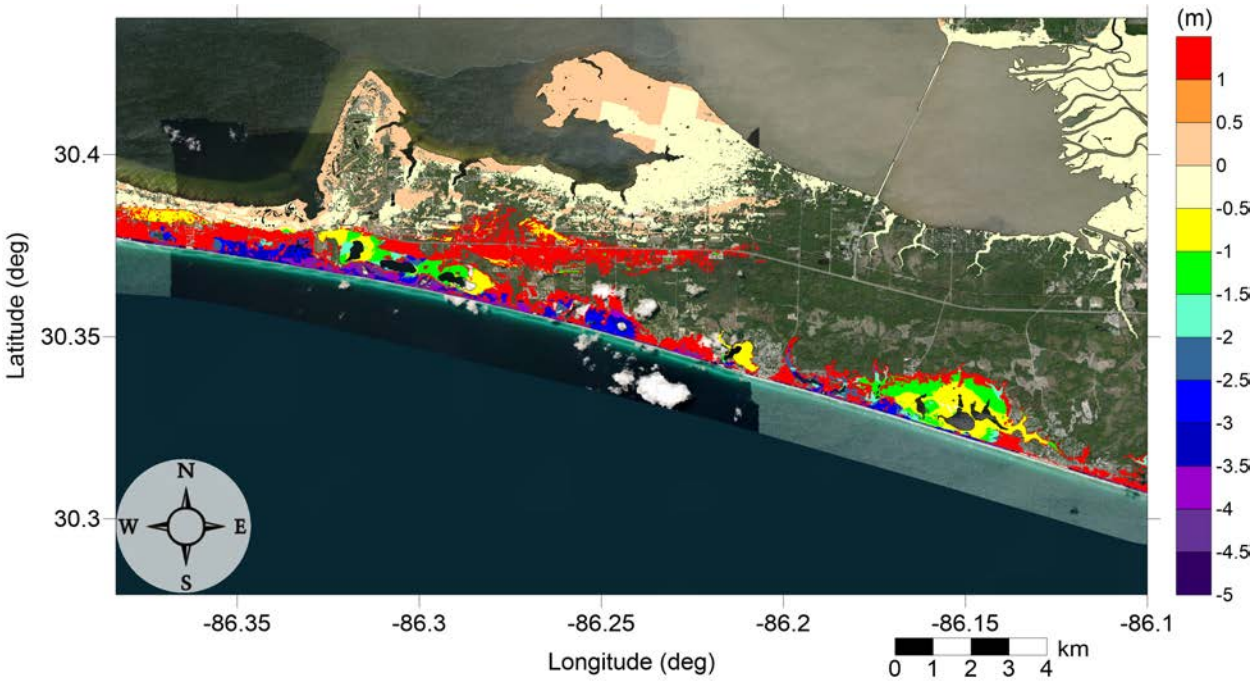

Figure 83: Actual difference $\Delta\zeta$ (in meters) between SLOSH MOM storm surge inundation and MOM tsunami inundation for the best-match hurricane category shown in Figure 82 for Miramar Beach, FL. Note that negative values indicate where tsunami inundation is higher than hurricane inundation, and pale colors indicate relatively good agreement between tsunami and storm surge inundation, i.e. $|\Delta\zeta| \leq 0.5$ m. The contours drawn and labeled are at -5 m, -10 m, and -15 m levels.

RosemaryBeach, FL
All Sources
SLOSH Storm Surge and MOM Tsunami Inundation Comparison

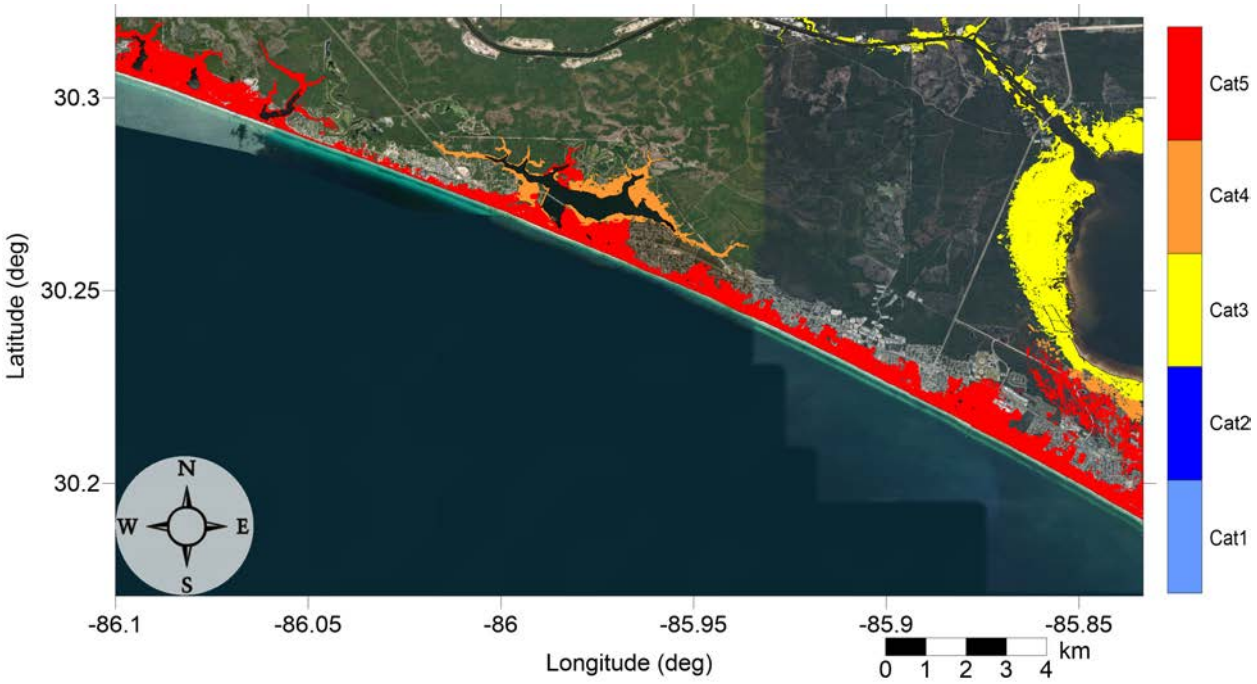

Figure 84: Hurricane category which produces inundation at high tide that best matches the MOM tsunami inundation shown in Figure 85 for Panama City Beach, FL. The contours drawn and labeled are at -5 m, -10 m, and -15 m levels.

RosemaryBeach, FL
All Sources
SLOSH Storm Surge and MOM Tsunami Inundation Comparison

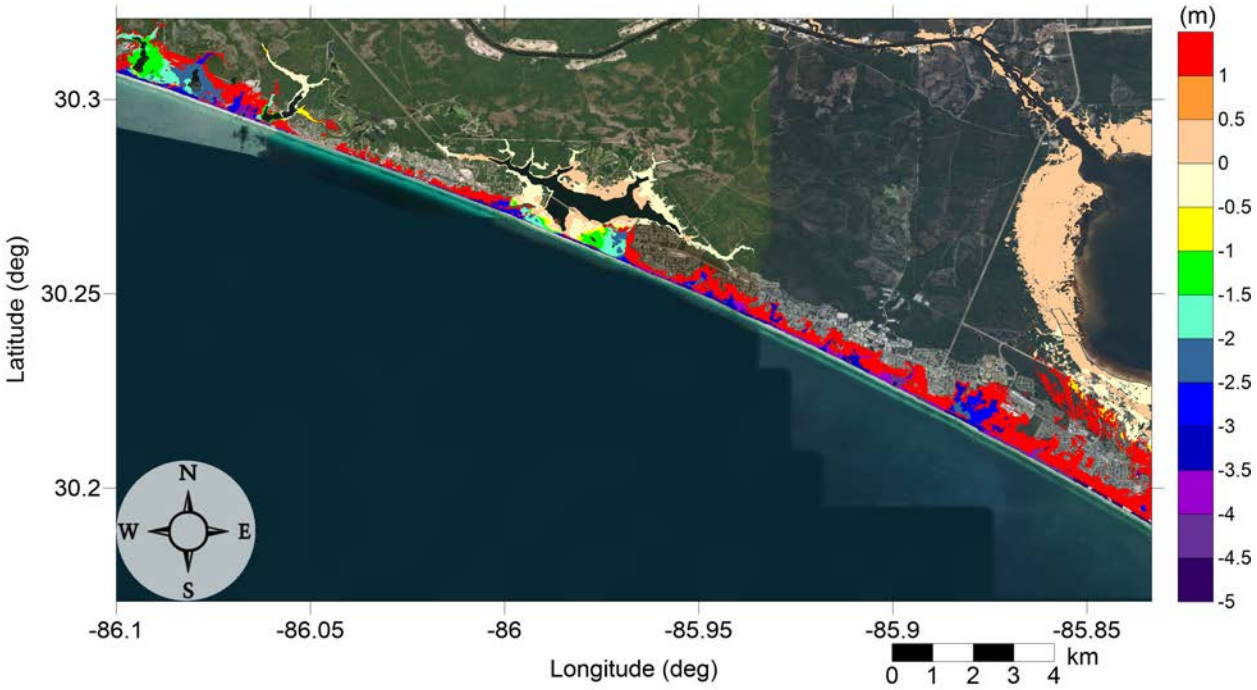

Figure 85: Actual difference $\Delta\zeta$ (in meters) between SLOSH MOM storm surge inundation and MOM tsunami inundation for the best-match hurricane category shown in Figure 84 for Panama City Beach, FL. Note that negative values indicate where tsunami inundation is higher than hurricane inundation, and pale colors indicate relatively good agreement between tsunami and storm surge inundation, i.e. $|\Delta\zeta| \leq 0.5$ m. The contours drawn and labeled are at -5 m, -10 m, and -15 m levels.

5.2 North Tampa Bay, FL

Fig. 78 and 79 shows the MOM tsunami inundation affecting the North Tampa Bay mapping area. Overall on the southern portion of this mapping area, the barrier islands from the Anclote Key (north) to the Caladesi Island (south) could be completely inundated under the worst case scenario (MOM), providing ample protection for the mainland. Inundation depth at the various barrier islands can reach over 2 m at GOM side, which decreases gradually toward the bay. On the mainland behind these barrier islands, the worst case scenario (MOM) inundation is mostly scattered around the inlet between the Anclote Key and the Three Rooker Island, with inundation depth up to 1.5 m. For the northern portion of the mapping area, the inundated region is mostly unpopulated. Inundation depth is less than 1 m. The Mississippi Canyon landslide is responsible for the MOM inundation (Fig. 80 and 81).

The hurricane category which best matches the tsunami inundation in this area is shown in Fig. 86 and 88. $\Delta\zeta$ for the best-match hurricane category satisfying Eq. 1 is shown in Fig. 87 and 89, respectively. The matching hurricane category distribution closely reflects that of tsunami inundation. Overall the tsunami inundation is comparable to hurricane Category 1 for the northern portion and all of the southern portion, except for part of the Clearwater Beach and Sand Key Beach where there is Category 2. The difference between hurricane flooding and tsunami inundation $\Delta\zeta$ is generally within $\pm$ 0.5 m for the barrier islands, except for the mainland where $\Delta\zeta$ is larger than 1. This large positive difference means storm surge inundation depth is much larger than tsunami inundation in this region.

North Tampa Bay, FL
All Sources
SLOSH Storm Surge and MOM Tsunami Inundation Comparison

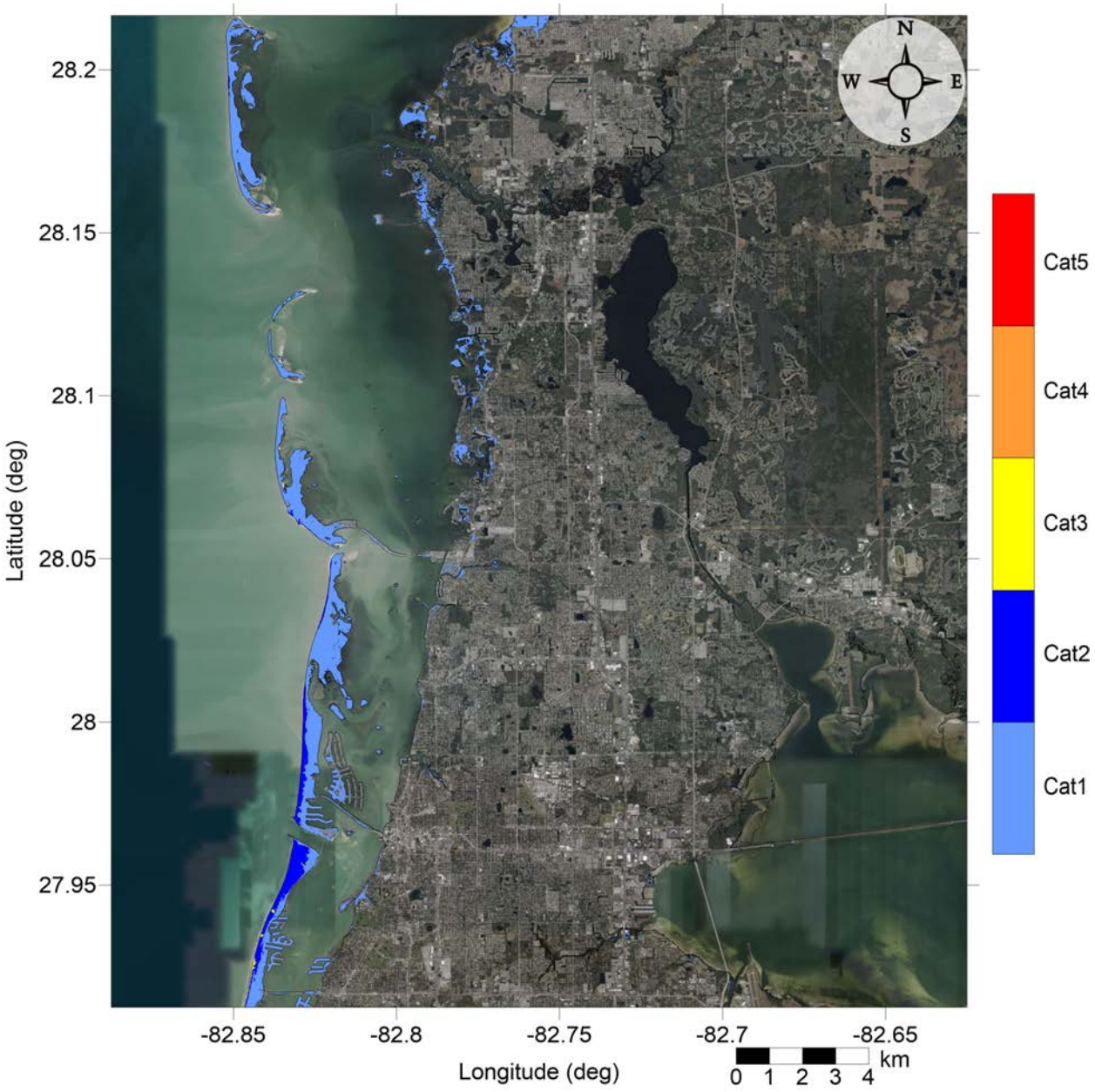

Figure 86: Hurricane category which produces inundation at high tide that best matches the MOM tsunami inundation shown in Figure 87 for Pasco County, FL. The contours drawn and labeled are at -5 m, -10 m, and -15 m levels.

North Tampa Bay, FL
All Sources
SLOSH Storm Surge and MOM Tsunami Inundation Comparison

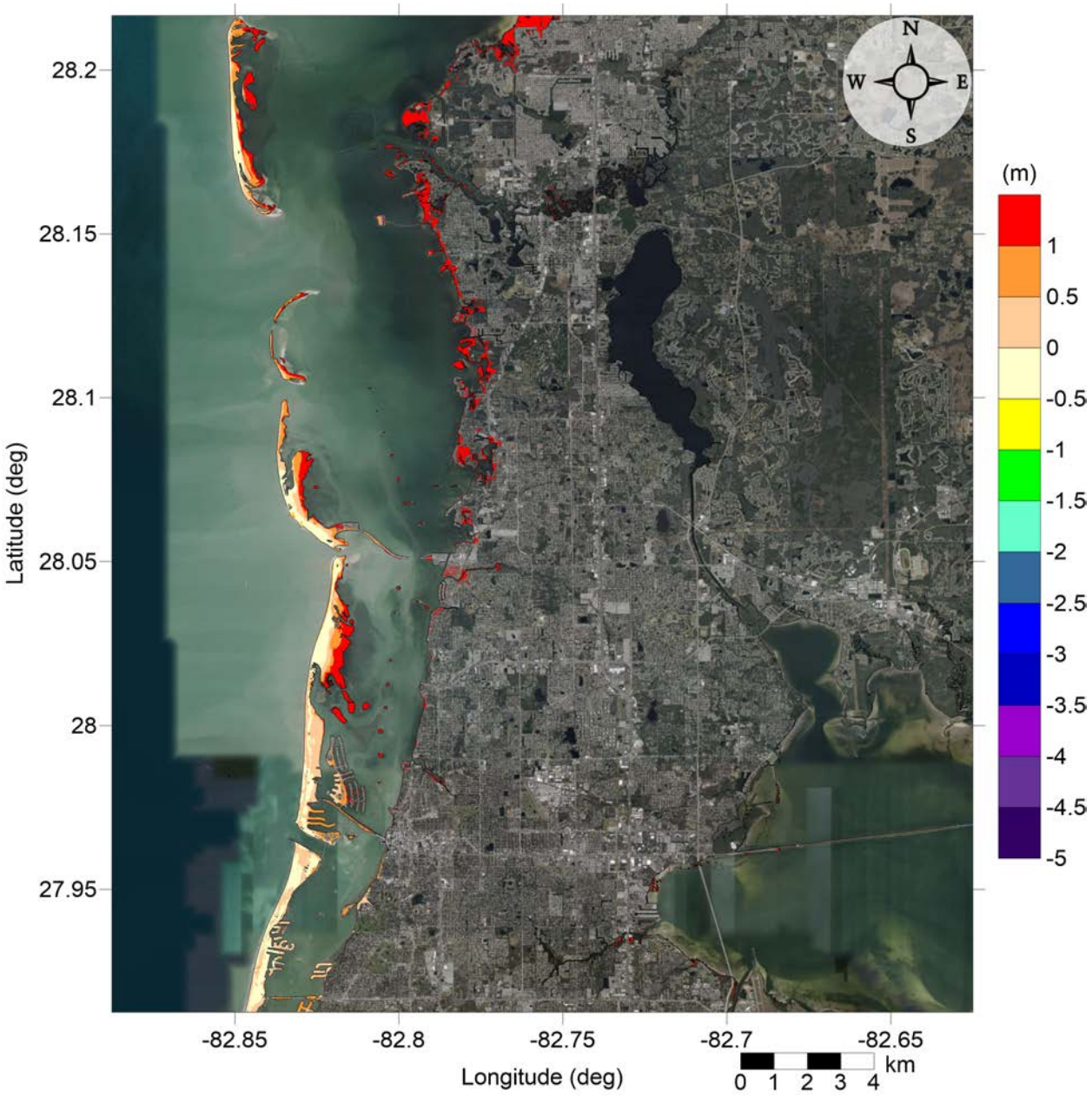

Figure 87: Actual difference $\Delta\zeta$ (in meters) between SLOSH MOM storm surge inundation and MOM tsunami inundation for the best-match hurricane category shown in Figure 86 for Pasco County, FL. Note that negative values indicate where tsunami inundation is higher than hurricane inundation, and pale colors indicate relatively good agreement between tsunami and storm surge inundation, i.e. $|\Delta\zeta| \leq 0.5$ m. The contours drawn and labeled are at -5 m, -10 m, and -15 m levels.

North Tampa Bay, FL
All Sources
SLOSH Storm Surge and MOM Tsunami Inundation Comparison

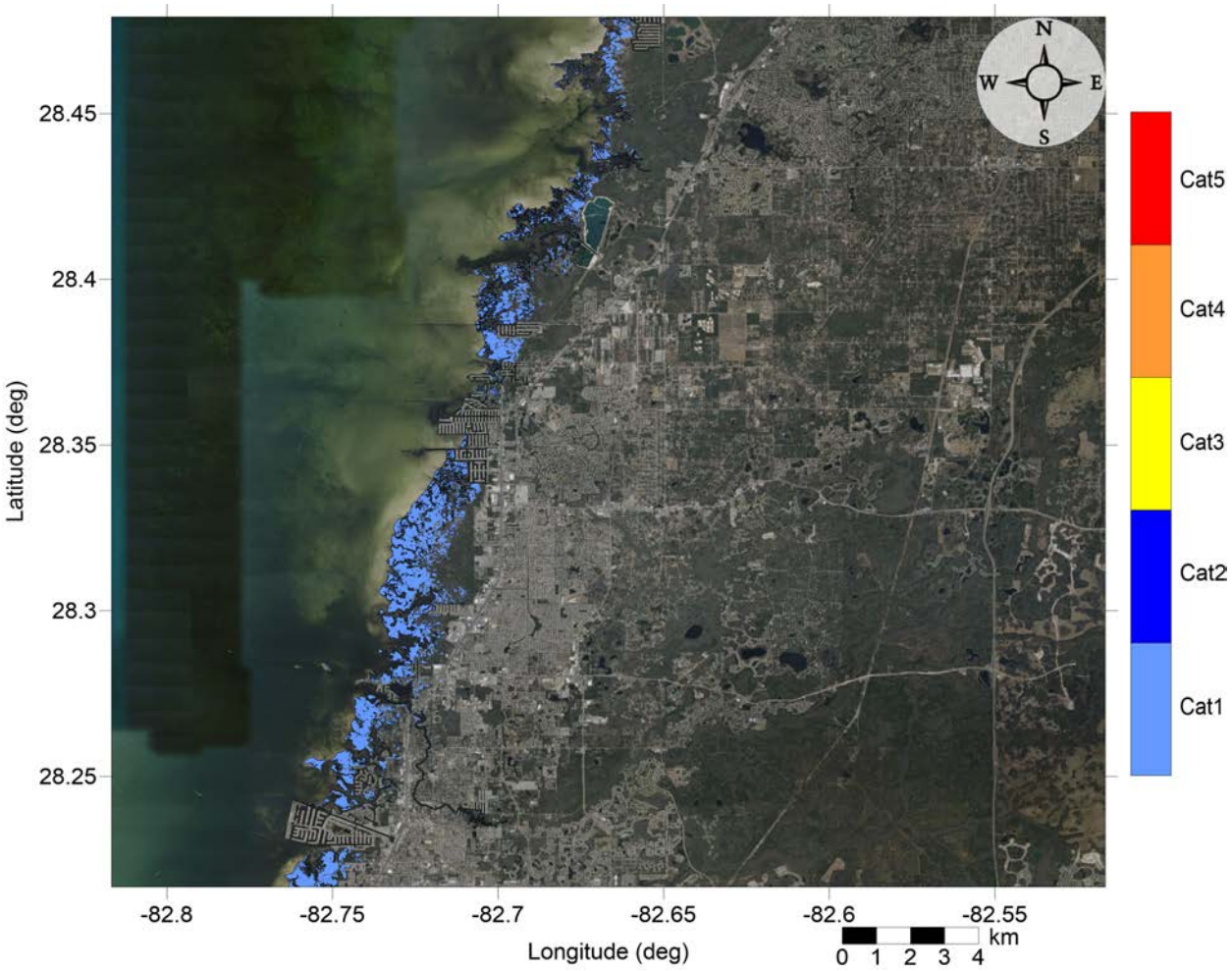

Figure 88: Hurricane category which produces inundation at high tide that best matches the MOM tsunami inundation shown in Figure **??** for North Pinellas County, FL. The contours drawn and labeled are at -5 m, -10 m, and -15 m levels.

North Tampa Bay, FL
All Sources
SLOSH Storm Surge and MOM Tsunami Inundation Comparison

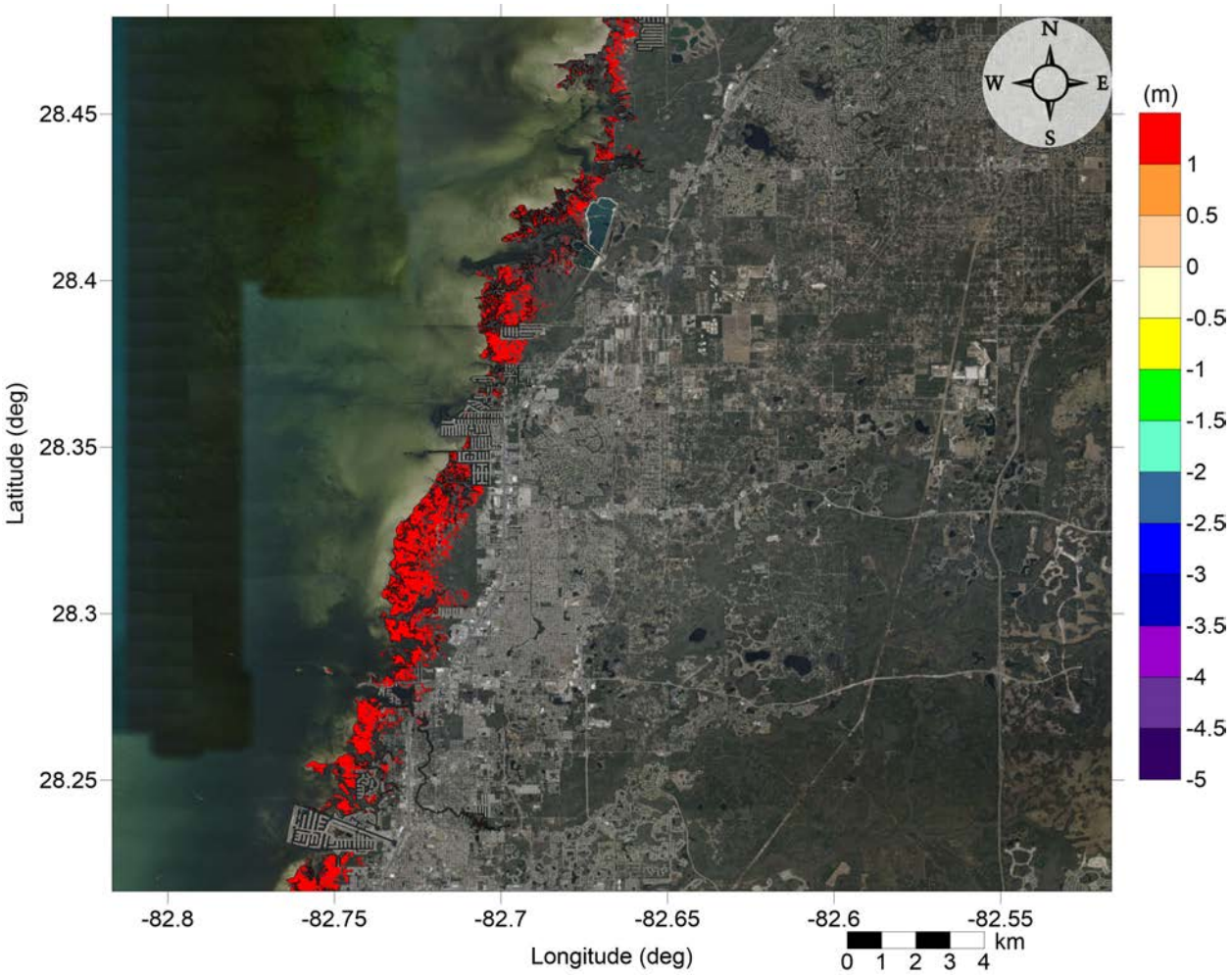

Figure 89: Actual difference $\Delta\zeta$ (in meters) between SLOSH MOM storm surge inundation and MOM tsunami inundation for the best-match hurricane category shown in Figure 88 for North Pinellas County, FL. Note that negative values indicate where tsunami inundation is higher than hurricane inundation, and pale colors indicate relatively good agreement between tsunami and storm surge inundation, i.e. $|\Delta\zeta| \leq 0.5$ m. The contours drawn and labeled are at -5 m, -10 m, and -15 m levels.

6 Tsunami Maritime Products

Accurate estimates of tsunami wave amplitude do not necessarily equate to the prediction of localized damaging currents in a basin or harbor [Lynett et al., 2012]. Furthermore, damage potential in ports is strongly related to the current speed. Therefore, tsunami hazard mitigation products need to be advanced to predict damage potential in basins or harbors. Past tsunamis have shown that the maritime community requires additional information and guidance about tsunami hazards and post-tsunami recovery [Wilson et al., 2012, 2013]. To accomplish mapping and modeling activities to meet NTHMP's planning/response purposes for the maritime community and port emergency management and other customer requirements, it is necessary to continue the process to include maritime products in our current inundation map development. These maritime products will help identify impact specifically on ship channels, bay inlets, harbors, marinas, and oil infrastructures (e.g., designated lightering and oil tanker waiting zones).

In this study, Rosemary Beach, FL and Tampa Bay North, FL are added to the maritime portfolio, where tsunami hazard maritime products such as tsunami current magnitude, vorticity, safe/hazard zones are generated.

Lynett et al. [2014] complied a general relationship between tsunami current speed and harbor damage based on observational data, in which the current speed is divided into four ranges of damaging potential, 0 - 3 knots means unharmful currents, 3 - 6 knots corresponds to minor-to-moderate damage, 6 - 9 knots moderate-to-major damage, and over 9 knots extreme damage. Since the extent of damage is very location-dependent, to make the text concise, we associate 0 - 3 knots to unharmful currents, 3 - 6 knots to minor damage, 6 - 9 knots to moderate damage, and finally over 9 knots to major damage. The four levels are denoted with white, blue, yellow and red colors, respectively, for all the velocity contour plots within our velocity maritime products.

Using this damage-to-speed relationship, we have plotted the maximum of maximum depth-averaged velocity for each computational subdomain of the two new communities. Fig. 90 shows the minimum offshore safe depth (approximately 200 m or 100 fathoms), and the maximum of maximum velocity magnitude contour plot across the entire Gulf of Mexico (15 arcsecond resolution) for all landslide scenarios (Eastbreaks, PSL-A, PSL-B1, PSL-B2, Mississippi Canyon, PSL-C, West Florida, Yucatán #3 and Yucatán #5). Potential damaging currents ($>$ 3 knots, blue, yellow and red areas) tend to be present in most of the area shallower than the minimum offshore safe depth. However, damaging currents could reach areas deeper than 200 m close to most of the landslide generation regions. Major damaging currents ($>$ 9 knots, red) can be expected in most of the landslide generation regions, in the continental shelf adjacent to Mississippi Canyon, offshore northwest Florida, and Yucatán shelf. Moderate ($>$ 6 knots and $<$ 9 knots, yellow) damaging current areas are scattered over the continental shelf, but mostly close to areas with major damage currents.

All locations
All Sources
Maximum of Maximum Velocity Magnitude

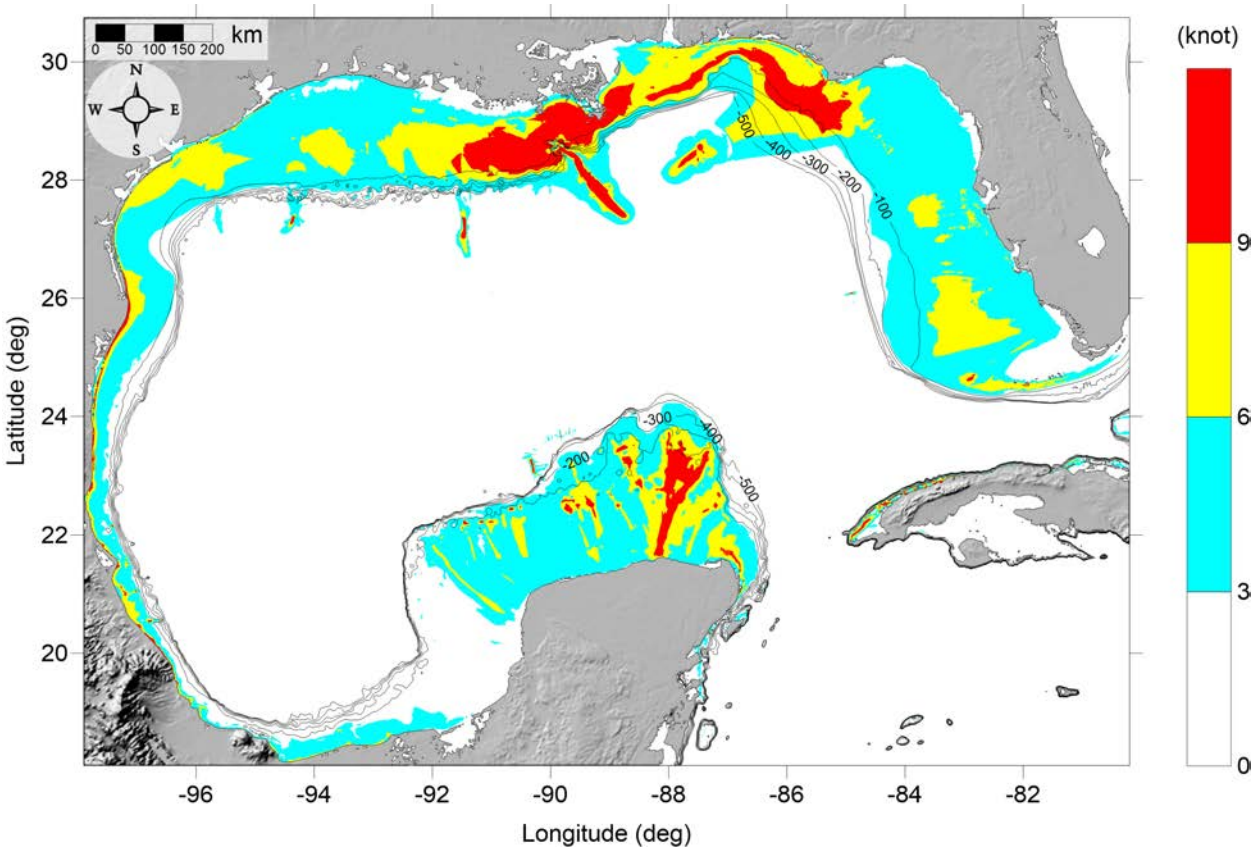

Figure 90: Maximum of maximum velocity magnitude contour in GOM for all landslide scenarios and all locations.

The MOM velocity magnitude (damaging potential) contour maps and the MOM vorticity magnitude contour maps for the finer computational subdomains of Rosemary Beach, FL and Tampa Bay North, FL are presented from Fig. 91 to Fig. 104.

Fig. 93 and Fig. 94 shows the MOM velocity magnitude contour plot result for the Rosemary Beach area. Most of offshore region is expected to have moderate to major damaging currents, with major damaging currents occurring along the coastline, inlets, and the various lakes. There is generally no moderate damaging currents farther behind the barrier islands. In Tampa Bay North, FL mapping region, the situation is much less severe than Rosemary Beach, FL. In general, the worst case (MOM) tsunami waves result in minor damaging currents in most areas offshore (Fig. 99). Behind the barrier islands and in the north region, there are much calmer tsunami current velocities (< 3 knots) that usually causes no harm.

For both Rosemary Beach, FL and Tampa Bay North, FL, vorticity distribution displays similar patterns to their velocity distribution, where high vorticity appears around the barrier island, and are more intense near the bay entrances.

6.1 Rosemary Beach, FL

Rosemary Beach, FL
All Sources
Maximum of Maximum Velocity Magnitude

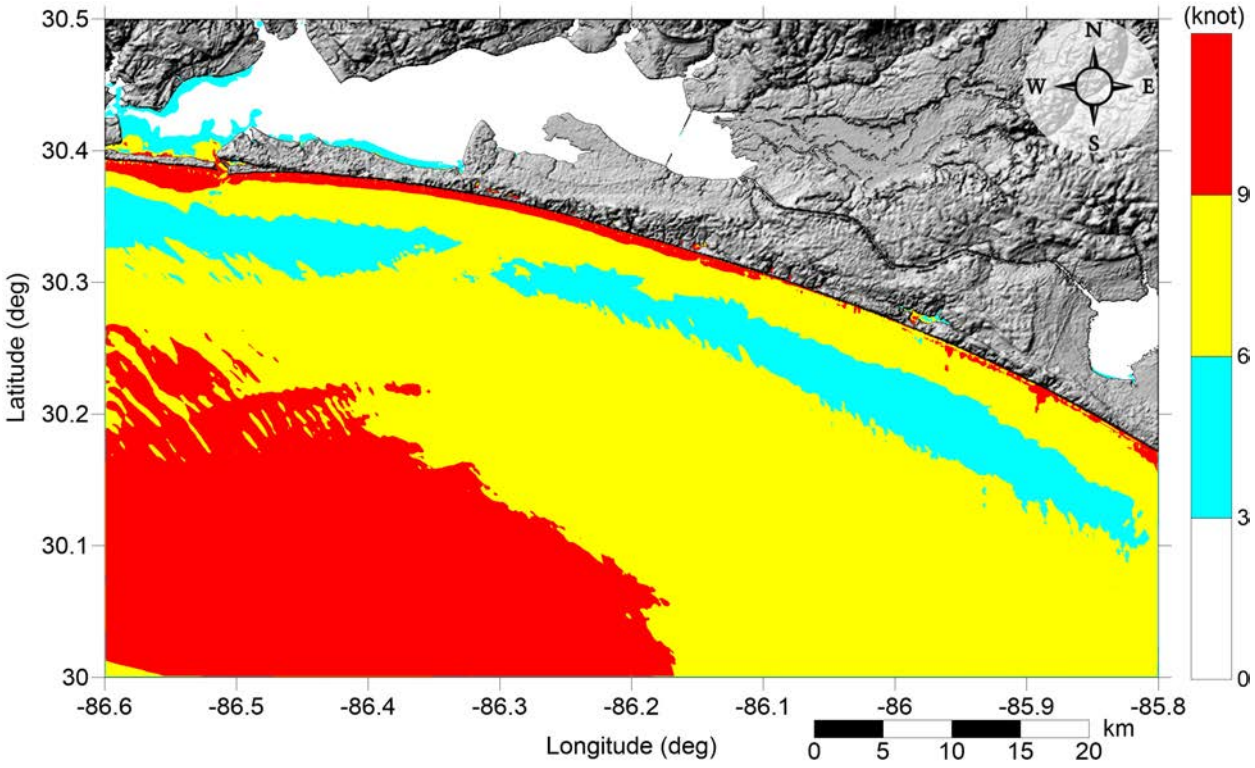

Figure 91: Maximum of maximum velocity magnitude contour in Rosemary Beach, FL (Grid 2 - 3 arcsecond) for all landslide scenarios.

Rosemary Beach, FL
All Sources
Maximum of Maximum Velocity Magnitude

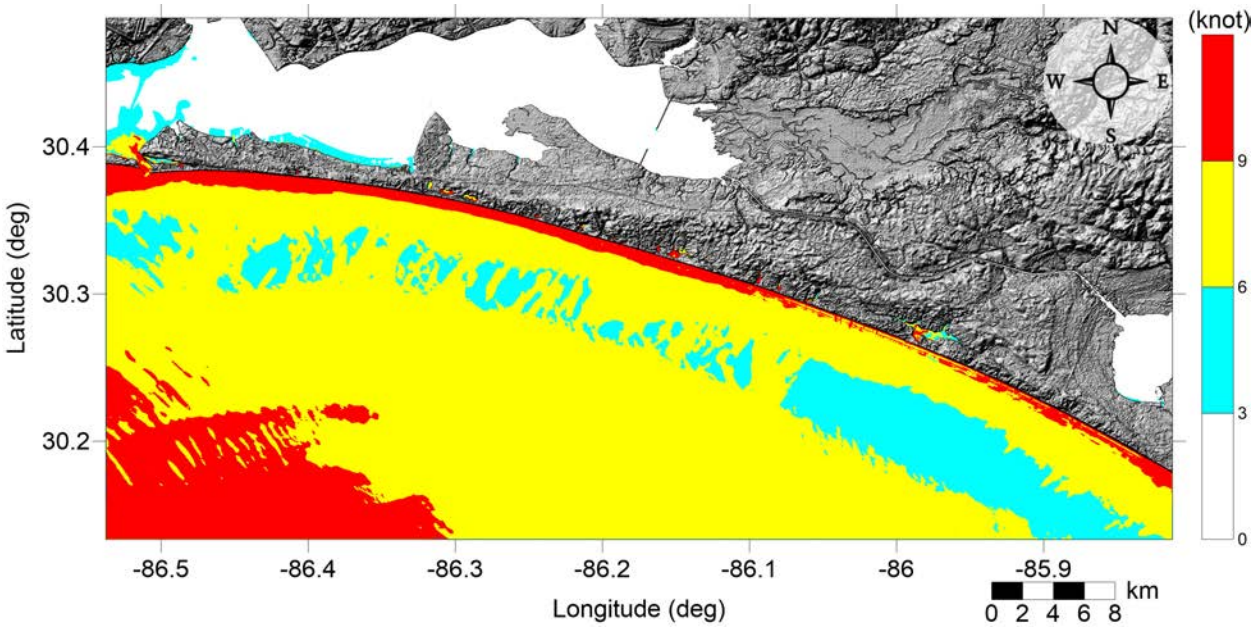

Figure 92: Maximum of maximum velocity magnitude contour in Rosemary Beach, FL (Grid 3 - 1 arcsecond) for all landslide scenarios.

Rosemary Beach, FL
All Sources
Maximum of Maximum Velocity Magnitude

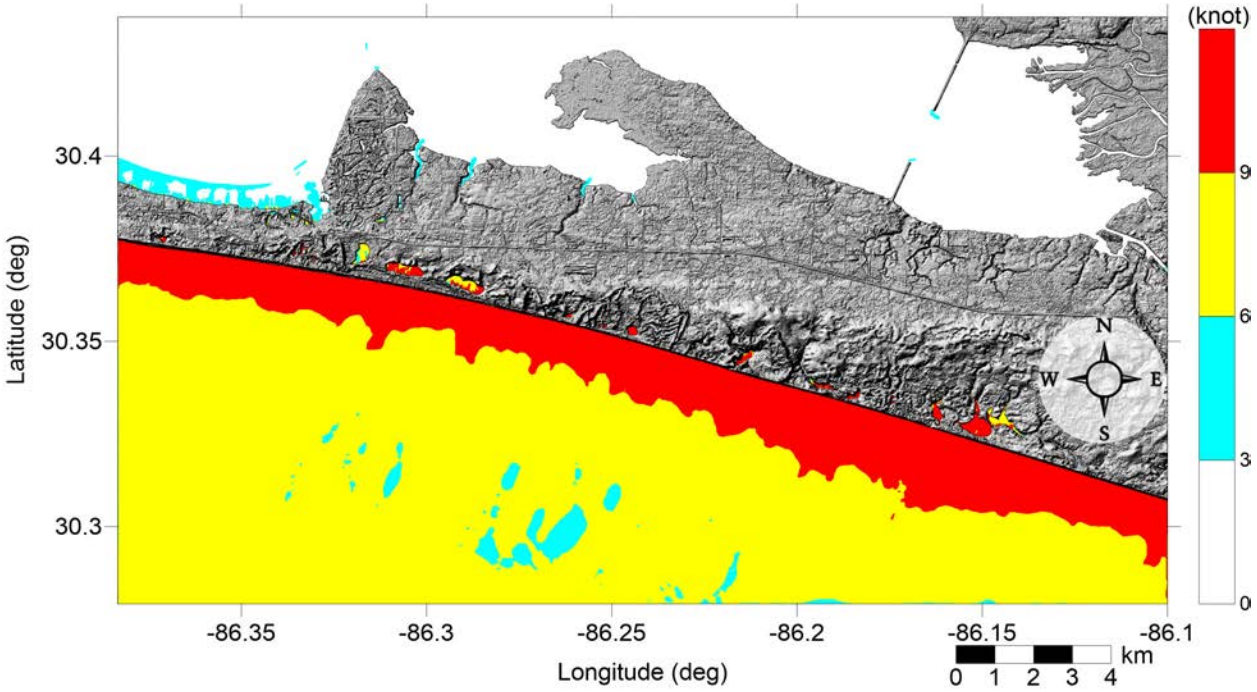

Figure 93: Maximum of maximum velocity magnitude contour in Gulf Shores, AL (Grid 4 - 1/3 arcsecond) for all landslide scenarios.

Rosemary Beach, FL
All Sources
Maximum of Maximum Velocity Magnitude

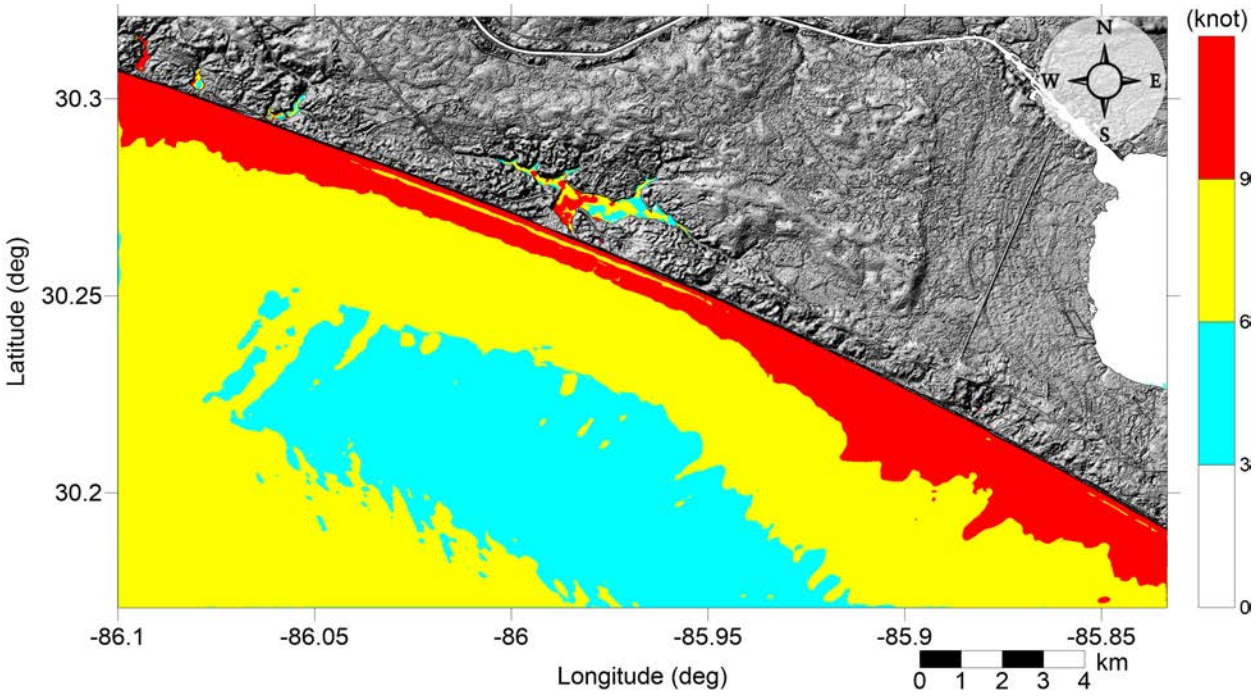

Figure 94: Maximum of maximum velocity magnitude contour in Rosemary Beach, FL (Grid 5 - 1/3 arcsecond) for all landslide scenarios.

Rosemary Beach, FL
All Sources
Maximum of Maximum Vorticity Magnitude

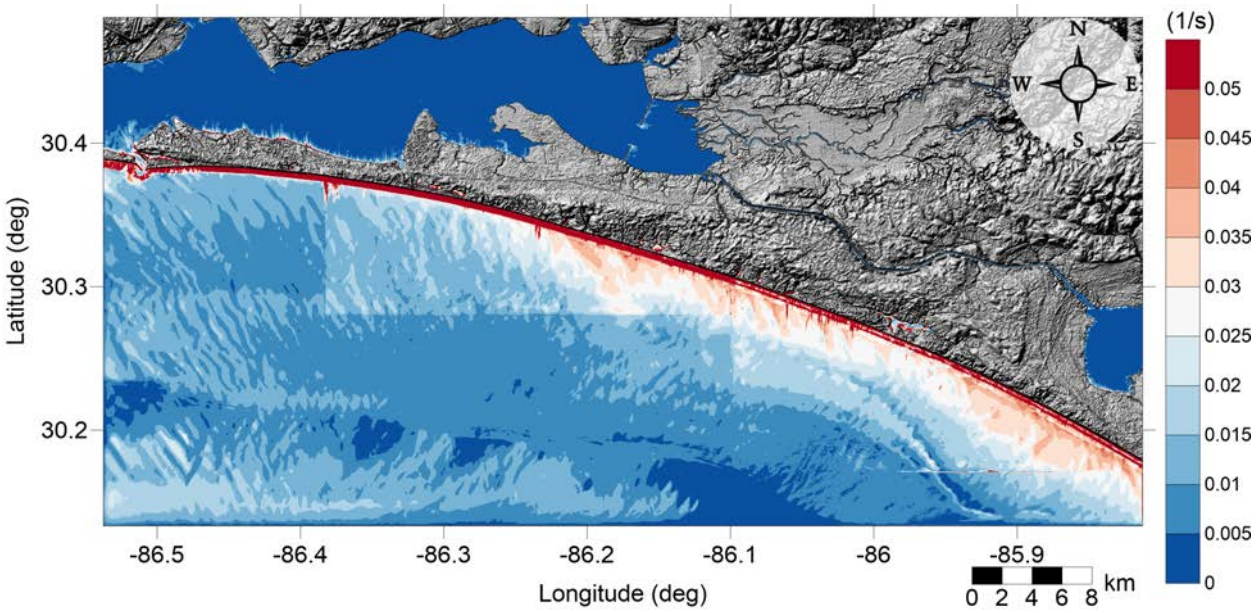

Figure 95: Maximum of maximum vorticity magnitude contour in Rosemary Beach, FL Grid 3 (1 arcsecond) for all landslide scenarios.

Rosemary Beach, FL
All Sources
Maximum of Maximum Vorticity Magnitude

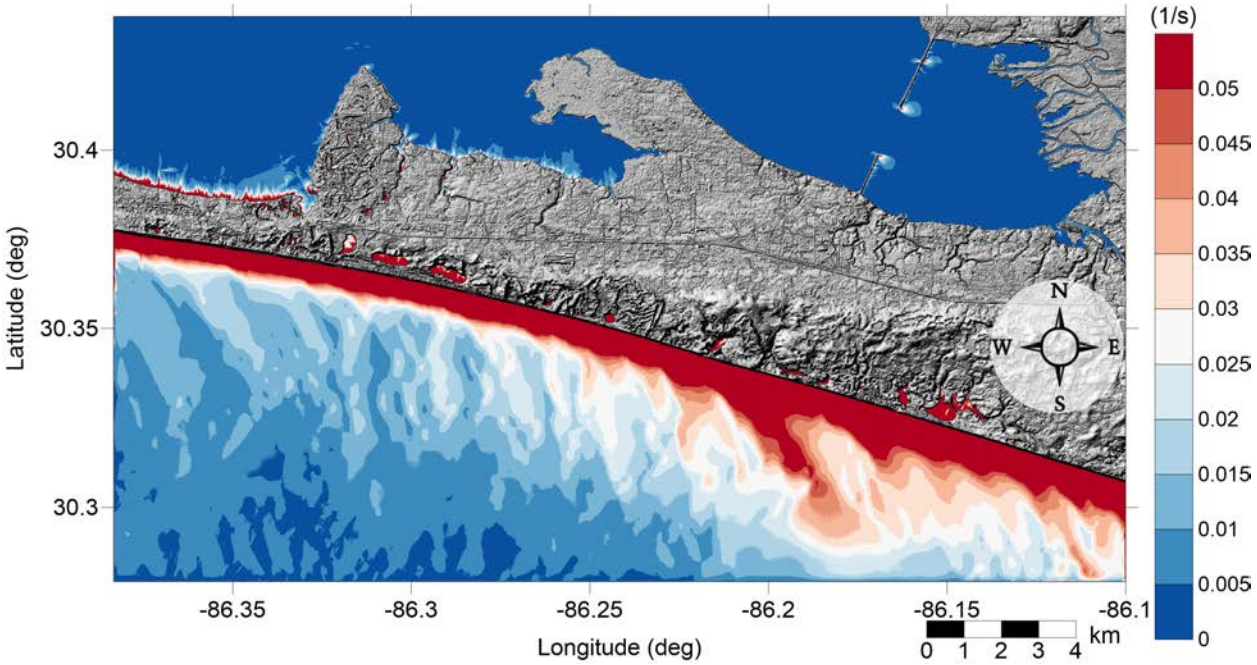

Figure 96: Maximum of maximum vorticity magnitude contour in Gulf Shores, AL Grid 4 (1/3 arcsecond) for all landslide scenarios.

Rosemary Beach, FL
All Sources
Maximum of Maximum Vorticity Magnitude

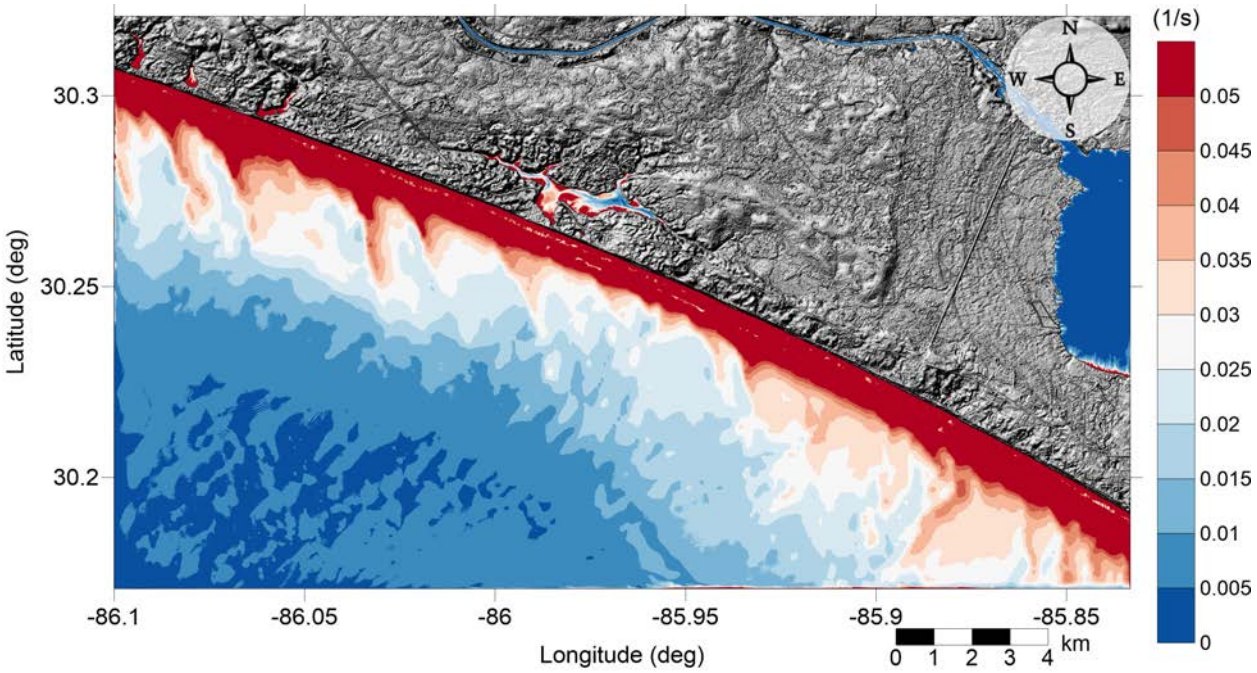

Figure 97: Maximum of maximum vorticity magnitude contour in Rosemary Beach, FL Grid 5 (1/3 arcsecond) for all landslide scenarios.

6.2 Tampa Bay North, FL

Tampa Bay North, FL
All Sources
Maximum of Maximum Velocity Magnitude

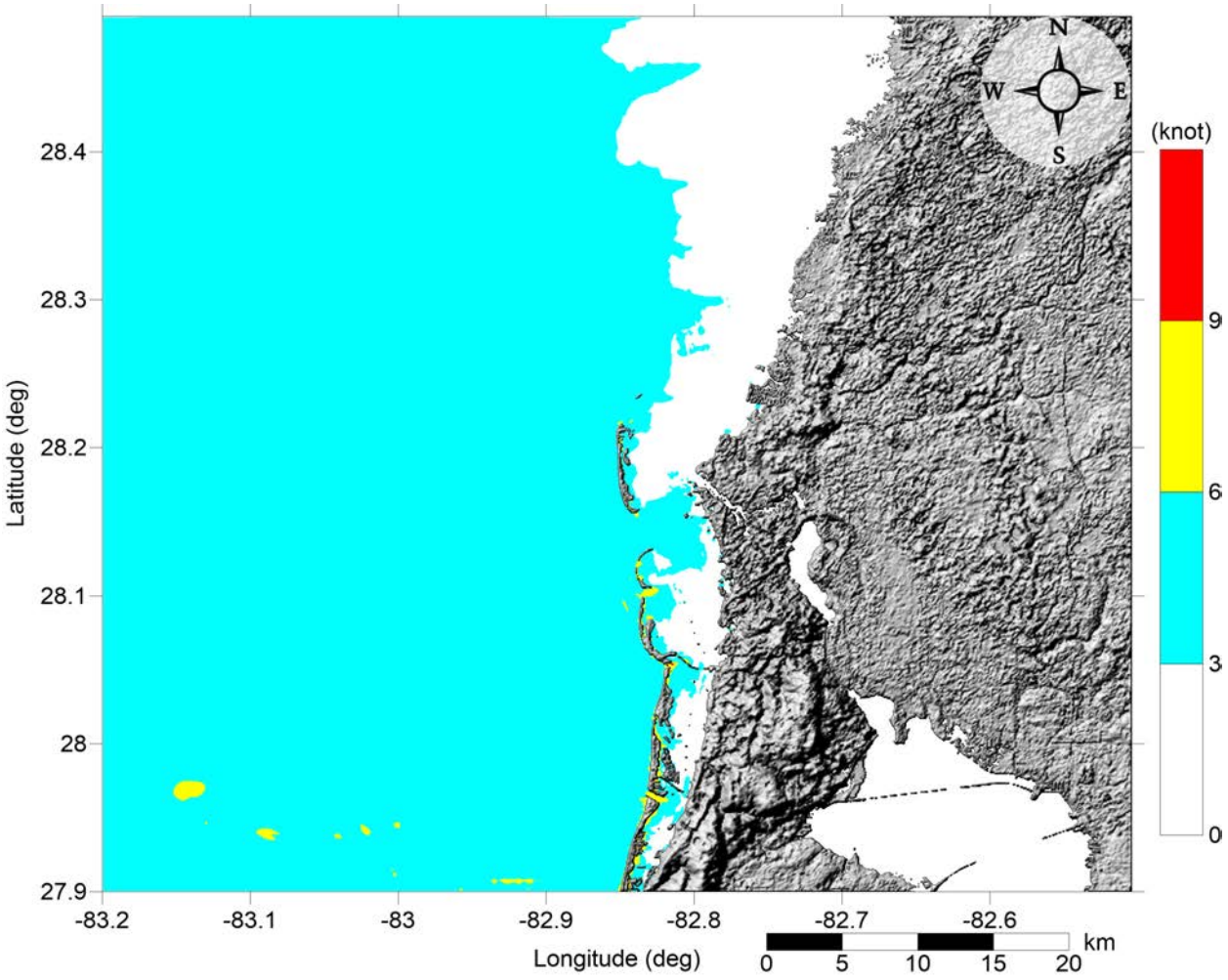

Figure 98: Maximum of maximum velocity magnitude contour in Tampa Bay North, FL (Grid 2 - 3 arcsecond) for all landslide scenarios.

Tampa Bay North, FL
All Sources
Maximum of Maximum Velocity Magnitude

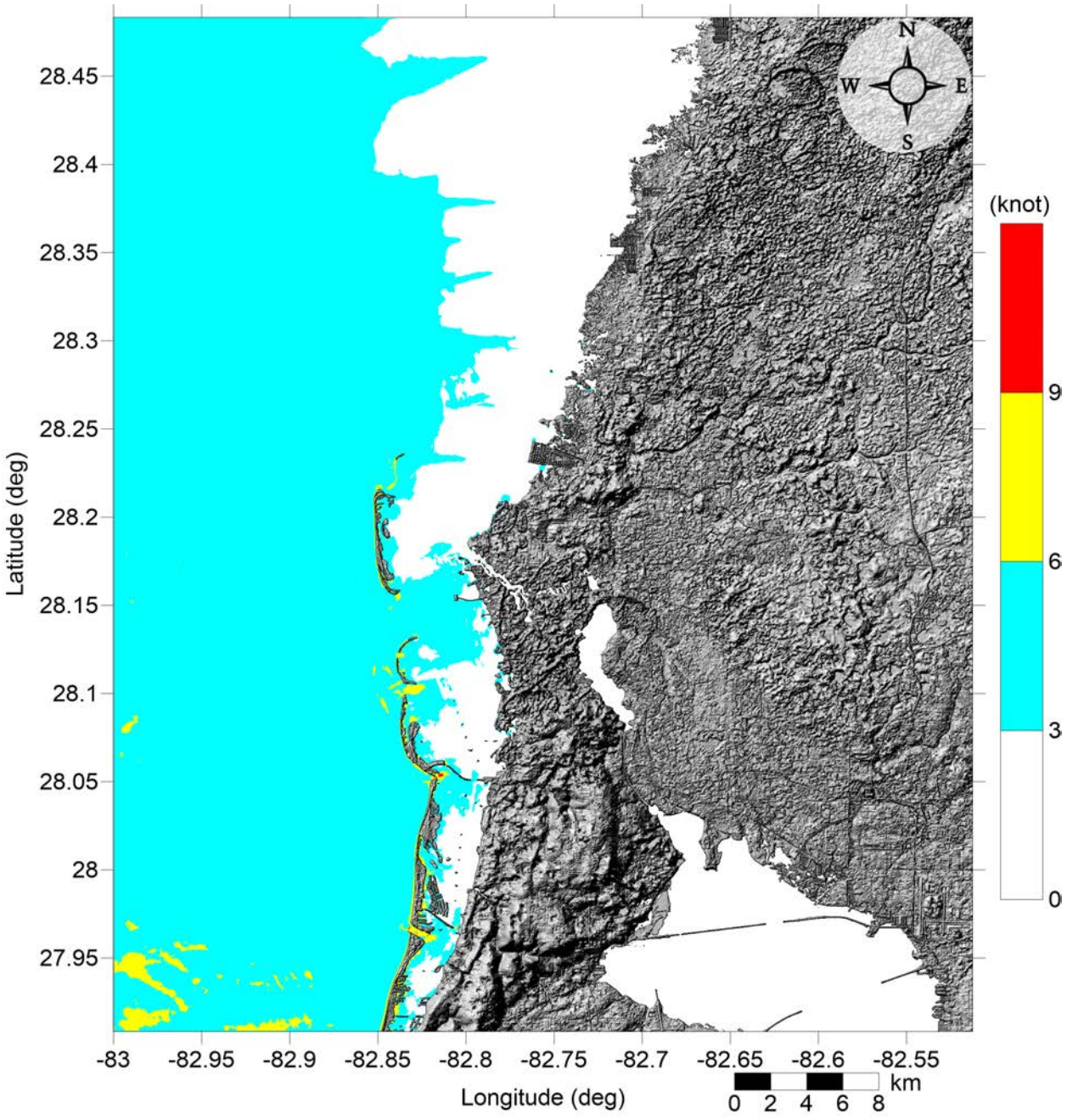

Figure 99: Maximum of maximum velocity magnitude contour in Tampa Bay North, FL (Grid 3 - 1 arcsecond) for all landslide scenarios.

Tampa Bay North, FL
All Sources
Maximum of Maximum Velocity Magnitude

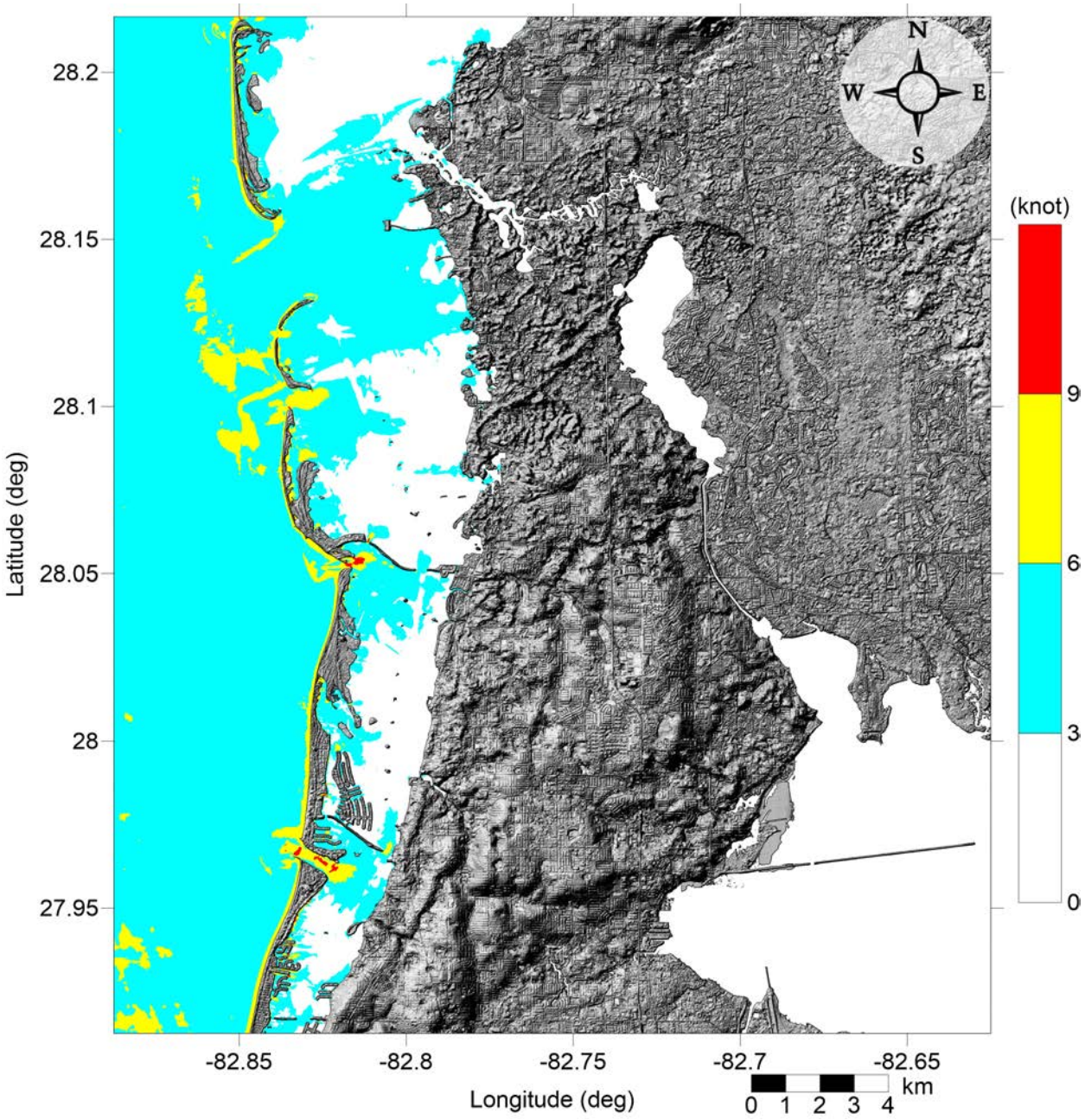

Figure 100: Maximum of maximum velocity magnitude contour in Tampa Bay North, FL (Grid 4 - 1/3 arcsecond) for all landslide scenarios.

Tampa Bay North, FL
All Sources
Maximum of Maximum Velocity Magnitude

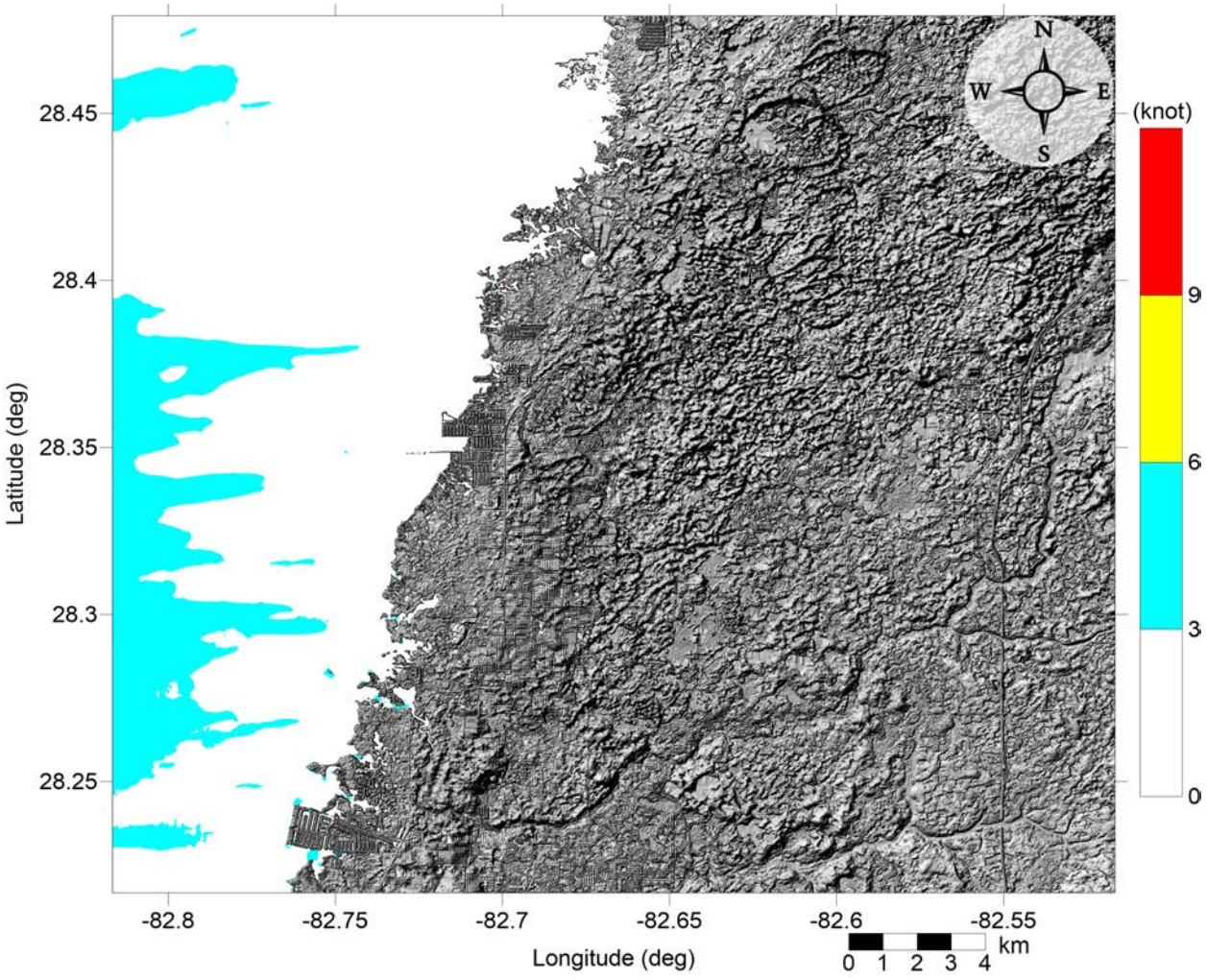

Figure 101: Maximum of maximum velocity magnitude contour in Port St. Joe, FL (Grid 5 - 1/3 arcsecond) for all landslide scenarios.

Tampa Bay North, FL
All Sources
Maximum of Maximum Vorticity Magnitude

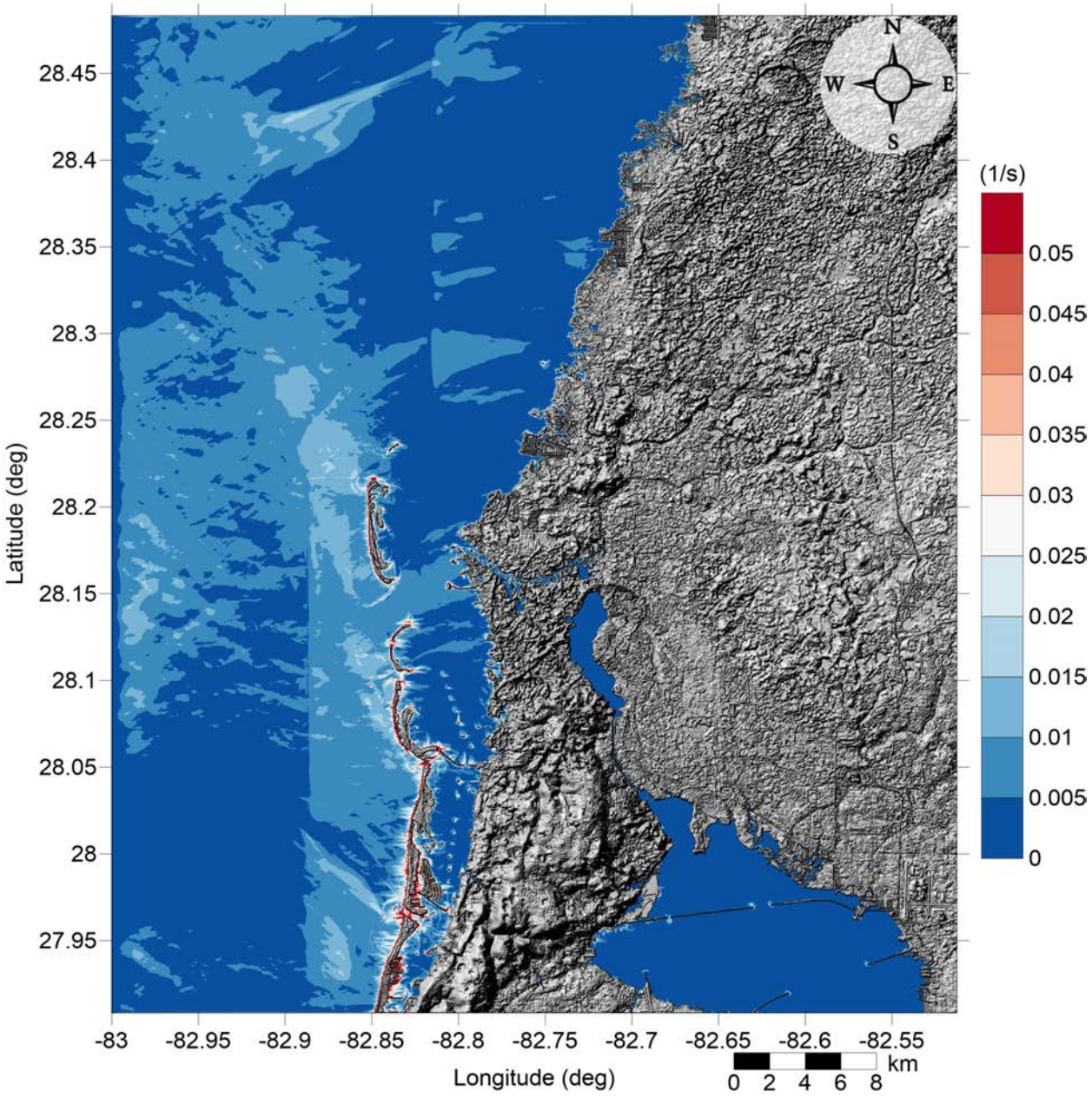

Figure 102: Maximum of maximum vorticity magnitude contour in Tampa Bay North, FL Grid 3 (1 arcsecond) for all landslide scenarios.

Tampa Bay North, FL
All Sources
Maximum of Maximum Vorticity Magnitude

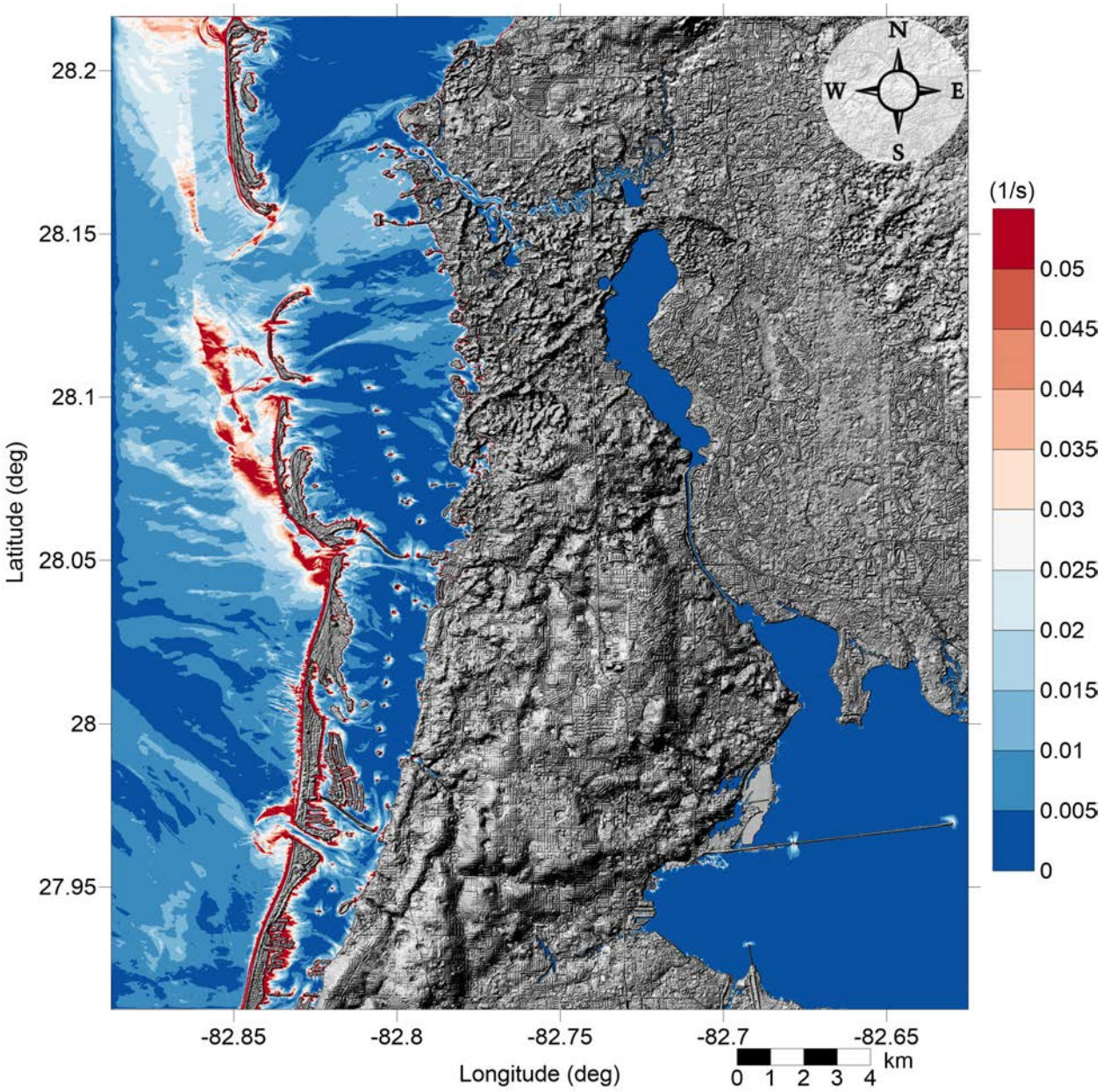

Figure 103: Maximum of maximum vorticity magnitude contour in Tampa Bay North, FL Grid 4 (1/3 arcsecond) for all landslide scenarios.

Tampa Bay North, FL
All Sources
Maximum of Maximum Vorticity Magnitude

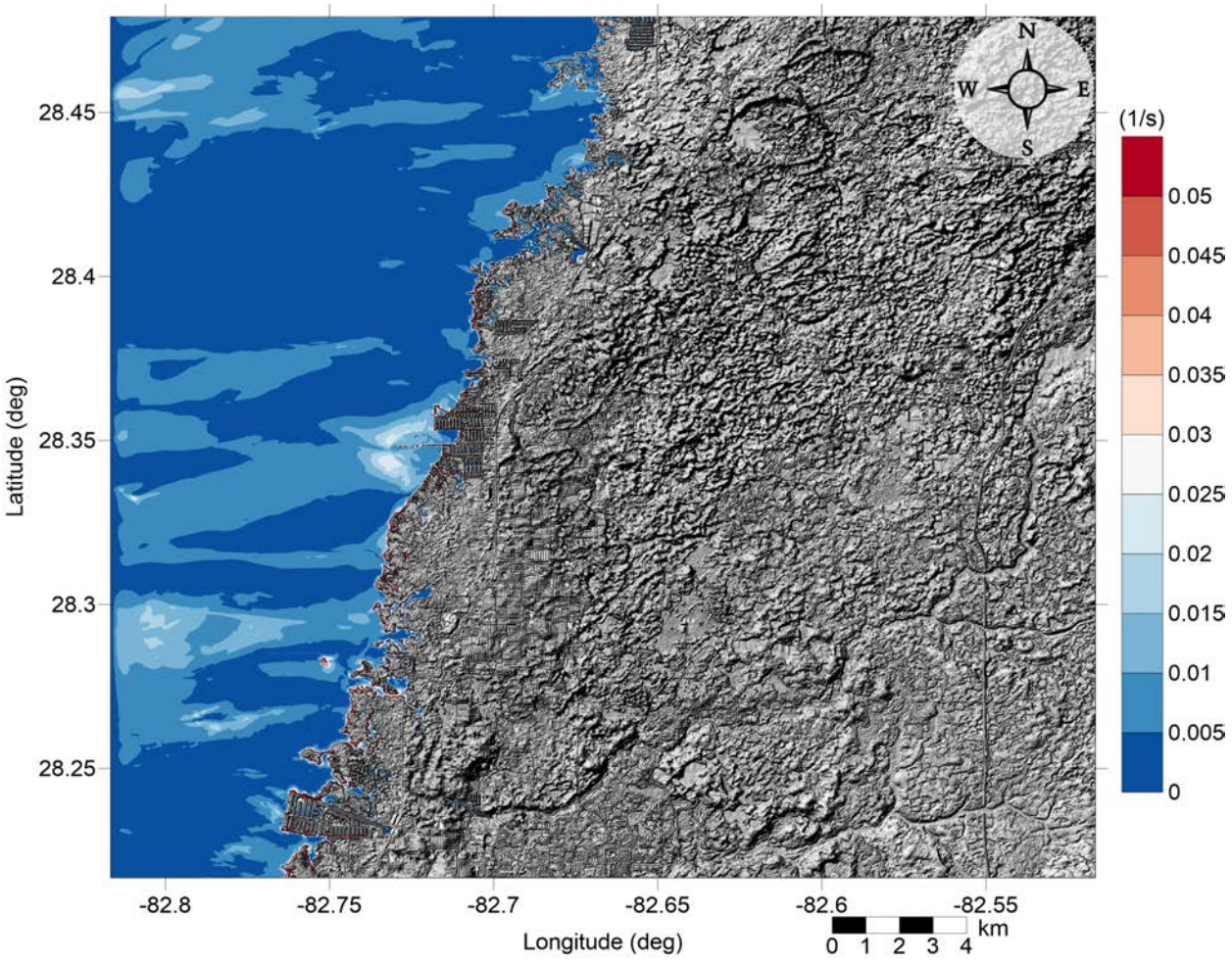

Figure 104: Maximum of maximum vorticity magnitude contour in Port St. Joe, FL Grid 5 (1/3 arcsecond) for all landslide scenarios.

7 Conclusions

This project focused on the implementation of recent developments in the tsunami science recommended by the National Tsunami Hazard Mitigation Program - Modeling Mapping Subcommittee - Strategic Plan (NTHMP-MMS-SP) into our current Gulf of Mexico (GOM) tsunami mitigation products. Three main developments for tsunami mitigation have been created under this project for two new communities in the GOM (Rosemary Beach, FL and North Tampa Bay, FL) that will provide guidance to state emergency managers for tsunami hazard mitigation and warning purposes. The first task is the development of tsunami inundation maps for the two selected communities with nine landslide sources. The second is the comparison between existing SLOSH hurricane flooding data and our tsunami inundation result for the two new communities in order to facilitate temporal-low-order estimate for tsunami hazard areas (community) where inundation studies have not yet been assigned/executed or where little bathymetric and elevation data exists. The third is to produce maritime products (maximum of maximum (MOM) velocity and velocity magnitude maritime maps) for both communities to help identify impact specifically on ship channels, bay inlets, harbors, marinas, and other infrastructures.

Tsunami wave propagation and inundation in Rosemary Beach, FL and North Tampa Bay, FL was modeled to obtain maximum inundation and extent, momentum flux, current velocity and vorticity maps considering the entire suite of nine landslide sources.

From Miramar Beach to Seaside, under the worst case scenario, the highest inundation (> 4 m) occurs at the immediate ocean front and around the various lakes, and the other potentially at-risk areas would expect less inundation further away from the lakes and the beach. Along the coastline near Miramar Beach, the high inundation appears south of US Highway 98. Around the Choctawhatchee Bay, high inundation (< 2.5 m) mostly appears around the Hogtown Bayou and east of Highway 331 bridge, which are caused by tsunami waves coming in from bay inlet, instead of overtopping water over the barrier island.

In Panama City Beach, FL, overall water depth exhibits decreasing trend from oceanfront toward the inland, with maximum over 4 m. The tsunami inundation is mostly contained south of E County Highway 30A (from Eastern Lake to Rosemary Beach) and Panama City Beach Parkway (from Rosemary Beach to Panama City Beach), while penetrating deeper inland via the various lakes (Eastern Lake, Deer Lake, Camp Creek Lake and the biggest Powell Lake via Philips Inlet). On the west bank of the West Bay, tsunami inundation could reach up to ~ 2 m, which extends upstream the West Bay Creek a few kilometers.

In the North Tampa Bay mapping area, overall on the southern portion, the barrier islands from the Anclote Key (north) to the Caladesi Island (south) could be completely inundated under the worst case scenario (MOM), providing ample protection for the mainland. Inundation depth at the various barrier islands can reach over 2 m at GOM side, which decreases gradually toward the bay. On the mainland behind these barrier islands, the worst case scenario (MOM) inundation is mostly scattered around the inlet between the Anclote Key and the Three Rooker Island, with inundation depth up to 1.5 m. For the northern portion of the mapping area, the inundated region is mostly unpopulated. Inundation depth is less than 1 m.

For both communities, MOM tsunami inundation is produced solely by the Mississippi

Canyon failure. This geological failure is the largest in both, area and volume of material removed, and therefore produces the highest amplitude wave of all simulated sources.

While high-resolution tsunami inundation studies have been completed for these 22 communities and are planned for additional locations, vulnerability assessments are still essential for coastal locations where inundation studies have not yet been performed or planned, or where there is a lack of high-resolution bathymetric and/or elevation data. Therefore, we aim to extend the results of the completed mapping studies in order to provide estimates of tsunami inundation zones for hazard mitigation efforts in unmapped locations. We anticipate that communities which lack detailed tsunami inundation maps, but which have modeled hurricane storm surge information, would be able to use the results presented here to estimate their potential tsunami hazard level based on their regional topographical/bathymetric features. We stress, however, that such results should be used only in a broad, regional sense given the differences seen among and within communities based on local details of bathymetry, topography, and geographical location within the GOM basin. There is no guarantee that comparison results will be identical in areas with similar topography, and comparisons should only be made after understanding the limitations and simplifications of the methodology presented here. Comparisons of MOM tsunami inundation results with the SLOSH MOM high tide storm surge inundation indicate that while the details of referencing tsunami inundation to hurricane storm surge is dependent on local topographic effects, general regional trends can be identified.

The hurricane category which best matches the tsunami inundation in Miramar Beach, FL is shown in Fig. 82, and Fig. 83 shows $\Delta\zeta$ for the best-matching hurricane category satisfying Eq. 1. The hurricane category that best matches tsunami inundation closely follows the MOM tsunami inundation trend. Category 5 appears near the beach and around Highway 98. Category 3 appears around the Choctawhatchee Bay and Category 4 mostly appears between Category 3 and 5. The difference between hurricane flooding and tsunami inundation is mostly within ± 1 m for Category 3 and 4, but < 3 m for Category 5, indicating that tsunami inundation greatly exceeds that of the most severe storms. The hurricane category which best matches the tsunami inundation in Panama City Beach area (grid 5) is shown in Fig. 84, and Fig. 85 shows $\Delta\zeta$ for the best-matching hurricane category satisfying Eq. 1. The hurricane category that best matches tsunami inundation closely follows the MOM tsunami inundation trend. On the coast line, tsunami inundation is mostly comparable to Category 5, while Category 4 only appears around the Powell Lake. Category 3 only appear around the Powell Lake. The difference between hurricane flooding and tsunami inundation is mostly within ± 0.5 m for Category 3 around the Powell Lake and can reach over 1 m for other inundated areas.

In the North Tampa Bay mapping area, the hurricane category which best matches the tsunami inundation is shown in Fig. 86 and 88. $\Delta\zeta$ for the best-match hurricane category satisfying Eq. 1 is shown in Fig. 87 and 89, respectively. The matching hurricane category distribution closely reflects that of tsunami inundation. Overall the tsunami inundation is comparable to hurricane Category 1 for the northern portion and all of the southern portion, except for part of the Clearwater Beach and Sand Key Beach where there is Category 2. The difference between hurricane flooding and tsunami inundation $\Delta\zeta$ is generally within $\pm$ 0.5 m for the barrier islands, except for the mainland where $\Delta\zeta$ is larger than 1. This

large positive difference means storm surge inundation depth is much larger than tsunami inundation in this region.

We produced the MOM velocity and vorticity magnitude maps for all the landslide scenarios, for Rosemary Beach, FL and North Tampa Bay, FL, based on a simplified current velocity damage scale where we associate 0 - 3 knots to unharmful currents, 3 - 6 knots to minor damage, 6 - 9 knots to moderate damage, and over 9 knots to major damage. The four damage levels are denoted with white, blue, yellow and red colors, respectively.

From the MOM velocity magnitude results in the entire Gulf of Mexico, it can be observed that, potential damaging currents ($>$ 3 knots, blue, yellow and red areas) tend to be present in most of the area shallower than the minimum offshore safe depth (approximately 200 m or 100 fathoms). However, damaging currents could reach areas deeper than 200 m close to most of the landslide generation regions. Major damaging currents ($>$ 9 knots, red) can be expected in most of the landslide generation regions, in the continental shelf adjacent to Mississippi Canyon, offshore northwest Florida, and Yucatán shelf. Moderate ($>$ 6 knots and $<$ 9 knots, yellow) damaging current areas are scattered over the continental shelf, but mostly close to areas with major damage currents.

Fig. 93 and Fig. 94 shows the MOM velocity magnitude contour plot result for the Rosemary Beach area. Most of offshore region is expected to have moderate to major damaging currents, with major damaging currents occurring along the coastline, inlets, and the various lakes. There is generally no moderate damaging currents farther behind the barrier islands. In Tampa Bay North, FL mapping region, the situation is much less severe than Rosemary Beach, FL. In general, the worst case (MOM) tsunami waves result in minor damaging currents in most areas offshore (Fig. 99). Behind the barrier islands and in the north region, there are much calmer tsunami current velocities ($<$ 3 knots) that usually causes no harm. For both Rosemary Beach, FL and Tampa Bay North, FL, vorticity distribution displays similar patterns to their velocity distribution, where high vorticity appears around the barrier island, and are more intense near the bay entrances.

Tsunami hazard maritime products such as tsunami current magnitude, vorticity, safe/hazard zones would be central for future developments of maritime hazard maps, maritime emergency response and as well as infrastructure planning.

Although the recurrence of destructive tsunami events have been verified to be quite low in the GOM, our work has confirmed that submarine landslide events with similar characteristics to those used here, have indeed the potential to cause severe damage to GOM coastal communities. Therefore, this work is intended to provide guidance to local emergency managers to help managing urban growth, evacuation planning, and public education with the final objective to mitigate potential landslide tsunami in the GOM.

Acknowledgments

This work was supported by the National Oceanic and Atmospheric Administration (NOAA) under awards NA22NWS4670022, "Tsunami Inundation Maps Development for the Gulf of Mexico". The authors wish to thank all NTHMP modeling and Mapping Subcommittee members and GOM's emergency manager representatives for their helpful insights. High

resolution inundation maps are available from http://www.tamug.edu/tsunami/NTHMP/NTHMP.html or by contacting corresponding author.

References

D. Basco and C. Klentzman. On the classification of coastal storms using principles of momentum conservation. In *Proc. 31st Int. Conf. on Coastal Eng.* ASCE, 2006.

J. D. Chaytor, E. L. Geist, C. K. Paull, D. W. Caress, R. Gwiazda, J. U. Fucugauchi, and M. R. Vieyra. Source characterization and tsunami modeling of submarine landslides along the yucatán shelf/campeche escarpment, southern gulf of mexico. *Pure and Applied Geophysics*, 173(12):4101–4116, Dec 2016. ISSN 1420-9136. doi: 10.1007/s00024-016-1363-3. URL `https://doi.org/10.1007/s00024-016-1363-3`.

W. Cheng, J. Horrillo, and R. Sunny. Numerical analysis of meteotsunamis in the northeastern gulf of mexico. *Natural Hazards*, Sep 2021. ISSN 1573-0840. doi: 10.1007/s11069-021-05009-9.

B. Dugan and J. Stigall. Origin of overpressure and slope failure in the Ursa region, northern Gulf of Mexico. In D. C. Mosher, R. C. Shipp, L. Moscardelli, J. D. Chaytor, C. D. P. Baxter, H. J. Lee, and R. Urgeles, editors, *Submarine Mass Movements and Their Consequences*, pages 167–178. Springer Netherlands, 2010.

P. K. Dunbar and C. S. Weaver. *U.S. States and Territories National Tsunami Hazard Assessment: Historical Record and Sources for Waves*. U.S. Department of Commerce, National Oceanic and Atmospheric Administration, National Geophysical Data Center Tech. Rep.No. 3, 2008.

E. L. Geist, J. D. Chaytor, T. Parsons, and U. ten Brink. Estimation of submarine mass failure probability from a sequence of deposits with age dates. *Geosphere*, 9(2):287–298, 2013.

S. T. Grilli, O.-D. S. Taylor, C. D. P. Baxter, and S. Maretzki. A probabilistic approach for determining submarine landslide tsunami hazard along the upper east coast of the United States. *Mar. Geol.*, 264:74–97, 2009.

C. B. Harbitz, F. Løvholt, and H. Bungum. Submarine landslide tsunamis: How extreme and how likely? *Nat. Hazards*, 72(3):1341–1374, 2014.

C. W. Hirt and B. D. Nichols. Volume of fluid method for the dynamics of free boundaries. *J. Comput. Phys.*, 39:201–225, 1981.

J. Horrillo. *Numerical Method for Tsunami calculations using Full Navier-Stokes equations and the Volume of Fluid method*. PhD thesis, University of Alaska Fairbanks, 2006.

J. Horrillo, A. Wood, C. Williams, A. Parambath, and G. Kim. Construction of tsunami inundation maps in the Gulf of Mexico. Technical report, Award Number: NA09NWS4670006 to the National Tsunami Hazard Mitigation Program (NTHMP), National Weather Service Program Office, NOAA, 2011. avail. from http://www.tamug.edu/tsunami/NTHMP.html.

J. Horrillo, A. Wood, G.-B. Kim, and A. Parambath. A simplified 3-D Navier-Stokes numerical model for landslide-tsunami: Application to the Gulf of Mexico. *J. Geophys. Res.-Oceans*, 118:6934–6950, 2013. doi:10.1002/2012JC008689.

J. Horrillo, A. Pampell-Manis, C. Sparagowski, L. Parambath, and Y. Shigihara. Construction of five tsunami inundation maps for the Gulf of Mexico. Technical report, Award Number: NA12NWS4670014 and NA13NWS4670018 to the National Tsunami Hazard Mitigation Program (NTHMP), National Weather Service Program Office, NOAA, 2015. avail. from http://www.tamug.edu/tsunami/NTHMP.html.

J. Horrillo, W. Cheng, A. Pampell-Manis, and J. Figlus. Implementing nthmp-mms strategic plan in tsunami hazard mitigation products for the Gulf of Mexico. Technical report, Award Number: NA14NWS4670049 to the National Tsunami Hazard Mitigation Program (NTHMP), National Weather Service Program Office, NOAA, 2016. avail. from http://www.tamug.edu/tsunami/NTHMP.html.

J. Horrillo, W. Cheng, and J. Figlus. Development of four additional tsunami inundation maps with revision of Port Aransas, TX and updating existing ones with maritime products. Technical report, Award Number: NA15NWS4670031 and NA16NWS4670039 to the National Tsunami Hazard Mitigation Program (NTHMP), National Weather Service Program Office, NOAA, 2017. avail. from http://www.tamug.edu/tsunami/NTHMP.html.

J. Horrillo, W. Cheng, and J. Figlus. Development of two tsunami inundation maps in the GOM and inclusion of the USGS' Yucatan landslide tsunami sources. Technical report, Award Number: NA17NWS4670015 to the National Tsunami Hazard Mitigation Program (NTHMP), National Weather Service Program Office, NOAA, 2018. avail. from http://www.tamug.edu/tsunami/NTHMP.html.

J. J. Horrillo, W. Cheng, R. Sunny, A. Jose, and Y. Shang. Development of two tsunami inundation maps and continuation of the meteotsunami characterization for the gom. Technical report, Award Number: NA19NWS4670015 to the National Tsunami Hazard Mitigation Program (NTHMP), National Weather Service Program Office, NOAA, 2020. avail. from http://www.tamug.edu/tsunami/NTHMP.html.

J. J. Horrillo, W. Cheng, A. Jose, and Y. Shang. Development of two tsunami inundation maps and continuation of the meteotsunami characterization for the gom. Technical report, Award Number: NA20NWS4670066 to the National Tsunami Hazard Mitigation Program (NTHMP), National Weather Service Program Office, NOAA, 2021. avail. from http://www.tamug.edu/tsunami/NTHMP.html.

J. L. Irish and D. T. Resio. A hydrodynamics-based surge scale for hurricanes. *Ocean Eng.*, 37:69–81, 2010.

L. Kantha. Time to replace the Saffir-Simpson hurricane scale? *Eos, Transactions American Geophysical Union*, 87(1):3–6, 2006.

W. Knight. Model predictions of Gulf and Southern Atlantic Coast tsunami impacts from a distribution of sources. *Sci. of Tsunami Hazards*, 24:304–312, 2006.

A. M. López-Venegas, J. Horrillo, A. Pampell-Manis, V. Huérfano, and A. Mercado. Advanced tsunami numerical simulations and energy considerations by use of 3D - 2D coupled models: The October 11, 1918, Mona Passage tsunami. *Pure Appl. Geophys.*, 172(6):1679–1698, 2015.

P. J. Lynett, J. C. Borrero, R. Weiss, S. Son, D. Greer, and W. Renteria. Observations and modeling of tsunami-induced currents in ports and harbors. *Earth and Planetary Science Letters*, 327:68–74, 2012.

P. J. Lynett, J. Borrero, S. Son, R. Wilson, and K. Miller. Assessment of the tsunami-induced current hazard. *Geophysical Research Letters*, 41(6):2048–2055, 2014.

S. Maretzki, S. Grilli, and C. D. P. Baxter. Probabilistic SMF tsunami hazard assessment for the upper east coast of the United States. In V. Lykousis, D. Sakellariou, and J. Locat, editors, *Submarine Mass Movements and Their Consequences*, pages 377–385. Springer Netherlands, 2007.

D. Masson, C. Habitz, R. Wynn, G. Pederson, and F. Lovholt. Submarine landslides: Processes, triggers and hazard protection. *Philos. Trans. R. Soc. A*, 364:2009–2039, 2006.

A. Pampell-Manis, J. Horrillo, Y. Shigihara, and L. Parambath. Probabilistic assessment of landslide tsunami hazard for the northern Gulf of Mexico. *J. Geophys. Res.-Oceans*, 2016. doi:10.1002/2015JC011261.

C. K. Paull, D. W. Caress, R. Gwiazda, J. Urrutia-Fucugauchi, M. Rebolledo-Vieyra, E. Lundsten, K. Anderson, and E. J. Sumner. Cretaceous–paleogene boundary exposed: Campeche escarpment, gulf of mexico. *Marine Geology*, 357:392–400, 2014.

U. S. ten Brink, H. J. Lee, E. L. Geist, and D. Twichell. Assessment of tsunami hazard to the U.S. East Coast using relationships between submarine landslides and earthquakes. *Mar. Geol.*, 264:65–73, 2009a.

U. S. ten Brink, D. Twichell, P. Lynett, E. Geist, J. Chaytor, H. Lee, B. Buczkowski, and C. Flores. Regional assessment of tsunami potential in the Gulf of Mexico. *U. S. Geol. Surv. Admin. Rep.*, 2009b.

R. Wilson, C. Davenport, and B. Jaffe. Sediment scour and deposition within harbors in california (usa), caused by the march 11, 2011 tohoku-oki tsunami. *Sedimentary Geology*, 282:228–240, 2012.

R. I. Wilson, A. R. Admire, J. C. Borrero, L. A. Dengler, M. R. Legg, P. Lynett, T. P. McCrink, K. M. Miller, A. Ritchie, K. Sterling, et al. Observations and impacts from the 2010 chilean and 2011 japanese tsunamis in california (usa). *Pure and Applied Geophysics*, 170(6-8):1127–1147, 2013.

Y. Yamazaki, Z. Kowalik, and K. F. Cheung. Depth-integrated, non-hydrostatic model for wave breaking and run-up. *Int. J. Numer. Meth. Fl.*, 61:473–497, 2008.